NATIONAL TECHNICAL UNIVERSITY OF ATHENS
SCHOOL OF NAVAL ARHITECTURE AND MARINE ENGINEERING

DIVISION OF SHIP DESIGN AND MARITIME TRANSPORT

Diploma Thesis

Dimitrios Bakogiannis

Examination of parametric rolling and excessive acceleration in the framework of the Second Generation Intact Stability Criteria with application to containerships

Supervisor: Nikolaos Themelis, Assistant Professor

Abstract

Several accidents involving intact stability failures related with modern hull designs have called into question the claim that the existing intact stability criteria can offer an adequate degree of safety. On the other hand, the International Maritime Organization (IMO) is finalizing the development of second generation intact stability criteria (IMO MSC.1-Circ.1627). Containerships due to their slender hulls with large bow flares tend to be sensitive to stability failures in waves. For this reason, in this diploma thesis, assessment of parametric rolling and excessive acceleration criteria, as well as the weather criterion (IMO MSC.267(85)), is applied on two different types of container vessels. In addition, an overview of accidents related with instabilities as well as the theoretical background of the criteria is presented. The results of the applications revealed certain inconsistencies between the two levels of the regulations. Specifically, the vessels examined fail the first level with ease while they pass the second level also easily. Regarding the parametric rolling criterion, it seems that the vessels are closer to the threshold value, in contrast to the excessive acceleration criterion were both ships have significantly lower value in relevance to the threshold value. Finally, the influence of bilge keel on the satisfaction of the criteria is examined.

Περίληψη

Αρκετά ατυχήματα που αφορούν αστοχίες άθικτης ευστάθειας σχετίζονται με γάστρες σύγχρονης σχεδίασης έχουν θέσει υπό αμφισβήτηση τον ισχυρισμό ότι τα υπάρχοντα κριτήρια άθικτης ευστάθειας μπορούν να προσφέρουν έναν επαρκή βαθμό ασφάλειας. Ο Διεθνής Ναυτιλιακός Οργανισμός (IMO) ολοκληρώνει την ανάπτυξη των κριτήριων άθικτης ευστάθειας δεύτερης γενιάς(IMO MSC.1-Circ.1627).Τα πλοία μεταφοράς εμπορευματο-κιβωτίων λόγω της λεπτόγραμμης γάστρας τους με έντονο ανοίγμα των γραμμών στην πλώρη τείνουν να είναι ευαίσθητα σε αστοχίες ευστάθειας υπό την επίδραση κυματισμών. Για το λόγο αυτό, η παρούσα διπλωματική εργασία εξετάζει την αξιολόγηση των κριτηρίων της παραμετρικής αστάθειας και των υπερβολικών επιταχύνσεων, όπως επίσης και το κριτήριο καιρού(IMO MSC.267(85) σε δύο διαφορετικούς τύπους πλοίων μεταφοράς εμπορευματοκιβωτίων. Επιπλέον, γίνεται μια επισκόπηση ατυχημάτων που σχετίζονται με αστάθειες καθώς και το θεωρητικό υπόβαθρο των κριτηρίων. Τα αποτελέσματα της εξέτασης των κριτηρίων έδειξαν ορισμένες ασυνέπειες μεταξύ των δύο επιπέδων των κανονισμών. Συγκεκριμένα, τα πλοία που εξετάστηκαν αποτυγχάνουν το πρώτο επίπεδο με μεγάλη ευκολία, ενώ περνούν εύκολα το δεύτερο. Όσον αφορά το κριτήριο της παραμετρικής αστάθειας, φαίνεται ότι τα πλοία είναι πιο κοντά στην οριακή τιμή, σε αντίθεση με το κριτήριο των υπερβολικών επιταχύνσεων όπου και τα δύο πλοία έχουν αρκέτα χαμηλότερη τιμή από την οριακή. Τέλος, εξετάζεται η επίδραση των παρατροπιδίων στην ικανοποίηση των κριτήριων.

Acknowledgments

I would like to thank my supervisor, Assistant Professor Nikolaos Themelis, for his support and advice during the elaboration of this thesis. Without his immediate response this project would be more difficult, since at the same time I was performing my obligatory military service. Finally, I would like to thank my family for always being by my side and providing help and encouragement throughout my whole university studies.

Contents

Chapter 1 Introduction 9
1.1. Introduction 9
1.2. Regulatory Review 10
1.3. Development of Second Generation Stability Criteria 10
1.3.1. Multi-Layered approach 11
Chapter 2 Critical review and aim of the study 13
2.1. Review of previous work 13
2.2. Thesis Objectives and Structure 15
Chapter 3 Review of accidents 16
3.1. Historical background of Container Vessels 16
3.2. Past Accidents 19
3.2.1. Introduction 19
3.2.2. APL China 19
3.2.3. Svendborg Maersk 21
3.2.4. CMV Chicago Express 24
Chapter 4 Presentation of the Regulatory criteria 27
4.1. Intact stability Weather Criterion 27
4.1.1. Introduction 27
4.1.2. Requirements 28
4.2. Parametric Rolling Regulations 32
4.2.1. Introduction 32
4.2.2. Physical Background 32
4.2.3. Level 1 Vulnerability criterion for Parametric Rolling 35
4.2.4. Level 2 Vulnerability criterion for Parametric Rolling 36
4.3. Excessive Acceleration Regulations 43
4.3.1. Introduction 43
4.3.2. Physical Background 43
4.3.3. Level 1 Vulnerability criterion for Excessive Acceleration 46
4.3.4. Level 2 Vulnerability criterion for Excessive Acceleration 48
Chapter 5 Application of the criteria 51
5.1. Introduction 51
5.2. Application of IMO weather Criterion 55
5.2.1. Application for “5,200 TEUs Post-Panamax” 55

5.2.2. Application for “2,200 TEUs Feedermax” 56
5.3. Application of Vulnerability criterion for Parametric Rolling 57
5.3.1. Application of Vulnerability Assessment for “5,200 TEUs Post-Panamax” 57
5.3.2. Application of Vulnerability Assessment for “2,200 TEUs Feedermax” 66
5.4. Application of Vulnerability criterion for Excessive Acceleration 72
5.4.1. Application of Vulnerability Assessment for “5,200 TEUs Post-Panamax” 72
5.4.2. Application of Vulnerability Assessment for “2,200 TEUs Feedermax” 78
5.4.3. Relationship between Level 1 check of EA and IMO Cargo Securing Manual [41] 80
Chapter 6 Impact of bilge keel 84
Chapter 7 Discussion & Conclusions 88
References 89

Chapter 1 Introduction

1.1. Introduction

The notorious accident of the Titanic concluded in the first-ever SOLAS Conference in 1914 since the need to protect life at sea and good transportation developed into a mandatory factor and led to the establishment of standards and rules for the ship design and the verification by classification societies in order to avoid significant scale accidents. On the other hand, the maritime industry has been cautious about dynamic stability in rough seas and how the ship behaves during lousy weather. These problems are complicated, and they are inextricably linked to basic design characteristics of the vessel. Since the nineteenth century, reduced stability on the wave crest in following seas and stability failure in waves like parametric rolling have been noted. Therefore, the International Maritime Organization constantly tried to establish a regulatory framework that could guarantee an adequate level of safety, at least for capsizing events in large vessels.

The need to minimize navigation time and consume less fuel since the increase of maritime demand in transport capacity led to a new generation in ship design. Researchers nowadays pursue high-efficiency and fine hulls with a higher speed and a larger deadweight than before, leading to instability in waves concerning the righting arm variations. These occasions raised academic interest as failures like parametric rolling, surf-riding, and pure loss of stability could be a considerable reason for accidents in the future. Furthermore, accidents that involve cargo damage and sailors' tipping proved to happen due to excessive accelerations noted in specific ship areas. In the past forty years, a series of stability-related incidents have sparked legitimate concerns about the existing intact stability regulations' suitability when applied to new era vessel designs. These events mainly include container and RoRo vessels, proving that while capsizing is exceptionally unlikely, container loss due to lashing equipment failures is common. The most notorious accident was the containership "APL China" in 1998 [14], which was the first confirmed parametric roll case and prompted ABS to publish a guide for evaluating parametric roll for containerships in 2004 [19]. Following "Nedlloyd Genoa" in 2006, "Jrs Canis" in 2007 [16], and many more accidents after, they will be further analyzed in the relevant chapter. Smaller vessels, such as fishing, are vulnerable to these phenomena and can cause more severe consequences. For instance is the Merry Jane fishing vessel, which, in 1986, heeled significantly and concluded in fatal injuries.

As a result, in 2002, IMO tasked the sub-committee on stability, load lines and fishing vessel safety (SLF) with initiating processes to establish enhanced intact stability criteria. By then, it became clear that the implementation of more effective but still more prone to wave stability failures, vessels necessitated the adoption of dynamic stability regulations. In 2008, IMO proceeded to the renovation of the Intact Stability Code starting from scratch. The new code should focus on the physics of the stability failures and not on statistics. Since then, the IMO committee has focused on the Second Generation Intact Stability Criteria because it was reported as the most challenging and vital issue to be solved.

The present thesis focuses on applying the Second Generation Intact Stability Criteria, especially the parametric rolling effect on two containerships. Specifically, parametric rolling levels of IMO will be evaluated and applied to modern designed vessels, and any critical issues will be highlighted. Moreover, the excessive acceleration criterion will also be investigated as containerships are prone to lateral accelerations, which can have a huge impact on stability. Finally, an influence on bilge keel will be executed in order to examine if their design can prove enough to reduce drastically rolling.

The 3D modeling for the ships' hull will be performed in MAXSURF Software as long as the stability calculations are needed. Numerical computations that are necessary will be accomplished through the programming environment of Matlab.

1.2. Regulatory Review

The first-ever worldwide intact stability regulation was released following the SOLAS'60 revision. Then, the Inter-Governmental Maritime Consultative Organization (IMCO) directed to begin research on ship stability on the SOLAS prototype. This project resulted in the birth of the General Stability Criteria on righting arm characteristics in 1968[23]. These criteria concerned ships under 100 meters, and they were a product of a statistical analysis of a significant number of ships classified as safe or not based on Rahola's Thesis[20]. The SOLAS'74 modification concluded in the Weather Criterion (1985), which first began as a recommendation and then was included in IMO's regulation (IMCO was replaced) according to [21]. All the criteria published from 1962 to 1985 were advisory, and none of them were obligatory. In 1975, Professor Kuo coordinated The International Conference on Stability of Ships and Ocean Vehicles, which resulted in the need to research wave effects and development on new methods for ship stability. As Francescutto in 1993[22] proposed, it was then made mandatory a Physical Approach to the hydrodynamics aspects to be taken into consideration concerning ship safety.

1.3. Development of Second Generation Stability Criteria

The desire for criteria based on the physics of stability failure and not on a statistical analysis led to a new era in ship stability. The physical approach proposed was necessary to decode the phenomena taking place in extreme weather and capsizing events to reduce drastically. The development of naval architecture in reference to hydrodynamics concluded in a breakthrough of modern ship designs with finer hulls for RoRo ships and containerships. The development of the Second Generation Stability Criteria started in 2002 since the new designs resulted in more efficient but often more prone vessels to stability failures in waves, like restoring arm variation. Due to the importance of revising the IS Code, the actual project for the second generation stability criteria began in September 2005, when the IMO Sub-Committee on Stability and Load Lines and Fishing vessel safety (SLF) working group in the

48th session determined that the criteria should concern performance and direct three basic modes of failures.

1. Parametric roll and pure loss of stability (restoring moment variations due to waves)
2. Stability failure under dead ship condition
3. Maneuvering-related problems (Surf-riding and broaching-to)

In 2014 the Sub-Committee on Ship Design and Construction (SDC) published the first draft of the second generation intact stability criteria. When the vulnerability criteria have been established, the Direct Stability Assessment (DSA), which constitutes the third level, began to be constructed. Finally, in December 2020 IMO published Interim Guidelines on the Second Generation Intact Stability criteria [30].

1.3.1. Multi-Layered approach

The regulation approach is set on a multi-level scale. Three different levels are assumed, two of them concern if the ship is vulnerable to the stability failures that are examined in order to identify if ships pass the vulnerability criterion, and the last one is a direct stability assessment. The concept of the multi-tiered approach is shown in Fig.(2.1).

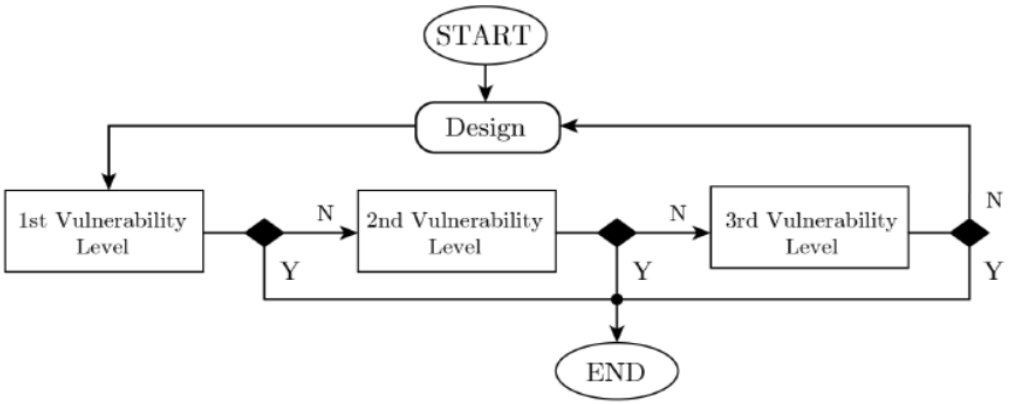

Figure 2.1: The multi-layered approach's operating concept[11]

The first level ***(L1)*** consists of simple mathematical calculations to find possible vulnerabilities, and its method is conservative so as to ensure that the vessel will not capsize in any wave case. For example, bulk carriers and VLCC vessels tend to have no issues with restoring arm variation in waves because of their hull type. Therefore, this kind of ship can pass the first check easily compared to ship types such as container and RoRo ships.

Level 2 ***(L2)*** requires very complicated calculations, including numerical solutions of high-order algebraic equations or non-linear ordinary differential equations. They are focused on a risk assessment process that incorporates the capsize probability in a known dangerous sea-state situation. The IACS wave scatter diagram of the North Atlantic in winter is used for the wave case calculations as it corresponds to the most extreme weather conditions and thus will be associated with the most adverse and uncontrolled operations.

It is approximated that a Level 3 ***(DSA)*** will be included in the future, consisting of the most advanced state-of-the-art technology concerning fluid dynamic calculations and research experiments to approach the vulnerability of vessels and their capsizing potential. The outcome of the DSA could be a change during the ship design process or the development of an Operation Guidance (OG). OG should contain information and recommendations on how the operator can navigate the ship when needed to avoid the probability of stability failures.

Although, these tools should be first verified and validated in order to be approved to use, which emerges as a challenging assignment. The criteria aim for a more detailed and challenging calculation at every level, so the difficulty bar rises as the levels pass on. In Fig.(2.2) the complete schematic structure of the application of SGISc is presented.

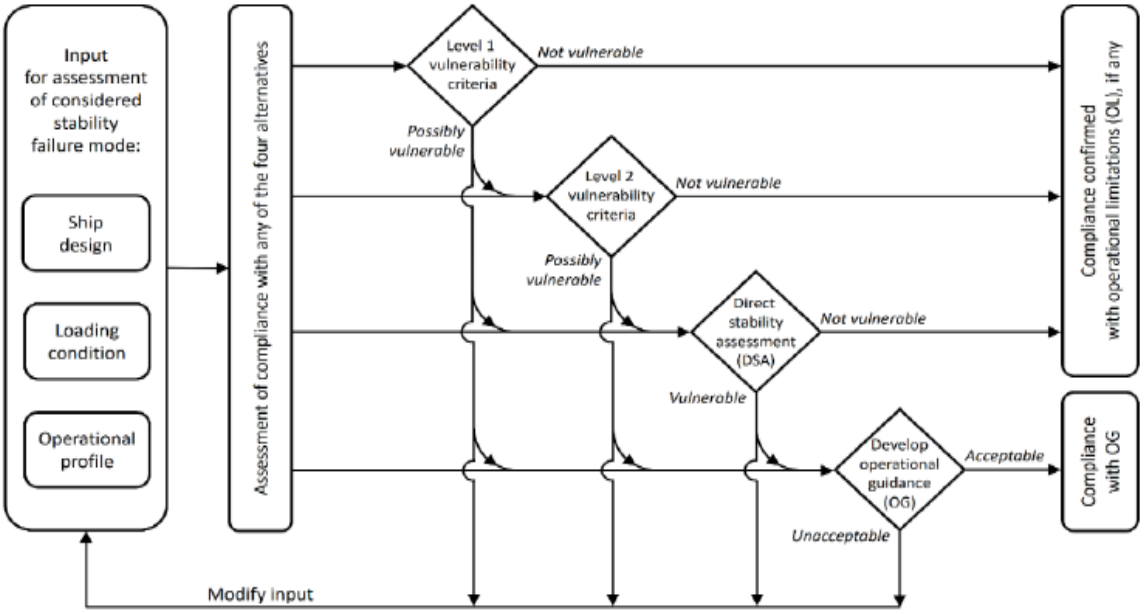

Figure 2.2: Scheme of the application structure of the Second Generation Intact Stability criteria [30]

Chapter 2 Critical review and aim of the study

2.1. Review of previous work

Parametric rolling is responsible for the loss of around 1000 containers per year, according to the World Shipping Council data[1,2], though the phenomenon is not as devastating as other ones, it has already attracted the attention of many research institutes and classification societies. With the combination of pioneers in the field and highly equipped labs, the naval community is trying to find a solution to minimize the frequency of this event and decrease the economic and environmental damage that occurs.

One of the most significant studies concerning the parametric rolling phenomenon was presented by the American Bureau of Shipping (ABS) in 2004, titled "Guide for the Assessment of Parametric Roll Resonance in the Design of Container Carriers"[19]. The study recommends guidelines for estimating the danger to developing parametric roll and calculation procedures for the roll amplitude in longitudinal waves. The criteria set focuses on the Mathieu equation, a one-degree-freedom model, and the metacentric height variation, and the Ince-Strutt diagram for the Mathieu equation is presented. Moreover, the influence of forward speed and wave direction on the phenomenon is discussed. Finally, the verification of the criteria model tests was executed with LAMP (Large Amplitude Motions Program) time-domain simulation software. Susceptibility Criteria presented in this paper were tested for nine different ships through numerical simulations using LAMP, and in every case, there was a correct prediction for the presence or not of the parametric roll.

Following the ABS paper, K.J.Spyrou [24] proposed design criteria to avoid parametric rolling. Pointed the issue that modern-day post-Panamax containerships set to sail without having inspected their proneness to parametric rolling in longitudinal waves. So, the need to develop computational tools to check vulnerability during the design process becomes mandatory. The paper's purpose was to demonstrate the relationship of deterministic and probabilistic aspects of the problem to set the design requirements needed. The deterministic analysis describes a model based on Mathieu's equation roll motion with a linear damping term, and the restoring force is modeled according to a 5^{th} order polynomial fitting. Finally, it presents a proposition for a criterion that binds the evaluation of roll response with the characteristic of extreme waves.

The following paper published by Spyrou et al.[25] was based on examining the parametric rolling behavior of a post-Panamax containership. It presents that even though the ABS and ITTC guidelines contain an analytical method, there is a need for a more structured evaluation. In order to approach both the deterministic and the probabilistic sides of the problem, an analytical prediction formula is structured, and stability charts present the parametric roll boundaries. A model in Maxsurf Software was designed for the calculation of the GZ curves in several positions. The GZ variation is fitted with a linear, cubic, and quantic fit. The next step consists of numerical simulations by time-domain code on SWAN2. In 2003,

[1] World-Shipping-Council-containers-lost-at-sea-2020.pdf (iims.org.uk)
[2] Parametric Rolling Movement - Skuld, Parametric Rolling Motion - a twist in the tail! - StratumFive Ltd

Umeda & Hashimoto [31] presented a study that focuses on parametric roll resonance of a container vessel in following and head seas by modeling the restoring moment as a non-linear function of wave steepness in a more analytical approach.

A different approach is presented in Grinnaert [6], where the second generation criteria of levels one and two are thoroughly investigated. KGmax curves are also used as a standard tool in stability booklets to compare the intact stability rules to the new criteria and approach different computation methods. Furthermore, Caloque software is presented, a three-dimension hydrostatic computer code. Caloque is a tool developed and used by French Naval Academy to calculate the equilibrium, the metacentric height, and the righting arm in still water and waves. Three main algorithms are analyzed on how to design a volume mesh. Finally, different methods are conferred on the results of future criteria and alternative ways to calculate the second check of level two of parametric roll since the calculation is complex. An energy method is applied, which consists of energy analysis and the assumption of linear GZ. The influence of speed, prediction of the width of the lock-in field, and shift angle are also taken into account.

Petacco [11] indicates an analysis and implementation of Second Generation Intact Stability criteria. The author evaluated the criteria on how they will affect existing ships and new project designs. The fundamental element of the thesis is the use of a computational code at UNIGE named Nautilus. Its usage concerns the calculation of hydrostatics and is applied in various vessel types,such as RoRo pax ferry , Navy vessel, mega yacht, and containership. Finally, the innovative element is the adoption of a systems engineering tool, the Design Structure Matrix. DSM is used as a tool to achieve a straightforward analysis to discern the relationship between the main design parameters and the stability failures.

Moreover, Anders Sjule [7] evaluated the parametric roll criteria of IMO for three generations of Pure Car/Truck Carriers (PCTC's) of the Wallenius fleet. The author cites a detailed description of the parametric roll and its physics, providing a more profound knowledge of the phenomenon. A tryout on different adjustments and basic parameters of the problem concludes in many observations, and modifications are suggested, such as the change of wave length and speed steps.

Finally, Panagiotelis[8] and Moulos[9] in their diploma thesis, present an extended evaluation of Second Generation Intact Stability criteria applying the draft regulations on modern-day RoRo ships. Explaining the theoretical and mathematical background of these phenomena and also exposing problems that arise. They also propose modifications and ways to improve the criteria and assess the draft regulations in their present form.

2.2. Thesis Objectives and Structure

The main objective of this thesis is to evaluate intact stability regulations, and specifically parametric rolling, excessive accelerations and the weather criterion, analyze their mathematical background and address any problems witnessed during the process. Specifically, ***Chapter 1*** includes the introduction and the evolution of intact stability code as it became a mandatory solution to minimize stability failures and large-scale accidents. ***Chapter 2*** consists of the regulatory context for the second generation intact stability criteria and the purpose they want to fulfill. Some previous works are considered critical on the development of the criteria. ***Chapter 3*** contains the historical background of the containerships' evolution, as this type of vessel is used to assess the vulnerability of the criteria. The most notorious, impactful past accidents of container vessels are also presented in this chapter as they led to the establishment of the SGISc. These accidents specify parametric rolling and excessive accelerations as the main focus in this thesis. The content of ***Chapter 4*** is the mathematical and theoretical background of the stability regulations assessed. The "weather criterion" (MSC.267(85)) and the first two levels of parametric rolling and excessive accelerations criteria as described in MSC.1/Circ.1627 are analyzed. ***Chapter 5*** introduces the vessels under investigation, and the application of the criteria analyzed before. A detailed approach is interpreted, and the computations used during the process are displayed in this chapter. ***Chapter 6*** contains the influence on bilge keels and how changing their dimension can affect the criteria and the vulnerability against roll. Finally, ***Chapter 7*** presents the final conclusions and thoughts for the criteria and future research.

Chapter 3 Review of accidents

3.1. Historical background of Container Vessels

Worldwide shipping has been the core of global trade throughout time. Even though the regulations are getting stricter and the shipping industry faces more challenges, the global fleet is getting more prominent, and transport is becoming more vital. From the beginning of container transport and the building of containerships until today, more than 60 years ago, the contribution to the global economy has been so outstanding that over 90% of non-bulk cargo worldwide is transported with containerships. Since then, containership designs have been optimized so as to go along with the legislation and simultaneously maximize TEU capacity. Naturally, these factors have a huge impact on the operation and performance nowadays, but since the shipping industry faces rapid changes, it is necessary to provide designs that comply with the rules and operate on a grand level.

The first containerships were made after modifications on oil tankers. The first converted tankers were built up from surplus T2 tankers after World War II. The first container vessel began operating in Denmark, Seattle, and Alaska in 1951, and the first commercially successful containership was named Ideal X, which was a T2 tanker owned by Malcom McLean, operated with 58 metal containers between Newark, New Jersey, Houston, and Texas(Fig.3.1). Malcom McLean is considered the innovator of container shipping, and he was the one who built the first company McLean Trucking which became one of the biggest fleets in the United States.

In 1966, a container liner service from the USA to Rotterdam was initiated. After that worldwide opening of transport, world trade was revolutionized, and through containerization, the whole shipping industry started sailing in new tides. The hours needed for loading and unloading were fewer than traditional ships, and shipping time between ports decreased, which concluded in high-efficiency shipping routes in terms of cost and contributed to the growing shipping industry and global trade.

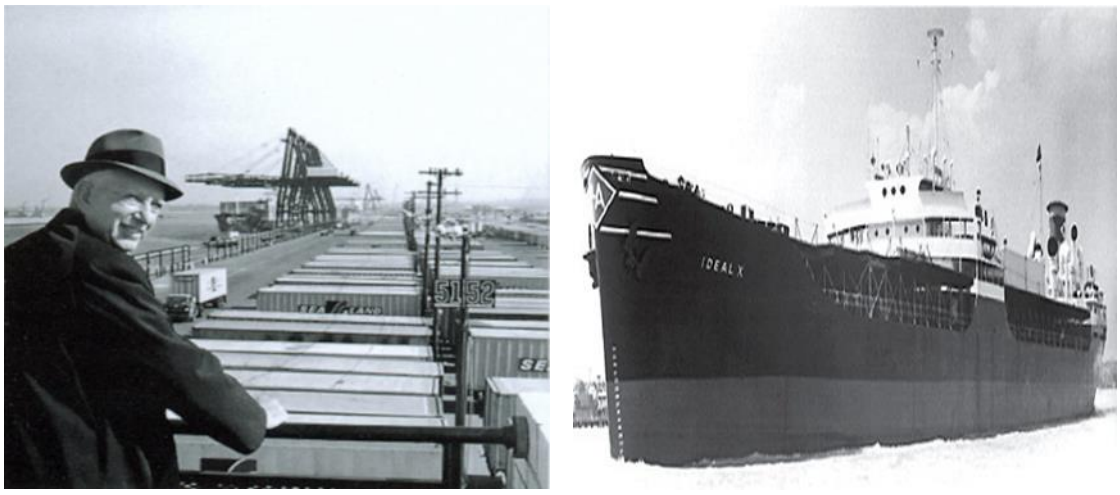

Figure 3.1:Malcom McLean and SS Ideal X 1956[43][44]

Today, container ships have huge bow flares, and they can travel at high speeds (approx.25 knots), and they carry their whole cargo in TEUs & FEUs (Twenty-foot Equivalent Unit & Forty-foot Equivalent Unit). A typical hull consists of hatch openings on the upper deck due to the vertical loading and unloading, and they are divided into cells by vertical guided rails. Since the burst of technology, modern ships can carry more than 20 thousand TEUs. These breakthroughs have led to a reduction of the total delivery time by 90% and the total cost by 35%.

Container vessels categories belong in the following classes relevant to their size and are presented in Table 3.1:

Table 3.1: Containerships' basic categories[47]

Name	Capacity(TEU)	L [m]	B [m]	T[m]
Small Feeder	< 1,000	-	-	-
Feeder	1,001-2,000	-	-	-
Feedermax	2,001-3,000	-	-	-
Panamax	3,001-5,000	294.13	32.31	12.04
Post-Panamax	5,101-10,000	366.00	49.00	15.20
New-Panamax	10,000-14,500	366.00	49.00	15.20
Ultra Large Container Vessel(ULCV)	>14,500	>366.00	>49	>15.20

Figure 3.2: Typical ULCV TEUcapacity:19462 L=400m B=58.85m T=15m [46]

& feeder L=146.2m B= 22.6m T=7.4 m[45]

The size of containerships is proliferating as maritime companies are anticipating monster ships like Maersk's Triple-E Vessels. This tendency is aimed at achieving economies of scale and adapting to the highly anticipated conditions of the market, so the parametric roll draws more interest and attention. The new ships that come to the market consist of large bow flare and wide beam in order to reduce the frictional resistance that is produced when the ship fore end passes through the water, making it streamlined with the hull. Although vessels increased in size, they retained a high service speed (approximately 25 knots) as used to be in traditional containerships, which used to carry 1,000 TEUs. Nowadays, container vessels can carry up to 20,000 TEUs, so a high speed can be achieved as the hull becomes thinner so that fuel consumption is not too high. However, this procedure poses complications, as it adapts some fundamental characteristics for the development of parametric roll resonance, which will be studied in a further chapter.

3.2. Past Accidents

3.2.1. Introduction

For several years, the naval architecture society has recognized the parametric roll, but it was never regarded as a significant concern for the intact stability. A series of events triggered the implementation of the Second Generation Intact Stability criteria, and a sequence of unusual accidents at sea occurred in recent years. These incidents included ships that were considered to be safe and compliable with the stability rules in place at the moment. Consequently, the concerns of the Administrations and experts arose. These incidents were chosen as case studies to be used as benchmarks and to evaluate the criteria established. The event that urged reconsideration was the APL China casualty in 1998[14] which made it evident that parametric roll affects either low freeboard vessels or low marginal stability, such as fishing vessels. Even though large vessels, such as containerships, are less vulnerable to capsizing than small vessels while under parametric roll excitation, this situation should not be neglected because that vessel's instability may lead to substantial loss of cargo and damage to the structure of the ship. Furthermore, such occurrences can generally cause severe economic damages to ship owners and disrupt the shipping industry.

3.2.2. APL China

It was stated already that the APL China accident was a pivotal moment for the researchers to launch a comprehensive investigation of the parametric roll resonance. The incident was detailed thoroughly in the research carried out by France et al.(2003). APL China is listed as a post-Panamax containership C11, and its dimensions are listed in the Table (3.2).

Table 3.2: APL China principal particulars[14]

APL China Overall Dimensions		
Length between perpendicular	L_{BP} [m]	262.0
Maximum Breadth	B [m]	40.0
Depth	D [m]	24.45
Maximum summer draught	$T_{s.}$ [m]	14.0

The C11 class has been thoroughly tested through numerical simulation or model tests for parametric rolling in following seas, but the state of head seas has never been addressed. This condition was not known to be significant until the accident involving APL China. The circumstances under which the incident took place were introduced at SNAME's annual meeting in 2001. The accident investigation revealed, using numerical simulations of various tools, that the stability failure was caused by parametric rolling in head seas.

On 20th October 1998, the vessel sailed from Kaohsiung (Taiwan) to Seattle with a two-way path suggested by the weather routing service as shown in Fig.(3.3). Due to changes in weather conditions at the territory, heavy seas of 10 to 11 Beaufort winds and waves and swell of 8.5 to 11.7 m. The two developing lows fused and developed an "explosively intensifying low." The storm approached the vessel's position within around 120 nm. On 26th and in the North Pacific Ocean, the storm encounter started at 00:00 and ended at 17:00. During the storm, the master has reduced the vessel's speed, and at the worst condition of

the storm, they were recorded extreme yaw, pitch, and heel angles up to 40 degrees, and the master reported that the ship was totally out of control. When the incident occurred, the mean draught was 12.34 m, with a freeboard of around 12 m. Furthermore, the deck log recorded winds of 11 Beaufort force and a sea state 9, which is the highest level on the International sea state scale, while the transverse metacentric height (GM_T) was 2 m and the rolling period (T_p) was 26 seconds. The weather conditions were described as “phenomenal,” and the wave heights averaged 14 m.

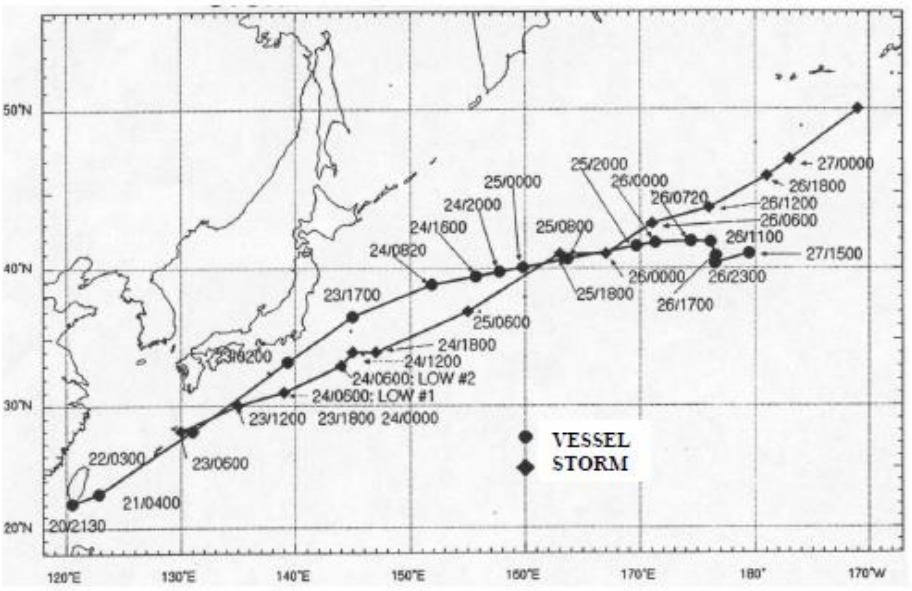

Figure3.3: Vessel and storm track[14]

In conclusion, when the vessel arrived at the Port of Seattle, as shown in Fig.(3.4), the gravity of the incident was obvious. It was defined that one third of the on-deck containers were lost, and another one was heavily damaged, luckily though there were no human fatalities. APL China was then recognized as the most significant container casualty in history, and it was claimed that the economic damage of cargo reached 50 million dollars, higher than the actual value of the ship.

Figure 3.4: APL China damaged containers[14]

3.2.3. Svendborg Maersk

Svendborg Maersk is a 1998 built containership sailing under the Danish flag, owned and operated by A.P. Moller-Maersk A/S, and its capacity rises to 8,160 TEUs. The vessel was operating in a regular trading service between ports in northern Europe and Asia via the Suez Canal. A typical trip would consist of 18 port calls and last about two months. Vessel's particulars and listed in Table(3.3).

Figure 3.5: Svendborg Maersk after departure from Rotterdam 13/02/2014[15]

Table 3.3: Svendborg principal particulars[15]

Svendborg Maersk Overall Dimensions		
Length overall	L_{OA} [m]	346.98
Maximum Breadth	B [m]	42.80
DWT	DWT[tons]	110,387
Maximum draught	T [m]	14.941
Service speed	V[kn]	25.0

On 13th February 2014, the Danish containership departed from the port of Rotterdam, heading to the Far East through the Suez Canal, averaging a speed of 19.8 knots during the trip. It was expected to experience unfavorable weather conditions, but there was no need to raise concerns. However, the following day, the weather forecast displayed that the weather conditions would start worsening. The cargo was then checked visually and physically in order to ensure that the lashings were adequately secured. In the afternoon, swiftly and abruptly, the vessel started rolling to extreme angles, and the speed through the water was decreased to three knots. It was recorded at a 38-degree starboard angle during the sudden roll, and then the rolling kept going at a more moderate pace. The crew then observed that a large number of containers were lost overboard from the bay positioned in front of the wheelhouse and another one from the aft part of the ship. Later in the day, the

ship started again heavily rolling with a result of a 41° angle to portside, and another vast amount of containers fell to the sea, and the master increased speed to 4-5 knots to ensure the capability of steering and to avoid parametric resonance as it was suspected to be the actual cause. The positions of lost containers are shown in Fig.(3.6).

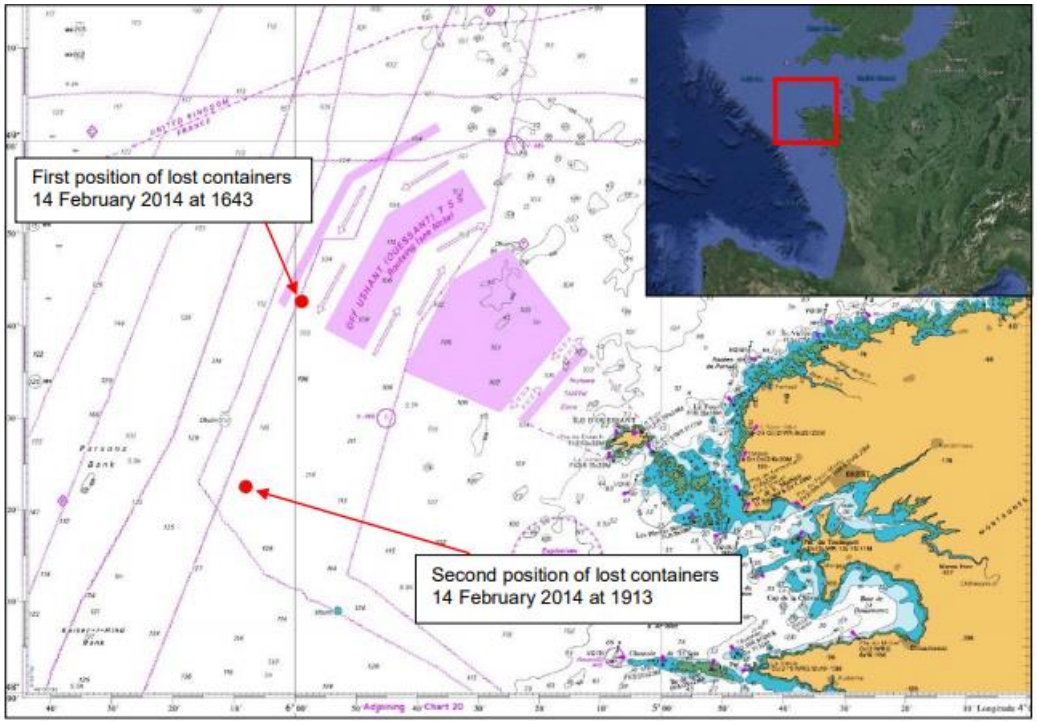

Figure 3.6: Scene of the accident (Bay of Biscay)[15]

On 15 February, the weather began to improve, and it was time to clean up the ship. A stability calculation carried out proved that there was a slight trim forward since many containers were lost overboard from the aft section. Master was informed to proceed to the port of Malaga to repair the minor damages to the ship's structure and remove the damaged containers. On 17th February, when the ship arrived in Malaga, an assessment to calculate the damages and the loss of the cargo was carried out.

Figure 3.7: Damaged lashing equipment and containers[15]

The result of the accident was that the lashing gear for 600-700 containers was damaged (Fig.3.7), and 517 containers were lost overboard, from which 75 contained cargo and the additional were empty, and another 250 containers were damaged(Fig.3.8). Finally, 17 floating containers were recovered from the area of the incident. In conclusion, the authorities reached the decision that the accident was caused by a combination of weather conditions and the ship's particulars, cargo loading, and cargo securing configuration as the cargo securing equipment could not withstand the forces that were induced during the heavy rolling.

Figure 3.8: Vessel's aft deck at arrival in Malaga[15]

3.2.4. CMV Chicago Express

On 24 September 2008, the Federal Bureau of Maritime Casualty Investigation[13] investigated the CMV Chicago Express accident and reported on 1st November 2009 with Investigation report 510/08. Chicago Express is a 2006 built containership (Figure 3.9) operating under the German flag, and its dimensions are listed in the Table (3.4).

Figure 3.9: CMV Chicago Express[13]

Table 3.4: Vessel's particulars[13]

CMV Chicago Express Overall Dimensions		
Length overall	L_{OA} [m]	336.19
Maximum Breadth	B [m]	42.80
DWT	DWT[tons]	103,691
Maximum draught	T [m]	14.61
Maximum speed	V[kn]	25.2

The vessel sailed from the port of Hong Kong on September 23 on a south-easterly course and followed the route displayed in Fig.(3.10), with a speed of 8-10 knots heading to Ningbo following strictly the directions of local authorities since there was a typhoon alarm because typhoon "HAGUPIT" was approaching. Unfortunately, the vessel was caught in strong gusts and began to roll exceptionally with up to 32 degrees heel angles. Corresponding to the voyage plan, the scheduled north-easterly path was modified in order to escape the approaching typhoon, and speed was decreased to around 3 to 5 knots because of the heavy weather, and during this time, the rolling angles were acceptable. On September 24, midnight winds of 10 Beaufort with strong gusts up to 12 hit the vessel, and a huge wave encountered in the starboard side as she rolled on it.

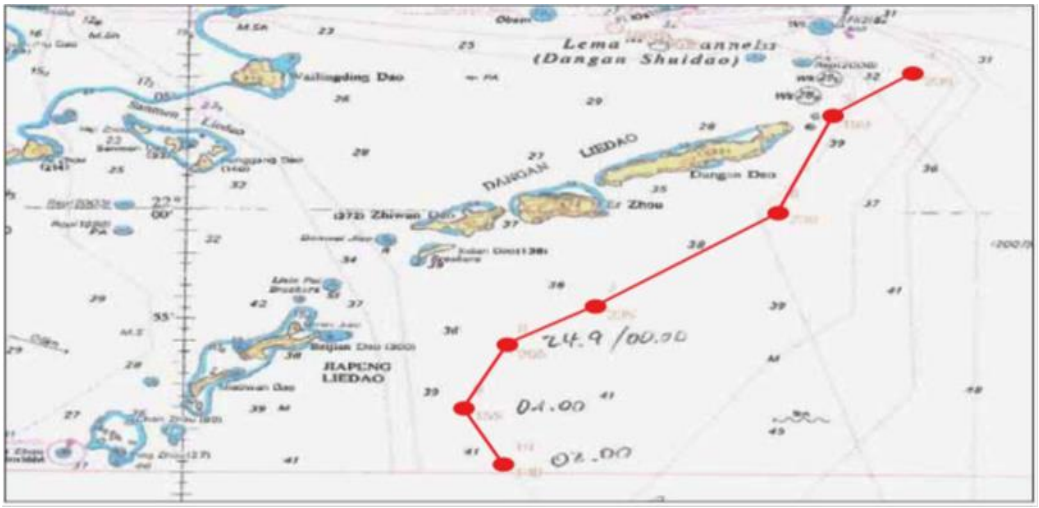

Figure 3.10: Route of the vessel [11]

As a result, the vessel heeled portside and back in a 10 seconds period while recording a transverse acceleration of 9.81 m/sec^2 and a maximum roll angle of 44 degrees. Owing to the abrupt and extreme roll motion of the ship in the navigation bridge, the master, the helmsman, and the lookout dropped down on the floor, bumping into the wheelhouse furniture, the path they followed after the fall is shown in Fig.(3.12). The Second Officer and the helmsman who recovered fast witnessed that the master and the lookout were still unconscious. For instance, the crash was informed to the appropriate inshore authority, and the injured were given first aids. Unfortunately, the lookout died on board a short time after the crash since he had clear signs of death(no pulse, respiration, etc.) due to a fatal head injury. In contrast, the master suffered from critical spinal injuries, and a rescue helicopter landed on the vessel immediately after the resumption of air service and was rushed to a Hong Kong hospital.

Figure 3.11: Impact damage and deformation of interior[13]

Thus, the master was actually in acute danger of losing his life for an extended period, and even after years of the incident, he has not regained total health since the internal injuries were too severe.

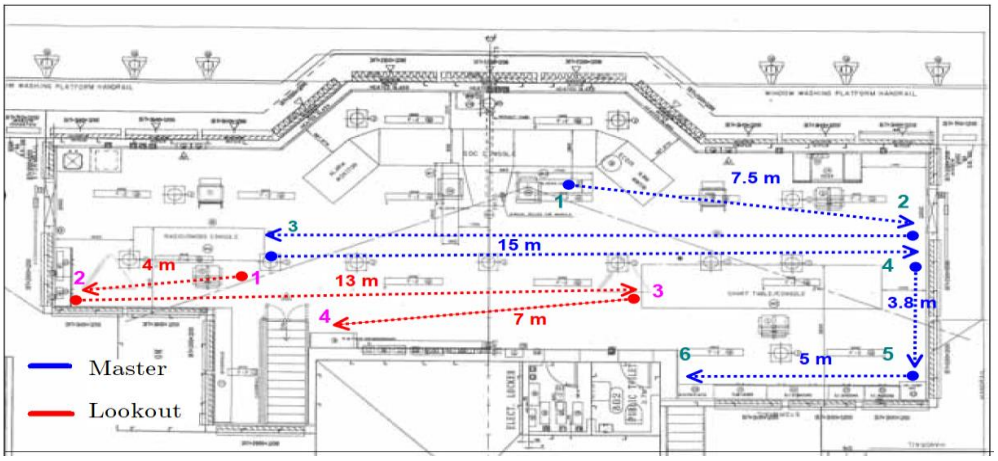

Figure 3.12: Path of the fall of the AB and the Master[13]

As a result, the experts found out that the critical cause of the crash was the combination of a high stability value of metacentric height GM=7.72 m and a low roll damping due to the reduced speed. In addition, drift abeam was not feasible because the islands were too close to the vessel there are no defects possible to trace to the crew members. Although, this incident caused the death of a member of the crew and the severe injury of the master while both were in the navigation bridge.

There are numerous accidents worth mentioning, such as Maersk Carolina 2003 loss of 133 containers, MSC Zoe loss of 342 containers in the North Sea in 2019, CMV CCNI GUAYAS 2009 where during the heavy rolling, crew members were injured, and the ship got several damages, JRS Canis 2007 loss of containers and MS Beluga 2006 where a person fell overboard, and the list of significant incidents goes on. The investigations for the above accidents will not be reported because some of the selected to be described in depth, but they can be found in[16] [17] [18]. Furthermore, the incident of ONE Apus on 20 November was also caused by severe weather, and even though it is too early for the investigation to report what happened, it is already known that it was identified heavy rolling which in combination with human errors led to the worst cargo loss counting the gigantic number of 1,816 containers overboard while 64 of them were containing Dangerous Goods.
From the above incidents, it was evident that containerships are incredibly vulnerable to severe weather conditions and heavy rolling, resulting in accidents with a massive impact on economic damage due to cargo loss or hull damage and threat to human life and the oceans on an environmental point of view. Furthermore, from the studies accomplished, it has been observed that parametric rolling develops when a combination of some key factors takes place. Specifically:

- The relationship between the wavelength and the ship length.
- The relationship between the ship's natural roll frequency and the encounter frequency.
- The ship roll damping.

Chapter 4 Presentation of the Regulatory criteria

4.1. Intact stability Weather Criterion

4.1.1. Introduction

The issue of stability, especially the avoidance of capsizing in severe weather, is a fundamental requirement in ship design. After the research publications of Rahola [20], which focused on a statistical analysis of ships recognized as safe or unsafe according to the intact ship stability, there was a strong interest in the shipbuilding industry for the establishment of an appropriate practical criterion. Driven by the need to avoid ship accidents, intact stability criteria were initially launched in individual countries such as USSR [33], the USA [34] , and Japan-Yamagata [32].

The framework of IMO stability criteria was presented with Resolution A.167 (1969), followed by the weather criterion adopted in Resolution A.562 (1985). The standard adopted by IMO was based on the Japanese criterion, and it was the first dynamic stability criterion. It determines the ability of the ship to withstand severe winds and rolling by comparing heeling and righting moments. Although, simplifications made regarding the motions of the vessel and the righting moments are estimated in calm water. It provides a dynamic aspect of the subject, but the criterion does not connect with modern ship designs since it applies to empirical data. In 1993 IMO adopted the first generation intact stability code Res A.749, which combined codes A.167 & A.562.The code was introduced in its original form until 2002 when the IMO re-formed the intact stability group to negotiate changes to the code as a response to the proposal of many who argued that the weather criterion was too strict for ships with a rolling period (T_r) above 20 seconds and large ratio B/d. Since the criterion was based on the Japanese, it was most applicable to ships with diverse design particulars from the modern ones. The main issues faced on the calculation of rollback angle φ_1 since the effective wave slope coefficient r and the wave steepness s were causing too large rollback angles for various types of ships.

There were no changes since the legislation of IMO's “Weather Criterion” of 1985 till 2005. In 2002 A.Francescutto[35] advised that the criterion was problematic because it only took lateral winds and waves into account. Furthermore, Spyrou [26] reviewed the criterion and proposed a radical change of it. At the SLF45 in 2002, many countries expressed their objections regarding the relevant criterion and its application to modern ships. Since the coefficients in A.562 IMO 1985 were based on statistical analysis on older ship designs, it could not keep up with modern design trends and led to strict results. The committee agreed that the parameters r should not exceed a value greater than one, and s should be calculated according to reviewed values.

Eventually, at conference SLF48 2005, utilizing the results of Japanese and Italian surveys, the standards of the experiments for the calculation of l_{w1} finalized. Thus, those standard instructions mentioned above were the creation of the code MSC.1/Circ.1227 (2007).

In 2008 IMO published the intact stability IS code where the criteria for the GZ curve and the weather criterion were presented. In addition, since 1995 IMO has published "Guidance to the master for avoiding a dangerous situation in following and stern quartering seas," which was revised in 2007 because of the need to decrease the danger of accidents due to wave instabilities.

4.1.2. Requirements

The criteria regarding the righting lever curve (GZ curve) in calm water are cited hereunder:

(a) The area under the righting lever curve (GZ curve) should not be less than 0.055 meter-radians up to θ=30° angle of heel and not less than 0.09 meter-radians up to θ=40° or the angle of flooding θf if this angle is less than 40°.Additionally, the area under the righting lever curve (GZ curve) between the angles of the heel of 30° and 40° or between 30° and θf if this angle is less than 40°, should not be less than 0.03 meter-radians.

(b) The righting lever GZ should be at least 0.20 m at an angle of heel equal to or greater than 30°.

(c) The maximum righting arm should occur at an angle of heel, preferably exceeding 30° but not less than 25°.

(d) The initial metacentric height GM0 should not be less than 0.15 m.

The main principles of severe wind and rolling criterion are:

- Ship's motion
- Steady wind pressure
- Beam waves
- External forces
- Wind gust

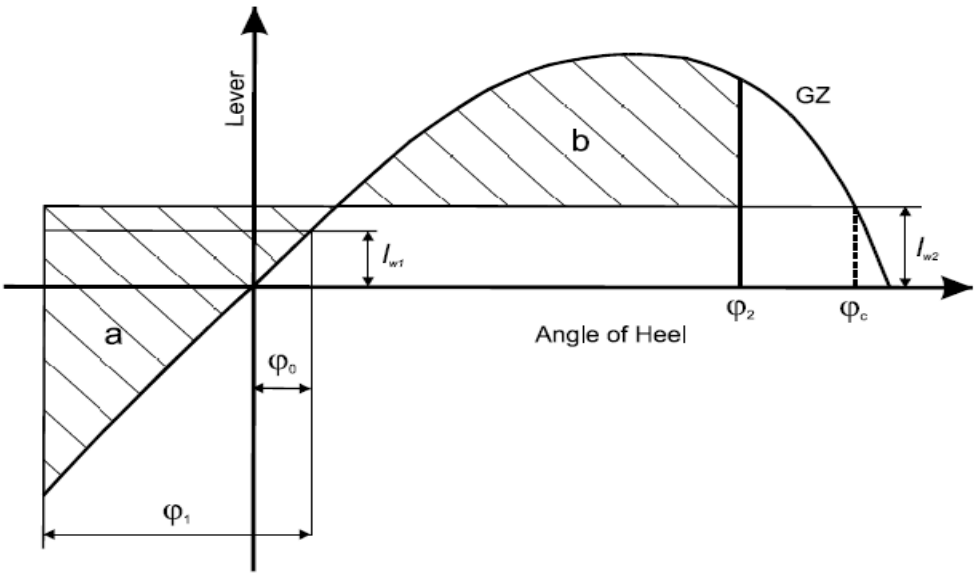

Figure 4.1: Severe wind and rolling diagram MSC.267(85)[27]

The angles in the figure are defined as:

$\boldsymbol{\varphi_0}$ = angle of heel under action of steady wind

$\boldsymbol{\varphi_1}$ = angle of roll to windward due to wave action

$\boldsymbol{\varphi_2}$ = angle of down-flooding ($\boldsymbol{\varphi_f}$) or 50^0 or $\boldsymbol{\varphi_c}$, whichever is less

Where:

$\boldsymbol{\varphi_f}$ = angle of heel at which openings in the hull, superstructures, or deckhouses cannot be closed weathertight immerse. In applying this criterion, small openings through which progressive flooding cannot take place need not be considered open
$\boldsymbol{\varphi_c}$ = angle of the second intercept between wind heeling lever $\boldsymbol{l_{w2}}$ and GZ curves.

The wind heeling levers $\boldsymbol{l_{w1}}$ & $\boldsymbol{l_{w2}}$ are constant values at all angles of inclination and shall be calculated as:

$$I_{w1} = \frac{P \cdot A \cdot Z}{1000 \cdot g \cdot \Delta} \; [m] \qquad (4.1)$$

$$I_{w2} = 1.5 I_{w1} \; [m] \qquad (4.2)$$

Where:

P = wind pressure of 504 Pa. The value of *P* used for ships in restricted service may be reduced subject to the approval of the Administration
A = projected lateral area of the portion of the ship and deck cargo above the waterline (m^2)
Z = vertical distance from the center of A to the center of the underwater lateral area or approximately to a point at one half the mean draught (m)
Δ= displacement (t)
g = gravitational acceleration of 9.81 m/s^2

Lugovski introduced the calculation method for the rolling amplitude using coefficients ***k***, $\boldsymbol{X_1}$, $\boldsymbol{X_2}$, which connect the vessel's response amplitude with its geometry. The first factor includes the ratio breadth to draft –B/d-, the second one the block coefficient C_B and factor k is the corresponding factor for the bilge keels.
The angle of roll (ϕ_1) is calculated as:

$$\varphi_1 = 109 * k * X_1 * X_2 * \sqrt{r * s} \quad [deg] \qquad (4.3)$$

where:

$\boldsymbol{X_1}$ = factor as shown in the table
$\boldsymbol{X_2}$ = factor as shown in the table
k = factor as follows:

- k = 1.0 for round-bilged ship having no bilge or bar keels
- k = 0.7 for a ship having sharp bilges
- k= as shown in the table for a vessel having bilge keels, a bar keel or both

r = 0.73 + 0.6 OG/d

where:

- OG = KG –d
- d = mean moulded draught of the ship (m)

s = factor as shown in the table, where T is the ship roll natural period. In the absence of sufficient information, the following approximate formula can be used:

$$T = \frac{2*C*B}{\sqrt{GM}}\ [s] \qquad (4.4)$$

where:

$$C = 0.373 + 0.023\left(\frac{B}{d}\right) - 0.043\left(\frac{L_{wl}}{100}\right) \qquad (4.5)$$

L_{wl} = length of the ship at waterline (m)
B = moulded breadth of the ship (m)
d = mean moulded draught of the ship (m)
C_B = block coefficient (-)
A_k = total overall area of bilge keels, or area of the lateral projection of the bar keel, or sum of these areas (m^2)
GM = metacentric height corrected for free surface effect (m)

Table 4.1: Values of factor k

$\frac{A_k \times 100}{L_{WL} \times B}$	k
0	1.0
1.0	0.98
1.5	0.96
2.0	0.88
2.5	0.79
3.0	0.74
3.5	0.72
≥4.0	0.70

Table 4.2: Values of factor s

T	s
≤ 6	0.100
7	0.098
8	0.093
12	0.065
14	0.053
16	0.044
18	0.038
≥20	0.035

Table 4.3: Values of factor X_1

B/d	X_1
≤ 2.4	1.0
2.5	0.98
2.6	0.96
2.7	0.95
2.8	0.93
2.9	0.91
3.0	0.90
3.1	0.88
3.2	0.86
3.4	0.82
≥3.5	0.80

Table 4.4: Values of factor X_2

C_B	X_2
≤0.45	0.75
0.5	0.82
0.55	0.89
0.60	0.95
0.65	0.97
≥0.7	1.00

The initial view of the weather criterion is based on ships with the following characteristics:

- B/d smaller than 3.5
- (KG/ d-1) between -0.3 and 0.5
- T smaller than 20 s.

For ships with parameters outside of the above limits, the angle of roll (ϕ_1) is calculated according to MSC.1/Circ.1200.

The Table 4.2 for the steepness factor s should be substituted with the steepness factor s, according to MSC.1/Circ.1200 “the Interim Guidelines for alternative assessment of the weather criterion” and presented in table 4.5.1 (Fig.4.2) below.

Ship roll period T_ϕ [s]	Wave steepness $s = H / \lambda$
<6	0.100
6	0.100
7	0.098
8	0.093
12	0.065
14	0.053
16	0.044
18	0.038
20	0.032
22	0.028
24	0.025
26	0.023
28	0.021
30	0.020
>30	0.020

Figure 4.2: Table 4.5.1 of MSC.1/Circ.1200[28]

4.2. Parametric Rolling Regulations

4.2.1. Introduction

Parametric rolling is a part of parametric resonance phenomena. The development of this kind of phenomenon is a system with changing parameters periodically with time. According to [10], parametric resonance was introduced by Faraday and afterward by Melde, and Mathieu structured the mathematical model that described the parametric resonance. William Froude was the first to recognize that parametric resonance applies in ships too. The first-ever research on parametric rolling was carried out in Germany. Krempf was the first one that observed back in 1938 that when the wave crest is amidships, the stability is decreased, and while the wave trough is at midship, the stability was increased. The model experiments for parametric rolling were introduced by Heckscher and Graff in 1941, since several incidents of capsizing of small ships, such as fishing boats, occurred in the following waves.

In 1950, professor Grim in Germany and MIT professor Kerwin reported that the metacentric height (GM) variations that occur while the ship is in motion in the head or following seas provide, as a result, a Mathieu-type differential roll equation. In 1961, Pauling and his associates for Berkeley University illustrated the effect of motions and waves on transverse stability through experiments and in 1980, Blocki used ship dynamics equations and function methods to determine the probability of capsizing.

4.2.2. Physical Background

Parametric Rolling is recognized as a kind of instability in waves where large roll angles develop and it is triggered by the periodic variations of transverse stability in longitudinal waves. Specifically, while the vessel is on the wave trough, the stability is increased, and when the vessel is on the wave crest, there is a decrease in stability. The GZ curve variations for different wave heights can depict the stability variations of a vessel in waves as presented in Fig.(4.3). As the wave height increases so does the difference between the GZ curve for wave trough amidship and wave crest amidship. This expansion in stability variation is the reason that the roll amplitude increases.

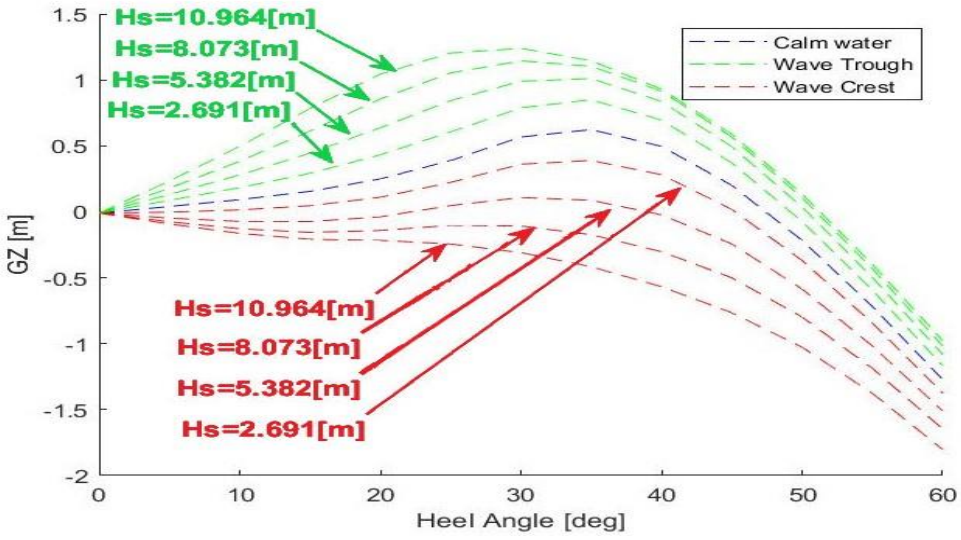

Figure 4.3: GZ curves for multiple wave heights and wave length equal to L_{WL} for Post-Panamax

As explained in [2], when on wave trough amidships, increased stability will add a stronger pushback and because of it when the ship returns to the upright position has an increased roll rate. When the wave crest reaches midship the ship will roll further to the opposite side, since the decrease in stability concludes in increased rolling speed and less resistance to heeling. Then, the wave trough is at midship, the ship reaches the maximum rolling amplitude and the stability increases again and this cycle repeats. The phenomenon observed when the wave encounter frequency $\boldsymbol{\omega_e}$ is about twice the natural roll frequency $\boldsymbol{\omega_f}$, as the stability change caused by the waves is synchronized with the rolling of the vessel and the roll damping is inadequate. Parametric roll resonance occurs when $\boldsymbol{\omega_e / \omega_f = 2}$ or $\boldsymbol{\omega_e / \omega_f = 1}$. The first verified parametric roll accident was APL China in 1998, and other significant accidents were presented in Chapter 3.

Mathematical Model for Parametric Roll

The analysis of the mathematical model for parametric roll that follows originates from [4].

The variation of GM under harmonic waves as a function of time is given by the equation below:

$$GM(t) = GM + \Delta GM \cdot \cos(\omega_e t) \tag{4.6}$$

GM is the value of metacentric height in calm water, and ΔGM is the amplitude of GM's harmonic variation.

By using the well-known linear roll equation below

$$(I_{xx} + A_{44}) \cdot \ddot{\varphi} + B_{44} \cdot \dot{\varphi} + m \cdot g \cdot GM(t) \cdot \varphi = 0 \tag{4.7}$$

And the time-dependent GM function, roll equation results in

$$(I_{xx} + A_{44}) \cdot \ddot{\varphi} + B_{44} \cdot \dot{\varphi} + m \cdot g \cdot [GM + \Delta GM \cdot \cos(\omega_e t)] \cdot \varphi = 0 \tag{4.8}$$

or $$\ddot{\varphi} + b \cdot \dot{\varphi} + {\omega_o}^2 \cdot [1 + h \cdot \cos(\omega_e t)] \cdot \varphi = 0 \tag{4.9}$$

where $h = \frac{\Delta GM}{GM}$ and $b = \frac{B}{(I + \Delta I)}$

Normalizing the equation and when the damping term *b* is neglected, the Mathieu equation is obtained as follows

$$\ddot{\varphi} + {\omega_o}^2 \cdot [1 + h \cdot \cos(\omega_e t)] \cdot \varphi = 0 \tag{4.10}$$

Although Mathieu is a linear differential equation, a closed-form solution is not obtainable. The Mathieu equation's numerical solution for several pairs of $(\omega_o^2/\omega_e^2, h)$ based on various studies proved stable and unstable solutions for specific values.

The Ince-Strutt diagram shows the bounded and unbounded solutions and is constructed by the coefficients ε, δ:

$$\varepsilon = h \cdot \left(\frac{{\omega_o}^2}{{\omega_e}^2}\right) \quad \text{and} \quad \delta = \frac{{\omega_o}^2}{{\omega_e}^2} \tag{4.11}$$

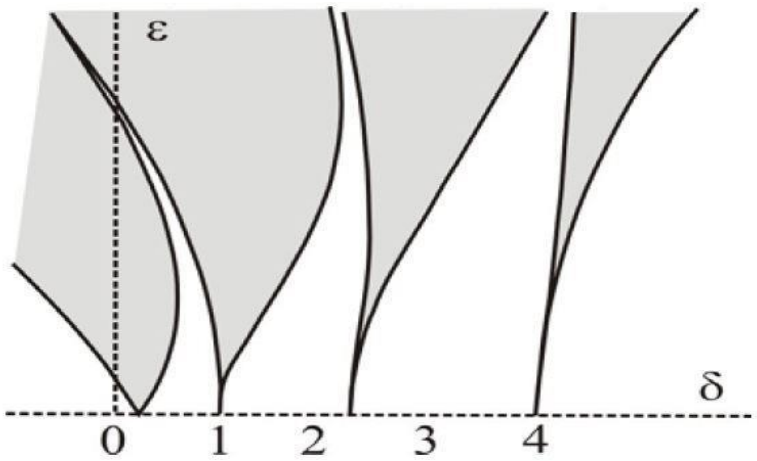

Figure 4.4: Ince-Strutt diagram[4]

The shaded areas represent the unstable pairs of *(δ,ε)*, where the roll motion does not exist, and the non-shaded ones where the pairs are stable and correspond to rolling motion.

Unbounded solutions of the Mathieu equation exist when for any h:

$$\frac{4\cdot{\omega_o}^2}{{\omega_e}^2} \approx n^2 \,, where\ n = 1,2,3,4 \ldots \qquad (4.12)$$

The value n=1 corresponds to "principal" resonance ($\omega_e = 2 \cdot \omega_o$), which refers to the most dangerous case and when n=2, the case is also considered critical and labeled as "fundamental" resonance($\omega_e = \omega_o$).

The damping term is not included in Mathieu equation, even though its impact is significant for the roll amplitude. As shown in figure, when damping is included, the unstable regions' boundaries are shifted upwards. Thus, small values of h will not conclude to extreme responses, and vessels will be safe against parametric rolling even if there is a principal or fundamental resonance situation. Roll damping can be increased with the use of bilge keels, stabilizer fins, and anti-rolling tanks.

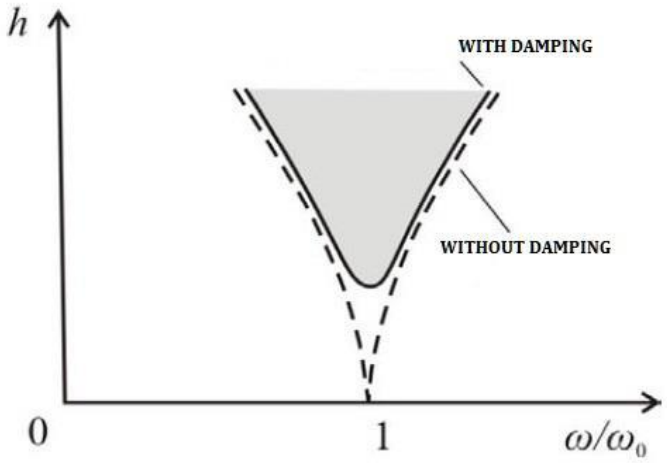

Figure 4.5: Effect of damping[4]

4.2.3. Level 1 Vulnerability criterion for Parametric Rolling

According to the first level of vulnerability [1], a ship is not considered vulnerable to the parametric rolling failure mode if:

$$\frac{\Delta GM}{GM} \leq R_{PR} \tag{4.13}$$

Where:

$R_{PR} = 1.87, if\ the\ ship\ has\ a\ sharp\ bilge\ ;\ otherwise,$

$$= 0.17 + 0.425 \left(\frac{100 \cdot A_k}{L \cdot B}\right), if\ C_m > 0.96; \tag{4.14}$$

$$= 0.17 + (10.625 \cdot C_m - 9.775) \left(\frac{100 \cdot A_k}{L \cdot B}\right), if\ 0.94 < C_m < 0.96$$

$$= 0.17 + 0.2125 \left(\frac{100 \cdot A_k}{L \cdot B}\right), if\ C_m < 0.94$$

and $\left(\frac{100 \cdot A_k}{L \cdot B}\right)$ should not exceed 4;

The value of GM and GM variation ΔGM is calculated using the simplified procedure as

$$\Delta GM = \frac{I_H - I_L}{2 \cdot \nabla}, only\ if\ \frac{\nabla_D - \nabla}{A_w (D-d)} \geq 1.0 \tag{4.15}$$

As an alternative approach, following the direct procedure shown in Fig.(4.6), the above value of metacentric height variation ΔGM can be calculated as one half the difference between the maximum and minimum value, $\Delta GM = \frac{GM_{MAX} - GM_{MIN}}{2}$, while considering the vessel balanced in sinkage and trim on a series of waves with a length equal to the ship length (λ=L) and a steepness coefficient S_W = 0.0167.

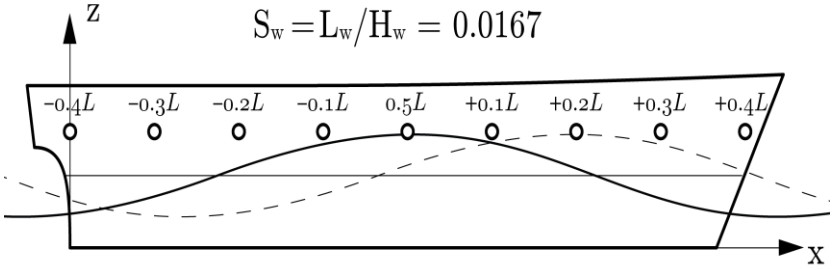

Figure 4.6: Direct procedure at parametric roll[11]

According to the simplified procedure, the moments of inertia of the waterplane area (I_H, I_L) are calculated for the drafts d_H, d_L respectively. Where:

$$d_H = d + \delta d_H\ , where\ \ \delta d_H = \min(D - d, L \cdot s_W/2) \tag{4.16}$$

$$d_L = d - \delta d_L\ , where\ \ \delta d_L = \min(d - 0.25 \cdot d_{full}, L \cdot s_W/2) \tag{4.17}$$

4.2.4. Level 2 Vulnerability criterion for Parametric Rolling

The second level consists of two different checks. The first one Level 2A checks the vulnerability based on parametric rolling, while the second one Level 2B, the magnitude of roll angle during parametric rolling as proposed in [1].

Level 2A Vulnerability Criterion

The first check judges stability variation in a series of waves. The ship is considered not to be vulnerable to parametric rolling if:

$$C1 = \sum_{i=1}^{16} W_i \cdot C_i \leq 0.06 \tag{4.18}$$

The C1 index is calculated as the weighted average of a series of waves where:

C_i = 0 if the requirements of either the variation of GM in waves eq.(4.19) or the vessel speed in waves eq.(4.20) are satisfied;

=1 if not satisfied,

W_i = the weighting factor for the respective wave cases as specified by the wave scatter diagram

The ship is considered to be balanced in sinkage and trim in a series of sinusoidal waves. The requirements of the variation of GM in waves are satisfied when the loading condition assessed agrees with the following equations:

$$GM(H_i, \lambda_i) > 0 \ \ and \ \frac{\Delta GM(H_i, \lambda_i)}{GM(H_i, \lambda_i)} < R_{PR} \tag{4.19}$$

Where:

$GM(H_i, \lambda_i)$ = The average value of GM calculated for a series of a wave characterized by wave height H_i and wave length λ_i (m)

$\Delta GM(H_i, \lambda_i)$ = The amplitude of GM variations, calculated as half the difference between the maximum and the minimum values of GM calculated. (m)

The second requirement consists of ship speed in waves, which is satisfied if the following equation is accepted:

$$V_{PR_i} = \left| \frac{2 \cdot \lambda_i}{T_r} \cdot \sqrt{\frac{GM(H_i, \lambda_i)}{GM}} - \sqrt{g \cdot \frac{\lambda_i}{2\pi}} \right| > V_S \tag{4.20}$$

Where:

$V_S =$ service speed of the vessel (m/s),

$V_{PR_i} =$ reference ship speed corresponding to parametric resonance (m/s)

$T_r =$ roll natural period in calm water (s)

$g =$ gravitational acceleration (m/s ^{2})

The 16 wave cases are obtained from the wave scatter diagram provided by IACS Recommendation No.34 as defined in the Explanatory notes.

Level 2B Vulnerability Criterion

Level 2B consists of the evaluation of roll motion in both head and following waves for a selection of operating speeds by using one degree of freedom time-domain simulations to calculate the rolling amplitude of steady-state parametric roll. It requires the calculation of maximum parametric roll amplitudes for 10 wave cases, where each wave length is equal to ship length (λ= L_{WL}) and wave height of h=0.01·j·L, j=1,2,…,10.

Calculations were made for three different wave directions, where the relative wave heading is β (0^0,30^0,60^0). Vulnerability index C2 is calculated as an average of values C2(Fn_i,β_i), each one is a weighted average for the series of waves for a specific Froude numbed and wave direction.

$$C2 = \left[\sum_{i=1}^{N} C2(Fn_i, \beta_h) + \frac{1}{2}\cdot\{C2(0, \beta_h) + C2(0, \beta_f)\} + \sum_{i=1}^{N} C2(Fn_i, \beta_f)\right]/25 \qquad (4.21)$$

Where,

$C2(Fn_i, \beta_h)$= vulnerability index when the ship is in head waves with a speed equal to V_i

$C2(Fn_i, \beta_f)$= vulnerability index when the ship is in following waves with a speed equal to V_i

$Fn_i = V_i/\sqrt{L \cdot g}$ = Froude number corresponding to speed V_i

$V_i = V_s \cdot K_i$= the speed for each encounter (m/s)

Where K_i is given by the table:

Table 5.10: Values for K_k

k	K_k	Corresponds to encounter with:
1	1.0	Head or following waves at V_s
2	0.866	Waves with 30º relative bearing to ship centerline at V_s
3	0.50	Waves with 60º relative bearing to ship centerline at V_s

N=3 since three different wave directions are used and *h, f* refers to head and following waves, respectively. For each condition, the C2 index is calculated as:

$$C2(Fn,\beta) = \sum_{i=1}^{N} W_i \cdot C_i \tag{4.22}$$

Where:

N = Total number of wave cases

W_i =is the weight factor for the respective wave cases,

C_i = 1 if the maximum parametric roll amplitude is larger than 25 degrees

= 0 otherwise

When the rolling amplitude is larger than 25° the criterion is violated. A check needs to be done for every wave case. Thus, ships are not considered to be vulnerable when:

$$C2 \leq R_{PR1} = 0.025 \tag{4.23}$$

The method used for the calculation of parametric roll amplitude is by numerically solving the one-degree-of freedom parametric roll differential equation (eq.4.26) as a time-domain simulation.
The 1-DOF which was used:

$$\ddot{\varphi} + 2 \cdot \alpha \cdot \dot{\varphi} + \gamma \cdot \dot{\varphi}^3 + {\omega_\varphi}^2 \cdot f(\varphi, t) = 0 \tag{4.24}$$

where ***α*** and ***γ*** represent the linear and cubic roll damping coefficients, $\boldsymbol{\omega_\varphi}$ the natural roll frequency, and ***f*** is the non-linear restoring force in the wave.

$$f(\varphi,t) = \varphi + I_3 \cdot \varphi^3 + I_5 \cdot \varphi^5 + \frac{1}{GM} \cdot \left(GM_{mean} + GM_{amp} \cdot \cos(\omega_e \cdot t) \cdot \left(1 - \left(\frac{\varphi}{\pi}\right)^2\right)\right) \cdot \varphi \tag{4.25}$$

Where $\boldsymbol{I_3}$ and $\boldsymbol{I_5}$ are the polynomial coefficients interpolating the GZ curve in calm water.

Finally, parametric resonance according to level 2B requirements is assessed by the following equation:

$$\ddot{\varphi} + 2 \cdot \alpha \cdot \dot{\varphi} + \gamma \cdot \dot{\varphi}^3 + {\omega_\varphi}^2 \cdot I_3 \cdot \varphi^3 + {\omega_\varphi}^2 \cdot I_5 \cdot \varphi^5 + {\omega_\varphi}^2 \cdot \frac{\varphi}{GM} \cdot \left(GM_{mean} + GM_{amp} \cdot \cos(\omega_e \cdot t) \cdot \left(1 - \left(\frac{\varphi}{\pi}\right)^2\right)\right) = 0 \tag{4.26}$$

To calculate the adequate variables I_3, I_5, an approximation of GZ curve in calm water is attempted by fitting a 5th order polynomial. In this step, it is imperative to find the correct heel angle where the polynomial has the most suitable fit to the GZ curve points, as shown in the figure below. Furthermore, it should also be noted that the first-order coefficient of the GZ equation represents the GMc and should be taken into account for calculating the roll angle. This follows from the fact that the first derivative's fixed term is the GMc. Thus, the righting lever is modeled as:

$$GZ = I_5 \cdot \varphi^5 + I_3 \cdot \varphi^3 + \varphi \tag{4.27}$$

The next step consists of the calculation of α,γ linear, and cubic roll damping coefficients, respectively. Following the procedure of Appendix 2 [2] of parametric rolling explanatory notes, the simplified Ikeda's prediction method will be used since it is the most adopted and studied one to calculate roll damping coefficient B_{44}. Finally, the roll damping is divided into five different components as mentioned in the equation below:

$$B_{44} = B_F + B_E + B_L + B_W + B_{BK} \tag{4.28}$$

The frictional (B_F), the wave (B_W), the eddy (B_E), and the bilge keel (B_{BK}) damping coefficients at zero forward speed and lift component (B_L) at forward speed. This prediction formula is based on systematic series of ships derived from the Taylor Standard Series. So, the formula requires basic design parameters, such as the main particulars and bilge keel dimensions.

For the calculation of skin friction damping (B_F), a different approach was executed. Educationally, when the ship rolls, the damping is caused by the viscous skin friction stress that acts on the hull surface. The skin friction value is obviously affected by the waves and the existence of a bilge keel. The frictional damping in a laminar flow field regarding linear damping coefficient was introduced by Kato [36]. In this thesis, the below process will be applied as proposed in Falzarano et.al[38] & Chakrabarti [37] to obtain the coefficient as shown in eq.(4.34).

$$B_{f0} = \frac{4}{3\pi}\rho S r_e^3 R_0 \omega C_f \tag{4.29}$$

$$C_f = 1.328\left[\frac{2\pi\nu}{3.22 r_e^2 R_0^2 \omega}\right]^{\frac{1}{2}} \tag{4.30}$$

$$r_e = \frac{1}{\pi}\left[(0.887 + 0{,}145 C_B)\frac{S}{L} - 2OG\right] \tag{4.31}$$

$$S = L(1.7D + C_B B) \tag{4.32}$$

where

S = wetter surface area
r_e = the effective bilge radius
R_0 = the roll amplitude
v = the kinematic viscocity

Though the full-scale ship experiences turbulent flow in order to adjust to it, the eq.(4.28) will be used as proposed.

$$B_{f0} = 0.787\rho S r_e^2 \sqrt{\omega\nu}\left\{1 + 0.00814\left(\frac{r_e^2 R_0^2 \omega}{\nu}\right)^{0.386}\right\} \tag{4.33}$$

Finally, in the case of a vessel moving with a forward speed ***U,*** the Schmitke[39] modification will be used to compute the frictional damping according to eq.(4.33).

$$B_f = B_{f0}\left(1 + 4.1\frac{U}{\omega L}\right) \tag{4.34}$$

B_{44} coefficient is calculated for roll amplitudes of 1 and 20 degrees, and these results are used for determining α,γ according to the procedure that follows:

$$a = \frac{B_{44,1}}{2\cdot(I_{xx}+J_{xx})}\frac{\pi}{\omega_\varphi} \qquad \alpha_e = \frac{B_{44,20}}{2\cdot(I_{xx}+J_{xx})}\frac{\pi}{\omega_\varphi} \tag{4.35}$$

$$where\ \ I_{xx} = \rho\cdot V\cdot(0.4\cdot B)^2\ and\ \ J_{xx} = 0.25\cdot I_{xx}$$

It should also be mentioned that the Ikeda's simplified formula normalization for B_{44} is given accordingly to:

$$\hat{B}_{44} = \frac{B_{44}}{\rho\nabla B^2}\sqrt{\frac{B}{2g}} \tag{4.36}$$

Finally:
The equation that gives the linear coefficient:

$$a = \frac{\omega_\varphi}{\pi} \cdot \alpha \tag{4.37}$$

And the cubic coefficient:

$$\gamma = \frac{4c}{3\pi^2}\left(\frac{2\pi}{\omega_\varphi}\right) \tag{4.38}$$

$$where\ c = \frac{\alpha - \alpha_e}{{\varphi_m}^2}\ (\varphi_m = 25\ deg = 0.436\ rad)$$

Since all the sufficient components for the solution of the eq.(4.26) have been presented, the follow-up incorporates the calculation of the representative wave height Hri. The formula used for the computation, assuming a Bretschneider sea spectrum as proposed in [2], is given below:

$$H_{ri} = 4.0043\sqrt{m_0} \tag{4.39}$$

$$m_0 = \int_{0.01\omega_L}^{3\omega_L} \left\{ \frac{\frac{\omega^2 L}{g} sin\left(\frac{\omega^2 L}{2g}\right)}{\pi^2 - \left(\frac{\omega^2 L}{2g}\right)^2} \right\}^2 A\omega^5 \exp(-B\omega^{-4})\, d\omega \tag{4.40}$$

$$A = 173\ H_s^2 T_{01}^{-4} \tag{4.41}$$

$$B = 691 T_{01}^{-4} \tag{4.42}$$

$$T_{01} = 1.086 \cdot T_z \tag{4.43}$$

$$\omega_L = \sqrt{\frac{2g\pi}{L}} \tag{4.44}$$

For each wave of the scattering diagram no.34 for North Atlantic (the number of occurrences divided by 100,000) characterized by a zero-crossing mean period Tz and a significant wave height Hs, a representative wave height Hri according to the equations above will be computed. Then, for these heights, the roll angle will be determined by linear interpolation with the already calculated ones for the cases mentioned before. The aftermath is a 17x16 matrix for every case, containing the max roll angles for each sea state (Hs, Tz). This method is used because a large number of wave cases (since many are not zero-weighted) is ordered to compute the weighting factor Wi faster. Ci is also calculated as the criteria oppose if the roll angle exceeds 25 degrees or not.

Table 4.5: Wave scatter diagram from IACS Recommendation No.34 of the North Atlantic

	T_z (s) = average zero up-crossing wave period															
H_s (m)	3.5	4.5	5.5	6.5	7.5	8.5	9.5	10.5	11.5	12.5	13.5	14.5	15.5	16.5	17.5	18.5
0.5	1.3	133.7	865.6	1186.0	634.2	186.3	36.9	5.6	0.7	0.1	0.0	0.0	0.0	0.0	0.0	0.0
1.5	0.0	29.3	986.0	4976.0	7738.0	5569.7	2375.7	703.5	160.7	30.5	5.1	0.8	0.1	0.0	0.0	0.0
2.5	0.0	2.2	197.5	2158.8	6230.0	7449.5	4860.4	2066.0	644.5	160.2	33.7	6.3	1.1	0.2	0.0	0.0
3.5	0.0	0.2	34.9	695.5	3226.5	5675.0	5099.1	2838.0	1114.1	337.7	84.3	18.2	3.5	0.6	0.1	0.0
4.5	0.0	0.0	6.0	196.1	1354.3	3288.5	3857.5	2685.5	1275.2	455.1	130.9	31.9	6.9	1.3	0.2	0.0
5.5	0.0	0.0	1.0	51.0	498.4	1602.9	2372.7	2008.3	1126.0	463.6	150.9	41.0	9.7	2.1	0.4	0.1
6.5	0.0	0.0	0.2	12.6	167.0	690.3	1257.9	1268.6	825.9	386.8	140.8	42.2	10.9	2.5	0.5	0.1
7.5	0.0	0.0	0.0	3.0	52.1	270.1	594.4	703.2	524.9	276.7	111.7	36.7	10.2	2.5	0.6	0.1
8.5	0.0	0.0	0.0	0.7	15.4	97.9	255.9	350.6	296.9	174.6	77.6	27.7	8.4	2.2	0.5	0.1
9.5	0.0	0.0	0.0	0.2	4.3	33.2	101.9	159.9	152.2	99.2	48.3	18.7	6.1	1.7	0.4	0.1
10.5	0.0	0.0	0.0	0.0	1.2	10.7	37.9	67.5	71.7	51.5	27.3	11.4	4.0	1.2	0.3	0.1
11.5	0.0	0.0	0.0	0.0	0.3	3.3	13.3	26.6	31.4	24.7	14.2	6.4	2.4	0.7	0.2	0.1
12.5	0.0	0.0	0.0	0.0	0.1	1.0	4.4	9.9	12.8	11.0	6.8	3.3	1.3	0.4	0.1	0.0
13.5	0.0	0.0	0.0	0.0	0.0	0.3	1.4	3.5	5.0	4.6	3.1	1.6	0.7	0.2	0.1	0.0
14.5	0.0	0.0	0.0	0.0	0.0	0.1	0.4	1.2	1.8	1.8	1.3	0.7	0.3	0.1	0.0	0.0
15.5	0.0	0.0	0.0	0.0	0.0	0.0	0.1	0.4	0.6	0.7	0.5	0.3	0.1	0.1	0.0	0.0
16.5	0.0	0.0	0.0	0.0	0.0	0.0	0.0	0.1	0.2	0.2	0.2	0.1	0.1	0.0	0.0	0.0

4.3. Excessive Acceleration Regulations

4.3.1. Introduction

The excessive acceleration criterion was introduced later than the other four criteria as a product of several incidents that included casualties because of stability failures in adverse weather. Precisely, as presented in Chapter 3, Chicago Express [13] and CCNI Guayas [17] involved crew injuries, since, as reported, lateral accelerations reached higher values than 1.0 g on the bridge deck. Based on [3], during vessel's rolling since the roll period is the same for every location, in higher locations in order to cover longer distances a larger linear velocity is developed. This larger velocity leads to larger linear acceleration, since every half roll period the roll motion changes direction. This larger linear acceleration means larger inertial force. This inertial force when acts on the horizontal plane can become too dangerous as crew can lose balance and get injured.

Moreover, accidents reports showed that lateral accelerations are highly related to the loading condition. In fact, a high value of metacentric height GM concludes to a small roll period, thus, accelerations are larger because for the same roll amplitude the linear velocity changes with a faster rate. This lead to the conclusion that ballast conditions are the most severe, since GM value is high and the roll period small and also when the ship travels at a low speed the roll damping is low. This sudden ship roll enhances the chance to crew injuries and cargo damage.

4.3.2. Physical Background

The following analysis is based on [29]. Assuming that the ship is under the effect of a harmonic roll with roll amplitude $\boldsymbol{\varphi_\alpha}$ and natural roll frequency $\boldsymbol{\omega}$, the roll angle and the roll acceleration are expressed as:

$$\varphi = \varphi_\alpha \cdot \sin \omega t \tag{4.45}$$

$$\ddot{\varphi} = -\varphi_\alpha \cdot \omega^2 \sin \omega t \tag{4.46}$$

The projections of relative acceleration on the y- and z-axes are given by the equations(4.47)&(4.48) :

$$a_y = (g + a_v) \cdot \sin \varphi + h \cdot \omega^2 \varphi \tag{4.47}$$

$$\alpha_z = (g + a_v) \cdot \cos \varphi - y \cdot \omega^2 \varphi \tag{4.48}$$

Where:

$h=z-z_R$ and y are the respective distances from the axes. The maximum value for the ratio α_y / α_z occurs when $\phi=\phi_\alpha$ and the equations (4.47),(4.48) take the below formation:

$$a_y = (g + a_v) \cdot \sin \varphi_a + h \cdot \omega^2 \varphi_a \tag{4.49}$$

$$\alpha_z = (g + a_v) \cdot \cos \varphi_a - y \cdot \omega^2 \varphi_a \tag{4.50}$$

As proposed in [3],the roll equation is given as:

$$I_\varphi \ddot{\varphi} + b_\varphi \dot{\varphi} + c_\varphi \varphi = M_{FK} \tag{4.51}$$

Where:
I_ϕ : roll moment of inertia
b_ϕ: roll damping coefficient
c_ϕ : restoring force coefficient($c_\varphi = mgGM$)
ω_e : encounter frequency
M_{FK} : Froude-Krylov exciting moment

The roll angle can be described as:

$$\varphi = \varphi_\alpha \cdot e^{i\omega_e t} \tag{4.52}$$

Neglecting the diffraction effect the amplitude of the exciting moment can be written as:

$$M_{FK} = (a + bi) \cdot e^{i\omega_e t} \tag{4.53}$$

Where:

a,b: the real and imaginary parts of the exciting roll moment calculated using Froude-Krylov assumption as:

$$a = \rho g \iint_{S_H} e^{k_0 z} \cos(k_0 y) \cdot n_4 dS \tag{4.54}$$

$$b = -\rho g \iint_{S_H} e^{k_0 z} \sin(k_0 y) \cdot n_4 dS \tag{4.55}$$

but for laterally symmetric hulls, the previous equations (4.54)&(4.55) can be calculated as:

$$a = 0 \tag{4.56}$$

$$b = \Delta \cdot GM_c \cdot r \cdot (\frac{\omega^2}{g}) \tag{4.57}$$

Where:
k_0 : is the wave number ($k_0 = {\omega_{wave}}^2 / g$)
x,y,z : the coordinates of mean wetted hull surface
s_H : the mean wetted hull surface
n_4 : the normal vector of roll
r: effective wave slope
Investigating accident data showed that at the time of the accident ships operated at very low speeds, so the effect of forward speed could be neglected on the encounter frequency

and roll damping. So if the assumptions are used then by changing $\omega_e=\omega_\phi$ and Fn=0, eq.(4.51), by substituting eq.(4.52) & (4.53) equals to:

$$I_\varphi(-\omega^2\varphi_\alpha)\cdot e^{i\omega_e t}+b_\varphi(i\omega\cdot\varphi_\alpha)\cdot e^{i\omega_e t}+c_\varphi\varphi_\alpha\cdot e^{i\omega_e t}=(a+bi)\cdot e^{i\omega_e t} \tag{4.58}$$

The solution of eq.(4.58) for the roll amplitude ϕ_α is :

$$\varphi_\alpha=\frac{a+ib}{\left(c_\varphi-I_\varphi\cdot\omega^2\right)+(ib_\varphi\cdot\omega)} \tag{4.59}$$

The eq.(4.47) assuming that the lateral acceleration due to yaw is not accounted and so the factor $\alpha_v=0$ and $\sin\phi_\alpha=\phi_\alpha$ becomes:

$$a_y=\varphi_\alpha\cdot(g+h\cdot\omega^2) \tag{4.60}$$

Finally, the root-mean-square value of lateral acceleration is calculated as:

$$\sigma=\sqrt{m_0} \tag{4.61}$$

where:

$$m_0=\int_0^\infty\int_0^{2\pi}\left|a_y(\omega)\right|^2 D\left(\beta-\frac{\pi}{2}\right)S_{zz}(\omega)d\omega d\beta \tag{4.62}$$

$D\left(\beta-\frac{\pi}{2}\right)$: is the non-dimensional seaway energy spreading function

$S_{zz}(\omega)$: is the frequency spectrum of the seaway

The seaway energy spreading function is calculated as:

$$D\left(\beta-\frac{\pi}{2}\right)=\begin{cases}\frac{2}{\pi}\cdot\cos^2(\beta-\pi/2)\,,if\left|\beta-\frac{\pi}{2}\right|<\pi/2\\0\,,otherwise\end{cases} \tag{4.63}$$

Using the eq.(4.61) & (4.62) the variance of roll is:

$$\sigma^2=\int_0^\infty\int_0^{2\pi}\left|a_y(\omega)\right|^2 D\left(\beta-\frac{\pi}{2}\right)S_{zz}(\omega)d\omega d\beta$$

The variance of roll σ_ϕ^2 will be used for the ship's vulnerability to excessive acceleration criteria as will be explained below to the regulations.

4.3.3. Level 1 Vulnerability criterion for Excessive Acceleration

The criterion for excessive accelerations can be applied only if the examined loading condition meets the below standards:

- The distance from the waterline to the highest location along the length of the ship where passengers or crew may be present exceeds 70% of the breadth of the ship
- The metacentric height exceeds 8% of the breadth of the ship

If the loading condition under examination passes the above thresholds then the vulnerability is checked by Level 1 as proposed in [3].

A ship is not considered to be vulnerable to the excessive acceleration criterion if the equation(4.64) is satisfied.

$$\varphi \cdot k_L \cdot \left(g + \frac{4\pi^2 h}{T_r^2}\right) < R_{EA1} \tag{4.64}$$

Where:

R_{EA1} = 4.64 [m/s^2]

ϕ = characteristic roll amplitude [rad]

k_L= coupling factor of the action of roll,pitch and yaw motions

h= height of the assessed point above the roll axis [m]

T_r =natural roll period [s]

The adequate equations (4.65) &(4.66) for the calculation of level 1 are presented:

$$k_L = \begin{cases} 1.125 - 0.625 \cdot \dfrac{x}{L}, if\ x < 0.2 \cdot L \\ 1.0 \quad , if\ 0.2 \cdot L < x < 0.65 \cdot L \\ 0.527 + 0.727 \cdot \dfrac{x}{L}, if\ x > 0.65 \cdot L \end{cases} \tag{4.65}$$

$$\varphi = 4.43 \cdot r \cdot s / \delta_{\varphi}^{0.5} \quad [rad] \tag{4.66}$$

Where:

r= effective wave slope coefficient

s= non-dimensional wave steepness

δ_ϕ= non-dimensional logarithmic decrement of roll decay

Non-dimensional wave steepness ***s*** is calculated from Figure(4.2) for the loading condition's roll period.

The non-dimensional logarithmic decrement of roll decay is calculated as:

$$\delta_{\varphi} = 0.5\pi \cdot R_{PR} \tag{4.67}$$

Where R_{PR} is calculated as eq.(4.14).

Finally, the effective wave slope coefficient is evaluated as:

$$r = \frac{K_1 + K_2 + OG \cdot F}{\frac{B^2}{12 \cdot C_B \cdot d} - \frac{C_B \cdot d}{2} - OG} \tag{4.68}$$

Where:

$$K_1 = g \cdot \beta \cdot T_r^2 \cdot \frac{\left(\tau + \tau \cdot \tilde{T} - \frac{1}{\tilde{T}}\right)}{4\pi^2} \tag{4.69}$$

$$K_2 = g \cdot \tau \cdot T_r^2 \cdot \frac{(\beta - cos\tilde{B})}{4\pi^2} \tag{4.70}$$

$$F = \beta \cdot \left(\tau - \frac{1}{\tilde{T}}\right) \tag{4.71}$$

$$OG = KG - d \text{ [m]} \tag{4.72}$$

$$\tilde{B} = \frac{2\pi^2 B}{g \cdot T_r^2} \tag{4.73}$$

$$\tilde{T} = \frac{4\pi^2 \cdot C_B \cdot d}{g \cdot T_r^2} \tag{4.74}$$

$$\beta = \frac{\sin\left(\tilde{B}\right)}{\tilde{B}} \tag{4.75}$$

$$\tau = \frac{\exp\left(-\tilde{T}\right)}{\tilde{T}} \tag{4.76}$$

4.3.4. Level 2 Vulnerability criterion for Excessive Acceleration

For the Level 2 a ship will not be considered as vulnerable to excessive acceleration stability failure if the equation(4.77) is satisfied:

$$C < R_{EA2} \tag{4.77}$$

Where:

R_{EA2} =0.00039

C = a long-term probability index calculated as eq.(4.78)

$$C = \sum_{i=1}^{N} W_i C_i \tag{4.78}$$

Where:

C_i = the short-term index evaluated as proposed in eq.(4.79)

W_i = the weighting factor for the respective wave cases as specified by the wave scatter diagram

N = Total number of wave cases

The short-term excessive acceleration failure index, C_i is a measure of the probability that the ship will exceed a specified lateral acceleration, evaluated as:

$$C_i = \exp[-R_2^2 \,/\, (2 \cdot \sigma_{LAi}^2)] \tag{4.79}$$

Where:

R_2 = 9.81 m/s^2

σ_{LAi} = standard deviation of the lateral acceleration

The standard deviation of the lateral acceleration is calculated according to the following formula or the equivalent one:

$$\sigma_{LAi}^2 = \frac{3}{4}\sum_{j=1}^{N}\left(a_y(\omega_j)\right)^2 Szz(\omega_j)\Delta\omega \;\; or \;\; \sigma_{LAi}^2 = \frac{3}{4}\int_{\omega_1}^{\omega_2}\left(a_y(\omega)\right)^2 Szz(\omega)\, d\omega \tag{4.80}$$

Where:

$\boldsymbol{\alpha_y}$ = lateral acceleration calculated as eq.(4.80) (m/s^2)

$\boldsymbol{k_L}$= as defined in Level 1 eq.(4.65)

$\boldsymbol{h}$= as defined in Level 1 (m)

$\boldsymbol{\varphi_\alpha(\omega_j)}$ = roll amplitude in regular beam waves and circular frequency ω_j as defined in eq.(4.85) (rad/m)

$\boldsymbol{\omega_j}$= wave frequency at midpoint of the interval (rad/s)

$\boldsymbol{\Delta\omega}$ = the interval of wave frequency (rad/s)

$\boldsymbol{\omega_1}$ = the lower limit of the wave frequency spectrum (rad/s)

$\boldsymbol{\omega_2}$ = the upper limit of the wave frequency spectrum (rad/s)

$\boldsymbol{N}$ = the number of intervals in the frequency spectrum, should be not taken under 100

$\boldsymbol{S_{zz}}$ = wave frequency spectrum (m^{2}s/rad)

The above factors are calculated according to the equations below:

$$a_y = k_L \cdot \left(g + h \cdot \omega_j^2\right) \cdot \varphi_\alpha(\omega_j)[m/s^2] \tag{4.81}$$

$$\Delta\omega = \frac{\omega_2 - \omega_1}{N}\ (rad/s) \tag{4.82}$$

$$\omega_1 = \max((0.5/T),0.2)\ \ (rad/s) \tag{4.83}$$

$$\omega_2 = \min((25/T),2.0)\ \ (rad/s) \tag{4.84}$$

$$\omega_j = \omega_1 + ((2j-1)/2) \cdot \Delta\omega\ (rad/s) \tag{4.85}$$

$$\varphi_\alpha(\omega_j) = \left(\varphi_r(\omega_j)^2 + \varphi_i(\omega_j)^2\right)^{0.5}(rad/m) \tag{4.86}$$

The response of roll amplitude is divided in the two components. The real one ϕ_r and the imaginary one ϕ_i, which are calculated according to the equations (4.87)&(4.88):

$$\varphi_r(\omega_j) = \frac{\alpha \cdot \left(mgGM - I_{xx}\omega_j^2\right) + bB_e\omega_j}{\left(mgGM - I_{xx}\omega_j^2\right)^2 + (B_e\omega_j)^2}\ (rad) \tag{4.87}$$

$$\varphi_i(\omega_j) = \frac{b \cdot \left(mgGM - I_{xx}\omega_j^2\right) + aB_e\omega_j}{\left(mgGM - I_{xx}\omega_j^2\right)^2 + (B_e\omega_j)^2}\ (rad) \tag{4.88}$$

Where:

α,b = the cosine and sine components of the Froude-Krylov roll moment (N·m)

m= ship displacement (t)

I_{xx} = roll moment of inertia calculated as:

$$I_{xx} = mgGMT^2/(4\pi^2)\ \ (t \cdot m^2) \tag{4.89}$$

B_e = the equivalent linear roll damping factor calculated as:

$$B_e = 2 \cdot I_{xx} \cdot \mu_e\ (kN \cdot m \cdot s) \tag{4.90}$$

μ_e = equivalent linear roll damping (1/s)

The equivalent linear roll damping coefficient needs to be calculated during this process according to the following method. If there is no sufficient test data, applying the simplified Ikeda's method is acceptable as it consists of the standard methodology suggested in the regulations. Firstly, the equivalent roll damping coefficient is calculated through Ikeda as a function of roll amplitude and then a least square fitting is used to compute the roll damping coefficient as presented below.

$$\frac{B_{44}(\varphi_\alpha) \cdot \omega_\varphi^2}{2W \cdot GM} \Rightarrow \mu + \frac{4}{3\pi} \cdot \beta \cdot \omega_\varphi \cdot \varphi_\alpha + \frac{3}{8} \cdot \delta \cdot \omega_\varphi^2 \cdot \varphi_\alpha^2 \tag{4.91}$$

Where:

$\boldsymbol{\omega_\varphi}$: natural roll frequency (rad/s)

$\boldsymbol{W}$: displacement force (N)

$\boldsymbol{B_{44}}$: equivalent linear damping coefficient as calculated with Ikeda's method

$\boldsymbol{\mu,\beta,\delta}$: linear, quadratic and cubic roll damping coefficients respectively

Finally, the equivalent roll damping coefficient for the calculation of the roll response was defined following the method proposed in [3]. Specifically, for the equivalent linear roll damping in irregular waves, an equivalent stochastic linearization method can be used. The roll amplitude is given by the equation (4.92)

$$\varphi_\alpha = 0.3 T_r \sigma_{\dot{\varphi}} \tag{4.92}$$

where, $\sigma_{\dot{\varphi}}$ is the square root of the variance of roll angular velocity

An iterative procedure will have to be used for each seaway, otherwise the equivalent linear roll damping coefficient can be defined at the 15 degree roll amplitude.

Chapter 5 Application of the criteria

5.1. Introduction

The “Second Generation” intact stability criteria will be included in SOLAS regulation and will therefore become mandatory for all commercial ships. However, certain ship types are known to be particularly vulnerable to specific stability failure modes. In this thesis, one Post-Panamax containership with a capacity of 5248 TEUs that is designed to operate worldwide and another one Feedermax containership of 2,200 TEUs are examined. Due to their slender hull form, these ship types are often vulnerable to stability failures caused by the variation of the righting lever curve in waves.

The vessels’ hulls were designed in Maxsurf Modeler and the hydrostatic calculations were executed with Maxsurf Stability. The loadcases chosen to apply the criteria are the Full Load Departure for parametric roll, Ballast Arrival for excessive acceleration. Vessels’ main particulars are presented in Table (5.1) and the Loading conditions particulars in Table (5.2). Finally, the GZ curves for the wave crest and wave trough for a wave of s_w=1/20 are presented in Figure(5.2).

Figure 5.1: Designed hull of the Post-Panamax vessel

Table 5.1: Post-Panamax main particulars

L_{OA} [m]	277.7	DWT@T_{DESIGN}[tons]	54622
L_{BP} [m]	263.0	C_B	0.586
B_{MLD} [m]	40.2	C_M	0.981
D_{MAIN}[m]	24.3	$V_{SERVICE}$[kn]	24.5
T_{DESIGN}[m]	12.5	A_{BK} [m^2]	40
l_{BK} [m]	79	b_{BK} [m]	0.45

Table 5.2: Basic particulars of the examined loadcases

Loadcase	Full Load Departure	Ballast Arrival
Displacement [tons]	92910.6	41,643.3
Draft [m]	14.0	7.47
GM[m]	0.60	9.95
Trim [m]	-0.25	-4.31
$T_{ROLLING}$[s]	33.8	9.82
KG [m]	18.9	11.82
Windage Area[m^2]	2893.59	4617.81

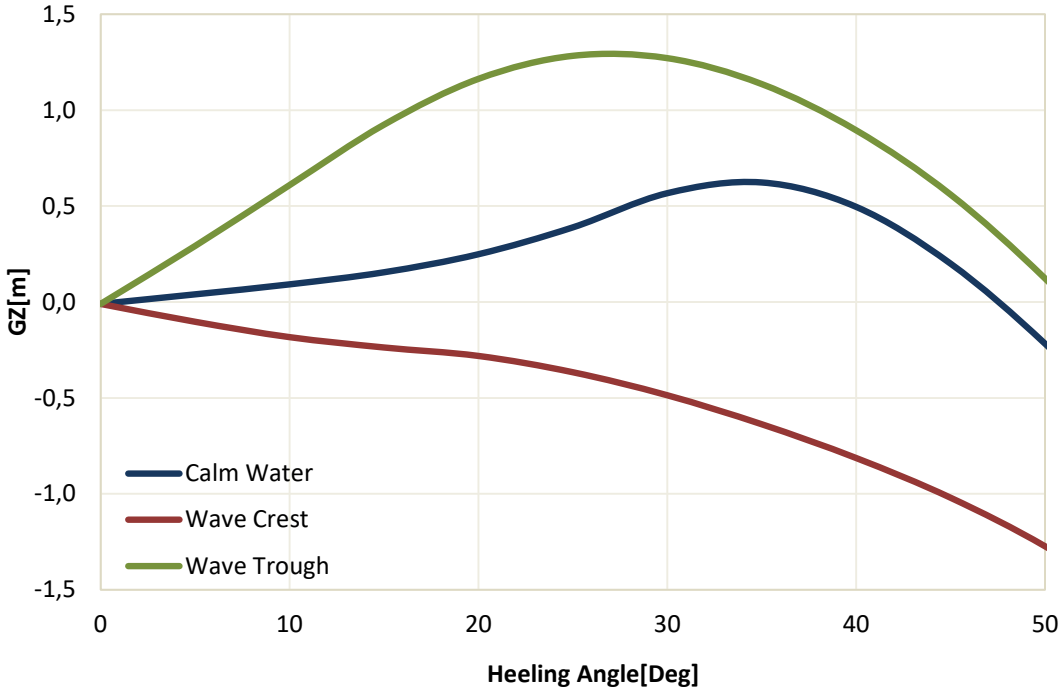

Figure 5.2: Full Load Departure GZ curve variations for wave of $\lambda=L_{WL}$ and Sw=1/20

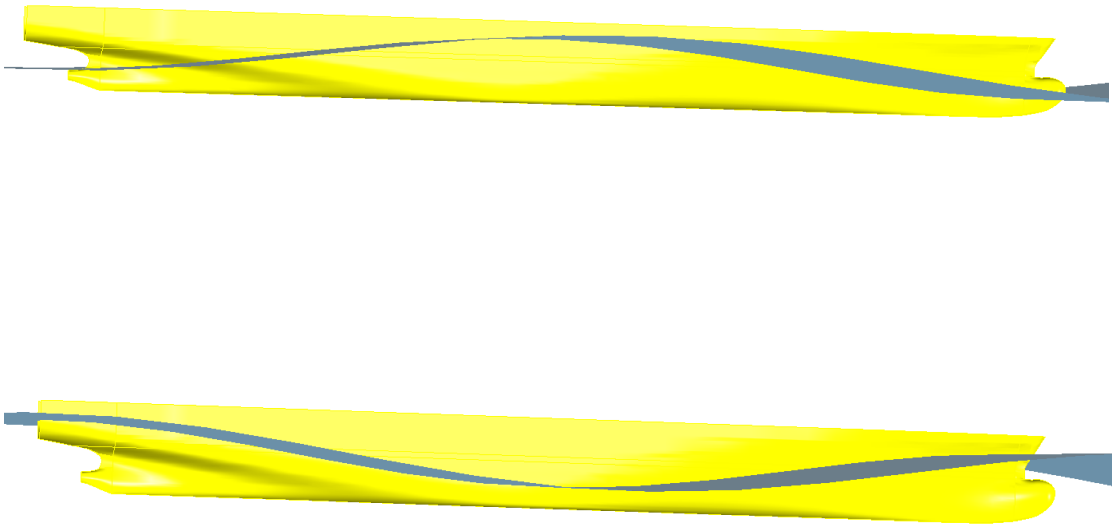

Figure 5.3: Vessel on wave crest and trough for wave of $\lambda=L_{WL}$ and Sw=1/20

Respectively, the main particulars and the loading conditions investigated for the Feedermax are presented in Table (5.3) & (5.4), as well as, the GZ curve variations in Figure(5.5)

Figure 5.4: Designed hull of the Feedermax vessel

Table 5.3: Feedermax main particulars

L_{OA} [m]	195.6	DWT@T_{DESIGN}[tons]	28006
L_{BP} [m]	185.5	C_B	0.655
B_{MLD} [m]	30.2	C_M	0.981
D_{MAIN}[m]	16.6	$V_{SERVICE}$[kn]	21.82
T_{DESIGN}[m]	10.5	A_{BK}[m^2]	30.11
l_{BK}[m]	43.01	b_{BK}[m]	0.35

Table 5.4: Basic particulars of the examined loadcases

Loadcase	Full Load Departure	Ballast Arrival
Displacement [tons]	42184	19526
Draft [m]	11.018	5.974
GM[m]	0.32	7.15
Trim [m]	0.652	-4.21
$T_{ROLLING}$[s]	37.4	9.31
KG[m]	13.8	9.21
Windage Area[m^2]	1417.35	2367.5

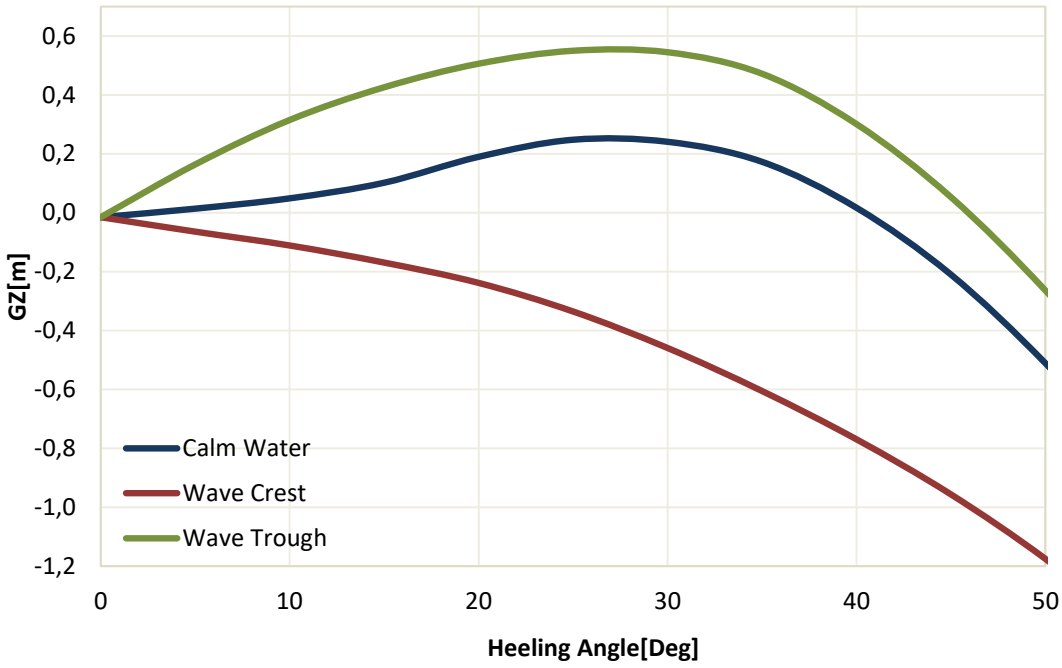

Figure 5.5: Full Load Departure GZ curve variations for wave of $\lambda=L_{WL}$ and Sw=1/20

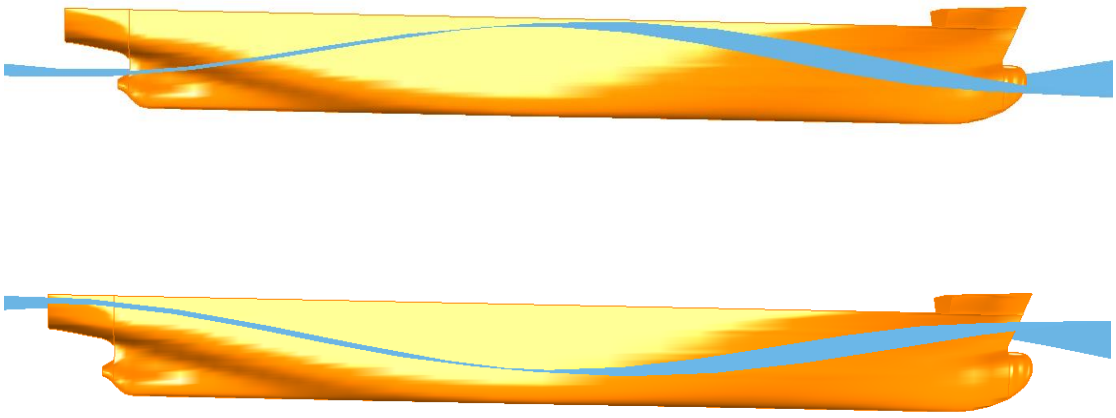

Figure 5.6: Vessel on wave crest and trough for wave of $\lambda=L_{WL}$ and Sw=1/20

5.2. Application of IMO weather Criterion

5.2.1. Application for "5,200 TEUs Post-Panamax"

The application of weather criterion on the designed vessels will be executed with the use of the programming software Maxsurf Stability. The main particulars needed are already in use through the model developed, so through hydrostatic calculations the results are shown below.

First step is to check the area under GZ curve following the methodology presented in Section 4.1. Through Maxsurf Software the calculations are:

2.2.1:

- Area 0 to 30 : E_{30} = 0.1044 ≥ 0.550 [m*rad]
- Area 0 to 40 : E_{40}= 0.1627 ≥ 0.090 [m*rad]
- Area 30 to 40: E_{30-40}=0.0583 ≥ 0.030 [m*rad]

2.2.2:

- Max GZ at 30 or greater : GZ_{30}= 0.626 ≥ 0.20 [m]

2.2.3:

- Maximum GZ angle: GZ_{MAX}=34.1 ≥ 25.0 [deg]

2.2.4:

- Initial GMt = 0.60 ≥ 0.150 [m]

In Figure (5.7) the application of the weather criterion is presented as exported from Maxsurf Stability and edited in Autocad.

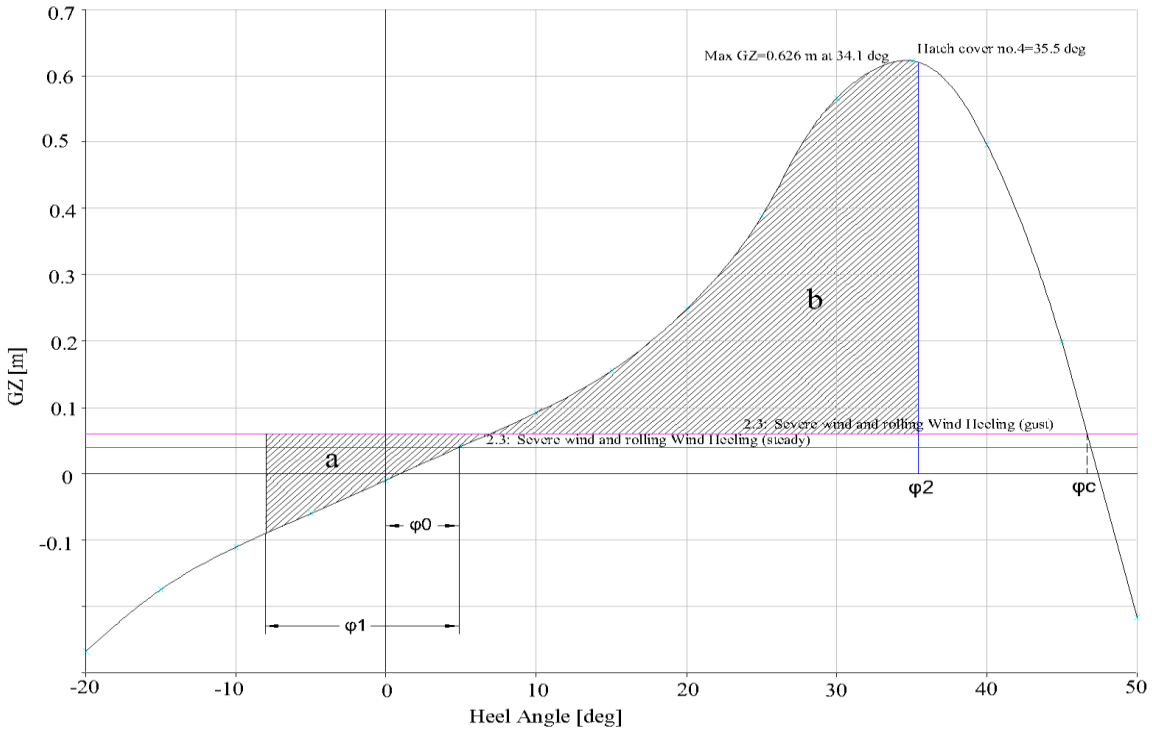

Figure 5.7: GZ curve Post-Panamax loading Condition FLD

2.3:

Table 5.5: Results of the application for Post-Panamax

Post-Panamax		
B/d=2.883 →	X_1 =0.913	φ_1=12.91[deg]
$(100 \cdot A_k)/(L \cdot B)$=0.368 →	X_2 =0.953	I_{w1}=0.03 m
C =0.324	k=0.993	I_{w2}=0.045 m
T_r=33.8 [sec]	r=0.939	a=0.0319 m*rad
OG=4.89 [m]	s=0.020	b=0.1302 m*rad
Since ***a < b***		**PASS**

5.2.2. Application for "2,200 TEUs Feedermax"

2.2.1:

- Area 0 to 30 : E_{30} = 0.063 ≥ 0.550 [m*rad]
- Area 0 to 40 : E_{40}= 0.095 ≥ 0.090 [m*rad]
- Area 30 to 40: $E_{30\text{-}40}$=0.032 ≥ 0.030 [m*rad]

2.2.2:

- Max GZ at 30 or greater : GZ_{30}= 0.241≥ 0.20 [m]

2.2.3:

- Maximum GZ angle: GZ_{MAX}=26.2 ≥ 25.0 [deg]

2.2.4:

- Initial GMt = 0.327 ≥ 0.150 [m]

In Figure (5.7) the application of the weather criterion is presented as exported from Maxsurf Stability and edited in Autocad.

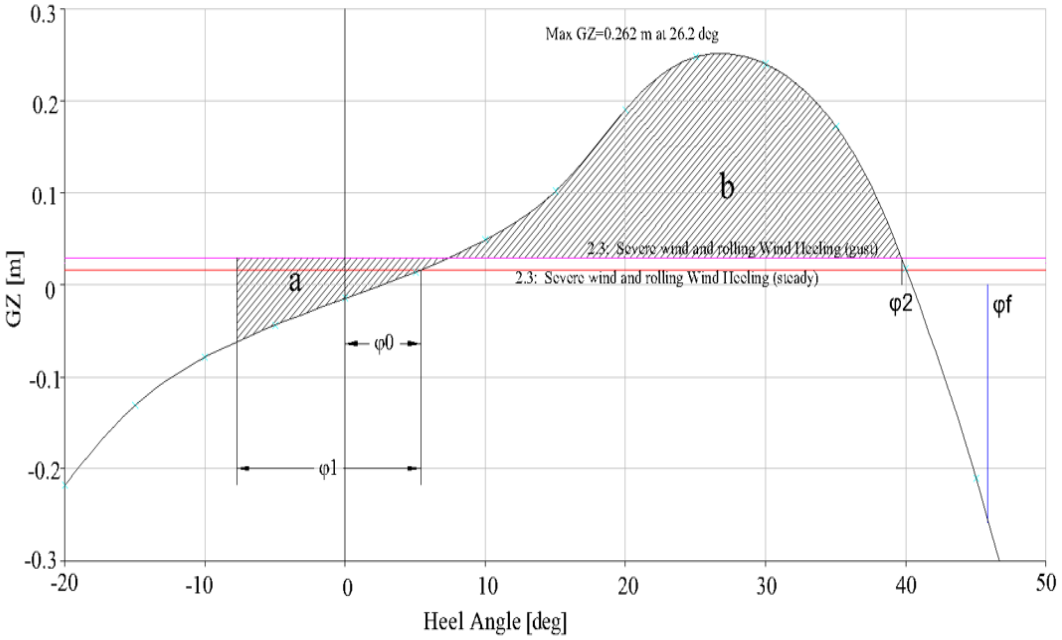

Figure 5.8:GZ curve for Feedermax Case Scantling draft FLD

2.3:

Table 5.6: Results of the application

B/d=2.741 →	X_1 =0.942	φ_1=13.12 [deg]	
$(100 \cdot A_k)/(L \cdot B)$=0.525 →	X_2 =0.972	I_{w1}=0.025 m	
C =0.354	k=0.99	I_{w2}=0.038 m	
T_r=37.44 [sec]	r=0.881	a=0.0183 m*rad	
OG=2.78 [m]	s=0.020	b=0.0760 m*rad	
Since ***a < b***			**PASS**

5.3. Application of Vulnerability criterion for Parametric Rolling

5.3.1. Application of Vulnerability Assessment for "5,200 TEUs Post-Panamax"

5.3.1.1.Level 1 Vulnerability Check

The criterion of parametric roll will be applied on both vessels for the Full Load Departure, following the procedure analyzed in Section 4.2. The Table (5.7) presents all the necessary values needed to apply the first level.

Table 5.7: Particulars for Level 1 Vulnerability Check[2]

L_{WL} [m]	269.1	V_D[m^3]	191300.4
V [m^3]	90644.6	d_H= d + min(D-d,L · s_w/2)[m]	16.25
A_w[m^2]	8969.47	d_L= d + min(D-0.25 · d_{FULL},L ·s_w/2)[m]	0.981
d_{DES}[m]	12.5	I_H[m^4]	1140706.7
d_{FULL} [m]	14.0	I_L[m^4]	905252.9

The ship considered not to be vulnerable if:

$$\frac{\delta GM_1}{GM_C} \leq R_{PR}$$

However, $$\frac{\nabla_D - \nabla}{A_W \cdot (D-d)} = 1.0896 > 1$$

and $$\delta GM_1 = \frac{I_H - I_L}{2 \cdot \nabla} = 1.299$$

$$\delta GM_1 / GM_C = 2.129$$

Using the direct procedure explained in Section 4.2.3 the amplitude of metacentric height variation is:

$$\delta GM = \frac{GM_{MAX} - GM_{MIN}}{2} = 1.081$$

So:

$$\delta GM_1 / GM_C = 1.81$$

Following the next step, the value R_{PR} and the ratio ΔGM/GM will be compared for level 1. Since C_M =0.98>0.96 then:

$$R_{PR} = 0.17 + 0.425 \cdot \left(\frac{100 \cdot A_K}{L \cdot B}\right) = 0.3272$$

After comparison, it is proven that the vessel is vulnerable to parametric roll for the examined loading condition as shown in table below. So a Level 2 check is needed. In Fig.(5.9) is presented the difference in waterplane for the same wave when the wave trough is at midship and the wave crest at midship respectively.

Table 5.8: Post-Panamax, Results for level 1 check for parametric roll

Vessel	Loadcase		ΔGM/GM Simplified	ΔGM/GM Direct	R_{PR}	Status
Post-Panamax	FLD	Full Load Departure	2.129	1.81	0.3272	**FAIL**

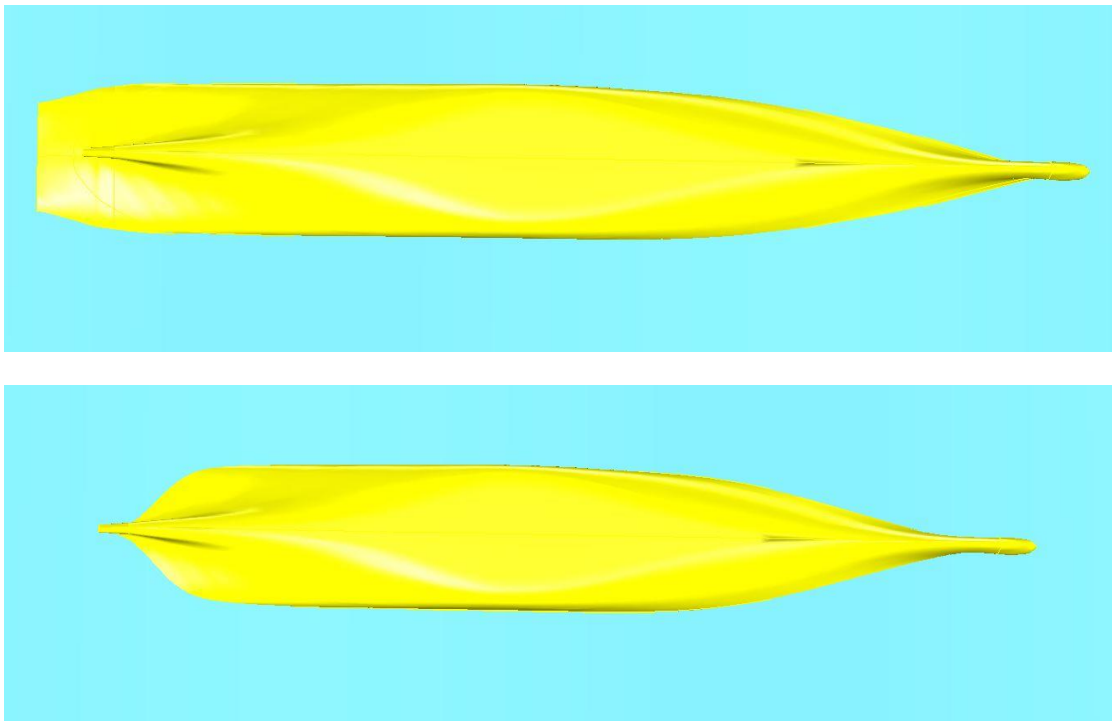

Figure 5.9: Waterplane on wave trough and wave crest for wave of Sw=0.0167

5.3.1.2.Level 2A Vulnerability Check

The value of C1 is calculated as the weighted average from a set of waves. Results of the necessary calculations are presented in the Table (5.9):

Table 5.9: Wave data and results for level 2A check for parametric roll

Case No.	Weight Wi	Wave Length λ_i[m]	Wave Height H_i[m]	ΔGM/GM	R_{PR}	V_s[kn]	V_{PR}[kn]	C_i
1	0.000013	22.574	0.35	0.0244	0.3272	24.5	8.976	0
2	0.001654	37.316	0.495	0.0610	0.3272	24.5	10.615	0
3	0.020912	55.743	0.8575	0.1645	0.3272	24.5	11.88	0
4	0.092799	77.857	1.2945	0.2875	0.3272	24.5	12.733	0
5	0.199218	103.655	1.732	0.6022	0.3272	24.5	13.176	1
6	0.248788	133.139	2.205	0.4106	0.3272	24.5	13.084	1
7	0.208699	166.309	2.6965	0.9765	0.3272	24.5	12.744	1
8	0.128984	203.164	3.1755	1.4434	0.3272	24.5	12.084	1
9	0.062446	243.705	3.625	1.534	0.3272	24.5	10.843	1
10	0.024790	287.931	4.04	1.3101	0.3272	24.5	7.0997	1
11	0.008367	335.843	4.4205	1.4616	0.3272	24.5	7.3423	1
12	0.002473	387.44	4.7695	1.3385	0.3272	24.5	4.8717	1
13	0.000658	442.723	5.097	1.1827	0.3272	24.5	2.1243	1
14	0.000158	501.691	5.3695	1.0514	0.3272	24.5	1.2944	1
15	0.000034	564.345	5.621	0.9318	0.3272	24.5	4.8926	1
16	0.000007	630.84	5.95	0.8069	0.3272	24.5	9.0953	1

The total C_i index for level 2A and the specific condition is:

$$C1 = \sum_{i=1}^{16} W_i \cdot C_i = 0.8846 > 0.06 = R_{PR0}$$

Table 5.10: Results for Level 2A of Parametric Rolling

Vessel	Loadcase		C1	R_{PR0}	Status
Post-Panamax	FLD	Full Load Departure	0.8846	0.006	**FAIL**

The conclusion is that the loading condition is considered vulnerable to parametric roll when the vessel is operating with the service speed of 24.5 knots, so in this case a level 2B check is required.

5.3.1.3.Level 2B Vulnerability Check

Level 2B requires the computation of parametric roll amplitude for seven different wave directions and ten different wave cases. The process followed is explained below.

For each wave case a calculation of the parametric rolling amplitude is executed for different directions to ship heading for both head and following waves. The maximum roll angle is calculated for 7 different cases:

- at zero speed where: $\omega_{enc} = \omega_{wave}\ and\ F_n = 0$
- in three speeds in head seas corresponding to relative wave heading ***β*** of 0^o, 30^o,60^o deg
- in three speeds in following seas corresponding to relative wave heading ***β*** of 120^o,150^o,180^o deg

For the above cases a wave encounter frequency is calculated according to the equation (5.1) with a speed equal to the service one but different heading. Results are listed below in Table (5.11):

$$w_{enc} = \omega_0 - \frac{\omega_0^2}{g} V_S \cdot cos\beta, where \quad \omega_0 = \sqrt{\frac{2\pi \cdot g}{L_{wl}}} \tag{5.1}$$

Table 5.11: Wave cases and their respective encounter frequencies

Wave direction***[deg]***	Encounter frequency ***[rad/s]***
0^o	0.1843
30^o	0.2238
60^o	0.3315
120^o	0.6257
150^o	0.7334
180^o	0.7729
V_S=0	0.4786

In the Table (5.12) that follows, the wave characteristics of Level 2B are listed. The wave height and the values of GM_{mean} and GM_{amp} are calculated as presented below:

$$\mathrm{h} = 0.01 \cdot \mathrm{n} \cdot \mathrm{L}_{wl} \ , \mathrm{n} = 1,2,\ldots,10 \tag{5.2}$$

$$GM_{mean} = \frac{GM_{max} + GM_{min}}{2} \tag{5.3}$$

$$GM_{amp} = \frac{GM_{max} - GM_{min}}{2} \tag{5.4}$$

Then, for the below wave cases (λ_i , H_i) through Maxsurf stability software the columns of GM_{mean} and GM_{amp} are calculated, applying the above equations respectively.

Table 5.12: Wave data and results for level 2B check for parametric roll

Case No.	Wave Length λ_i[m]	Wave Height H_i[m]	GM_{mean}	GM_{amp}
1	269.1	2.691	0.5335	0.6755
2	269.1	5.382	0.5265	1.1595
3	269.1	8.073	0.6075	1.5685
4	269.1	10.764	0.889	1.865
5	269.1	13.455	1.190	2.236
6	269.1	16.146	1.405	2.610
7	269.1	18.837	1.612	3.086
8	269.1	21.528	1.626	3.162
9	269.1	24.219	1.6535	3.2355
10	269.1	26.91	1.394	2.577

Further, a quantic fit approximation of GZ curve in calm water is used in order to calculate the restoring coefficients I_3,I_5, following the method stated in equation(4.27). The polynomial fit is shown in figure (5.11).

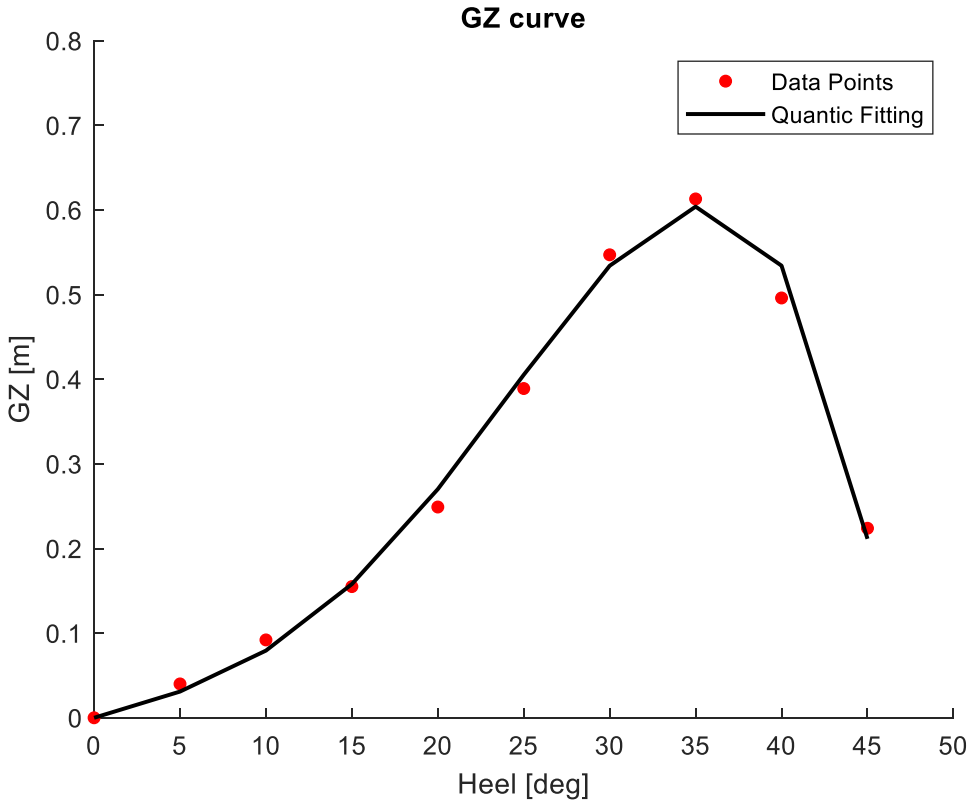

Figure 5.11: GZ curve in calm water fitting

The results for the restoring coefficients are:

$$I_3 = 14.57 \; and \; I_5 = -24.04$$

During this process, the fifth order approximation must fit accurately to the restoring arm's data points towards its greatest value. The need for higher angles is not necessary since the capsize becomes practically unavoidable. It is really crucial to do a strict fit in order to obtain the right results during the simulations.Damping coefficients will be calculated using Ikeda's simplified method as presented in Section 4.2.

Since all the mandatory parameters are calculated, the initial conditions are set. A 5^{o} heel and zero roll angular velocity are accounted. The equation(4.26) is solved numerically for each wave case and wave direction for a time duration of 500 seconds. The solution provided will be examined if the parametric amplitude overpass the angle of 25 degrees. In Figures (5.12) & (5.13) are presented two solutions of the equation. In the first one, in head seas, parametric roll is not detected opposing to the second one where in following seas is detcted

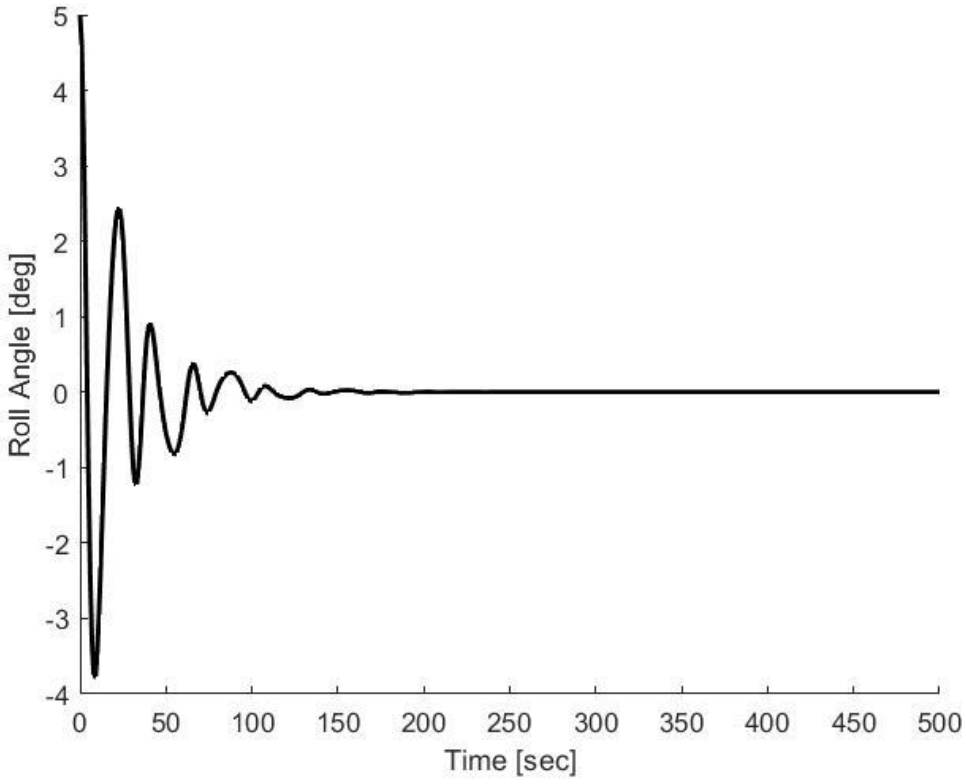

Figure 5.12: Roll response time history for Hw=2.7m in head seas where parametric roll is not detected

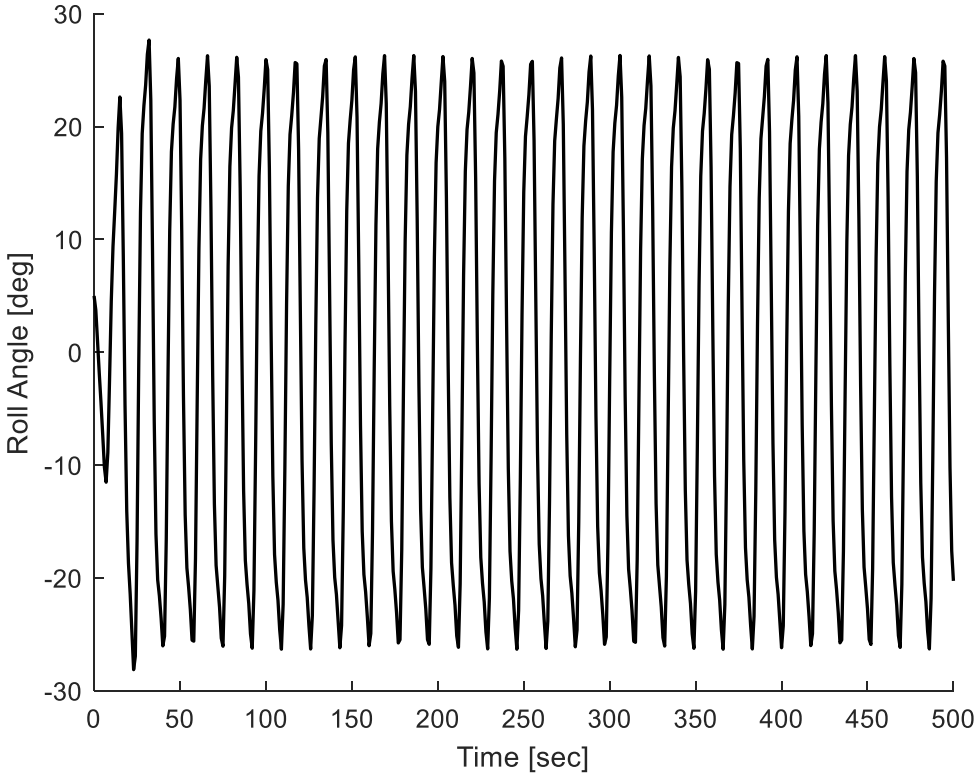

Figure 5.13: Roll response time history for Hw=13.5 m in following seas where parametric roll is detected

For the wave scattering diagram, the roll angle ϕ_i in each sea state will be established from the previously calculated max roll angles by linear interpolation, creating then seven 17x16 matrices consisting of max roll angles.

From these matrices the below procedure is followed:

C_i is determined as:

$$C_i = \begin{cases} 1\,, if\ \varphi_i > 25^o \\ 0, otherwise \end{cases}$$

Then, the weighting factor W_i is calculated following the method proposed above. Now, the C2 factor is calculated with one value for zero speed, three values for following waves and 3 for head waves.

at zero speed:

$$C2^O = \sum_i^N W_i C_i \tag{5.5}$$

in three speeds of following seas:

$$C2^{follow} = \sum_i^N W_i C_i \tag{5.6}$$

in three speeds of head seas:

$$C2^{head} = \sum_i^N W_i C_i \tag{5.7}$$

In Table (5.13) the relationship between encounter and roll frequency are presented for every case that was checked. In Table (5.14) is shown the results from the simulation for the 7 different cases in the North Atlantic wave scatter. Colored marked cells display the cases that max roll angle overpass the limit of 25 degrees. Blank cases oppose that no case overpassed 25 degrees and so correspond to a 0% probability.

Table 5.13: Wave direction and ratio of encounter to natural roll frequency

Ship speed & Wave direction	ω_{enc} / ω_{roll}
24.5 kn 0° Head	0.992
21.2 kn 30° Head	1.204
12.25 kn 60° Head	1.783
Vs=0	2.575
12.25 kn 120° Following	3.366
21.2 kn 150° Following	3.945
24.5 kn 180° Following	4.158

Table 5.14: Cases of different sea states with roll angles over 25 degrees

	Tz[s]=average zero up-crossing wave period															
Hs[m]	3,5	4,5	5,5	6,5	7,5	8,5	9,5	10,5	11,5	12,5	13,5	14,5	15,5	16,5	17,5	18,5
0,5	1,3	133,7	865,6	1186	634,2	186,3	36,9	5,6	0,7	0,1	0	0	0	0	0	0
1,5	0	29,3	986	4976	7738	5569,7	2375,7	703,5	160,7	30,5	5,1	0,8	0,1	0	0	0
2,5	0	2,2	197,5	2158,8	6230	7449,5	4860,4	2066	644,5	160,2	33,7	6,3	1,1	0,2	0	0
3,5	0	0,2	34,9	695,5	3226,5	5675	5099,1	2838	1114,1	337,7	84,3	18,2	3,5	0,6	0,1	0
4,5	0	0	6	196,1	1354,3	3288,5	3857,5	2685,5	1275,2	455,1	130,9	31,9	6,9	1,3	0,2	0
5,5	0	0	1	51	498,4	1602,9	2372,7	2008,3	1126	463,6	150,9	41	9,7	2,1	0,4	0,1
6,5	0	0	0,2	12,6	167	690,3	1257,9	1268,6	825,9	386,8	140,8	42,2	10,9	2,5	0,5	0,1
7,5	0	0	0	3	52,1	270,1	594,4	703,2	524,9	276,7	111,7	36,7	10,2	2,5	0,6	0,1
8,5	0	0	0	0,7	15,4	97,9	255,9	350,6	296,9	174,6	77,6	27,7	8,4	2,2	0,5	0,1
9,5	0	0	0	0,2	4,3	33,2	101,9	159,9	152,2	99,2	48,3	18,7	6,1	1,7	0,4	0,1
10,5	0	0	0	0	1,2	10,7	37,9	67,5	71,7	51,5	27,3	11,4	4	1,2	0,3	0,1
11,5	0	0	0	0	0,3	3,3	13,3	26,6	31,4	24,7	14,2	6,4	2,4	0,7	0,2	0,1
12,5	0	0	0	0	0,1	1	4,4	9,9	12,8	11	6,8	3,3	1,3	0,4	0,1	0
13,5	0	0	0	0	0	0,3	1,4	3,5	5	4,6	3,1	1,6	0,7	0,2	0,1	0
14,5	0	0	0	0	0	0,1	0,4	1,2	1,8	1,8	1,3	0,7	0,3	0,1	0	0
15,5	0	0	0	0	0	0	0,1	0,4	0,6	0,7	0,5	0,3	0,1	0,1	0	0
16,5	0	0	0	0	0	0	0	0,1	0,2	0,2	0,2	0,1	0,1	0	0	0

Since all the parameters have been determined the final level concerns the total value of the C2 which is reckoned as:

$$C2 = \left[\sum_{i=1}^{3} C2^{head}(Fn_i) + C2^{0}(Fn_0 = 0) + \sum_{i=1}^{3} C2^{following}(Fn_i)\right] /7 = 0.0022$$

$$C2 < R_{PR1} = 0.025$$

Table 5.15: Results for Level 2B of Parametric Rolling

Vessel	Loadcase		C2	R_{PR1}	Status
Post-Panamax	FLD	Full Load Departure	0.0022	0.025	**PASS**

In conclusion, from the Table[5.15], the vessel is considered not to be vulnerable to Level 2 criterion of parametric rolling.

DNV Worldwide wave scatter Table (5.16), according to [42], was also used for the vulnerability check. Following the above method, the results are presented below in Table (5.17).

Table 5.16: DNV Worldwide Wave Scatter Diagram

Tz(s)	3.5	4.5	5.5	6.5	7.5	8.5	9.5	10.5	11.5	12.5	13.5	14.5	15.5	16.5	17.5	Sum
Hs (m)																
1.0	311	2 734	6 402	7 132	5 071	2 711	1 202	470	169	57	19	6	2	1	0	26 287
2.0	20	764	4 453	8 841	9 045	6 020	3 000	1 225	435	140	42	12	3	1	0	34 001
3.0	0	57	902	3 474	5 549	4 973	3 004	1 377	518	169	50	14	4	1	0	20 092
4.0	0	4	150	1 007	2 401	2 881	2 156	1 154	485	171	53	15	4	1	0	10 482
5.0	0	0	25	258	859	1 338	1 230	776	372	146	49	15	4	1	0	5 073
6.0	0	0	4	63	277	540	597	440	240	105	39	13	4	1	0	2 323
7.0	0	0	1	15	84	198	258	219	136	66	27	10	3	1	0	1 018
8.0	0	0	0	4	25	69	103	99	69	37	17	6	2	1	0	432
9.0	0	0	0	1	7	23	39	42	32	19	9	4	1	1	0	178
10.0	0	0	0	0	2	7	14	16	14	9	5	2	1	0	0	70
11.0	0	0	0	0	1	2	5	6	6	4	2	1	1	0	0	28
12.0	0	0	0	0	0	1	2	2	2	2	1	1	0	0	0	11
13.0	0	0	0	0	0	0	1	1	1	1	0	0	0	0	0	4
14.0	0	0	0	0	0	0	0	0	1	0	0	0	0	0	0	1
Sum	331	3 559	11 937	20 795	23 321	18 763	11 611	5 827	2 480	926	313	99	29	9	0	100 000

Table 5.17: Results for Level 2B for DNV Wave Scatter

Vessel	Loadcase		C2	R_{PR1}	Status
Post-Panamax	FLD	Full Load Departure	0.0005	0.025	**PASS**

The DNV wave scatter seems to result to less vulnerable cases than the North Atlantic wave scatter since the prone cases concern wave heights above 10 meters and zero up-crossing wave periods above 9.5 seconds. For a different loading condition or a different vessel which would be more prone to lower significant heights and periods a vulnerability assessment would be interesting as this wave scatter has a higher relativity in these cases.

5.3.2. Application of Vulnerability Assessment for "2,200 TEUs Feedermax"

5.3.2.1. Level 1 Vulnerability Check

The criterion of parametric roll will be applied on both vessels for the Full Load Departure, following the procedure analyzed in Section 4.2. The Table (5.18) presents all the necessary values needed to apply the first level.

Table 5.18: Particulars for Level 1 Vulnerability Check

L_{WL} [m]	189.93	V_D[m³]	69841.92
V [m³]	41155.2	d_H= d + min(D-d,L · s_w /2)[m]	12.6
A_w[m²]	4861.85	d_L= d + min(D-0.25 · d_{FULL},L ·s_w/2)[m]	9.43
d_{DES}[m]	10.5	I_H[m⁴]	351840.0
d_{FULL} [m]	11.0	I_L[m⁴]	295278.1

The ship considered not to be vulnerable if:

$$\frac{\delta GM_1}{GM_C} \leq R_{PR}$$

However, $\frac{\nabla_D - \nabla}{A_W \cdot (D-d)} = 1.0572 > 1$

and $\delta GM_1 = \frac{I_H - I_L}{2 \cdot \nabla} = 0.6872$

$$\delta GM_1 / GM_C = 2.1474$$

Using the direct procedure explained in Section 4.2.3 the amplitude of metacentric height variation is:

$$\delta GM = \frac{GM_{MAX} - GM_{MIN}}{2} = 0.586$$

So:

$$\delta GM_1 / GM_C = 1.675$$

Following the next step, the value R_{PR} and the ratio ΔGM/GM will be compared for level 1. Since C_M =0.982>0.96 then:

$$R_{PR} = 0.17 + 0.425 \cdot \left(\frac{100 \cdot A_K}{L \cdot B}\right) = 0.3931$$

After comparison, it is proven that the vessel is vulnerable to parametric roll for the examined loading condition as shown in table below. So a Level 2 check is needed.

Table 5.19: Results for Level 1 of Parametric Rolling

Vessel	Loadcase		ΔGM/GM simplified	ΔGM/GM direct	R_{PR}	Status
Feedermax	FLD	Full Load Departure	2.1474	1.675	0.3931	**FAIL**

5.3.2.2. Level 2A Vulnerability Check

Results of the necessary calculations are presented in the table below:

Table 5.20: Feedermax, Results for level 2A check for parametric roll

Case No.	Weight Wi	Wave Length λ_i[m]	Wave Height H_i[m]	ΔGM/GM	R_{PR}	V_s[kn]	V_{PR}[kn]	C_i
1	0.000013	22.574	0.35	0.06835	0.3931	21.82	8.3431	0
2	0.001654	37.316	0.495	0.15993	0.3931	21.82	9.573	0
3	0.020912	55.743	0.8575	0.27348	0.3931	21.82	10.336	0
4	0.092799	77.857	1.2945	0.59587	0.3931	21.82	10.586	0
5	0.199218	103.655	1.732	0.4714	0.3931	21.82	10.324	1
6	0.248788	133.139	2.205	1.1399	0.3931	21.82	9.3966	1
7	0.208699	166.309	2.6965	1.5202	0.3931	21.82	8.1586	1
8	0.128984	203.164	3.1755	1.5711	0.3931	21.82	6.5219	1
9	0.062446	243.705	3.625	1.4943	0.3931	21.82	4.1614	1
10	0.024790	287.931	4.04	1.3841	0.3931	21.82	1.3198	1
11	0.008367	335.843	4.4205	1.2109	0.3931	21.82	1.831	1
12	0.002473	387.44	4.7695	1.0641	0.3931	21.82	5.725	1
13	0.000658	442.723	5.097	0.9039	0.3931	21.82	9.964	1
14	0.000158	501.691	5.3695	0.7967	0.3931	21.82	15.04	1
15	0.000034	564.345	5.621	0.6972	0.3931	21.82	20.34	1
16	0.000007	630.84	5.95	0.6123	0.3931	21.82	26.394	0

The total C_i index for level 2A and the specific condition is

$$C1 = \sum_{i=1}^{16} W_i \cdot C_i = 0.88461 > 0.06 = R_{PR0}$$

Table 5.21: Results for Level 2A of Parametric Rolling

Vessel	Loadcase		C1	R_{PR0}	Status
Feedermax	FLD	Full Load Departure	0.88461	0.006	**FAIL**

The conclusion is that the loading condition is considered vulnerable to parametric roll when the vessel is operating with the service speed of 21.82 knots, so in this case a level 2B check is required.

5.3.2.3.Level 2B Vulnerability Check

Level 2B requires the computation of parametric roll amplitude for seven different wave directions and ten different wave cases. The process followed is the same as used in section 5.3.1.3.The wave encounter frequency is calculated according to the equation (5.1) with a speed equal to the service one but different heading. Results are listed in Table(5.22):

$$w_{enc} = \omega_0 - \frac{\omega_0^2}{g} V_S \cdot cos\beta, where \quad \omega_0 = \sqrt{\frac{2\pi \cdot g}{L_{wl}}}$$

Table 5.22: Wave cases and their respective encounter frequencies

Wave direction***[deg]***	Encounter frequency ***[rad/s]***
0^o	0.1528
30^o	0.2086
60^o	0.3612
120^o	0.7782
150^o	0.9308
180^o	0.9866
V_S=0	0.5697

In the table (5.23) that follows, the wave characteristics that were used for the calculation of Level 2B are listed. In Figure (5.14) is presented the waterplane for the wave case No.5.

Table 5.23: Wave data and results for level 2B check for parametric roll

Case No.	Wave Length λ_i[m]	Wave Height H_i[m]	GM_{mean}	GM_{amp}
1	189.93	1.8993	0.314	0.363
2	189.93	3.7986	0.316	0.649
3	189.93	5.6979	0.3845	0.7895
4	189.93	7.5972	0.5135	0.9985
5	189.93	9.4965	0.7645	1.3025
6	189.93	11.396	0.8415	1.4285
7	189.93	13.295	0.6795	1.3045
8	189.93	15.194	0.8395	1.301
9	189.93	17.094	0.835	1.345
10	189.93	18.993	0.815	1.433

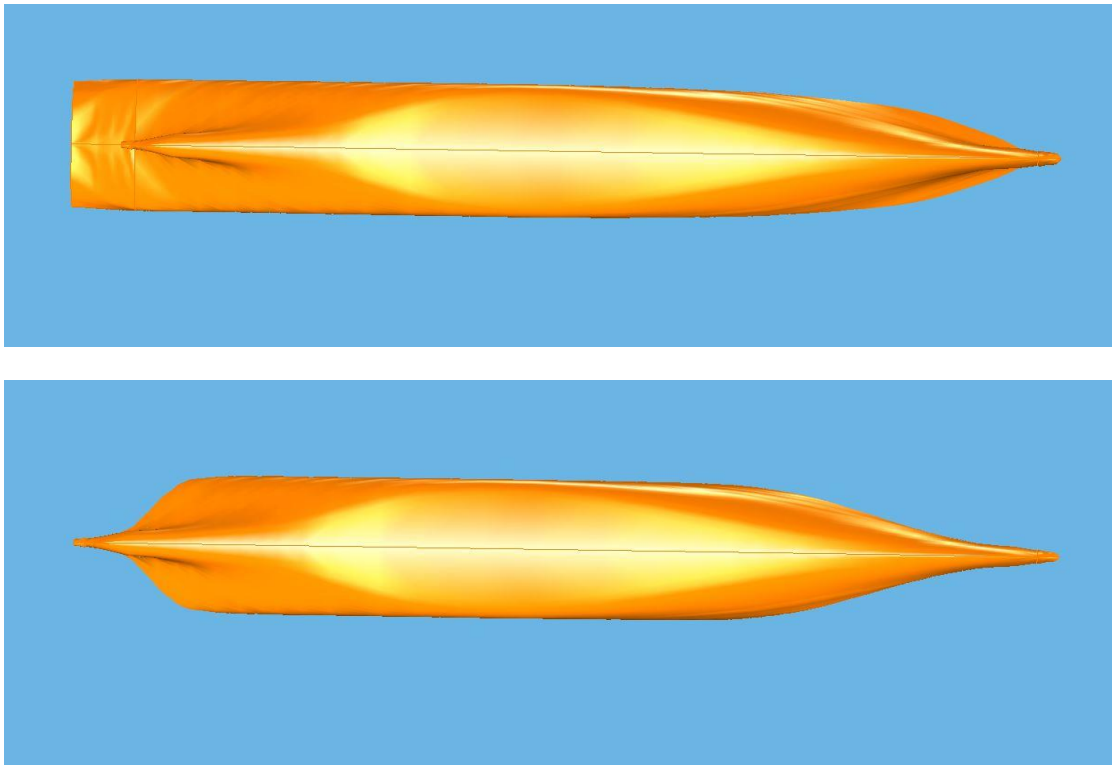

Figure 5.14: Waterplane on wave trough and crest for a wave of $\lambda=L_{WL}$ and $s_w=1/20$

Further, a quantic fit approximation of GZ curve in calm water is used in order to calculate the restoring coefficients I_3,I_5 .The polynomial fit is shown in Figure (5.12).

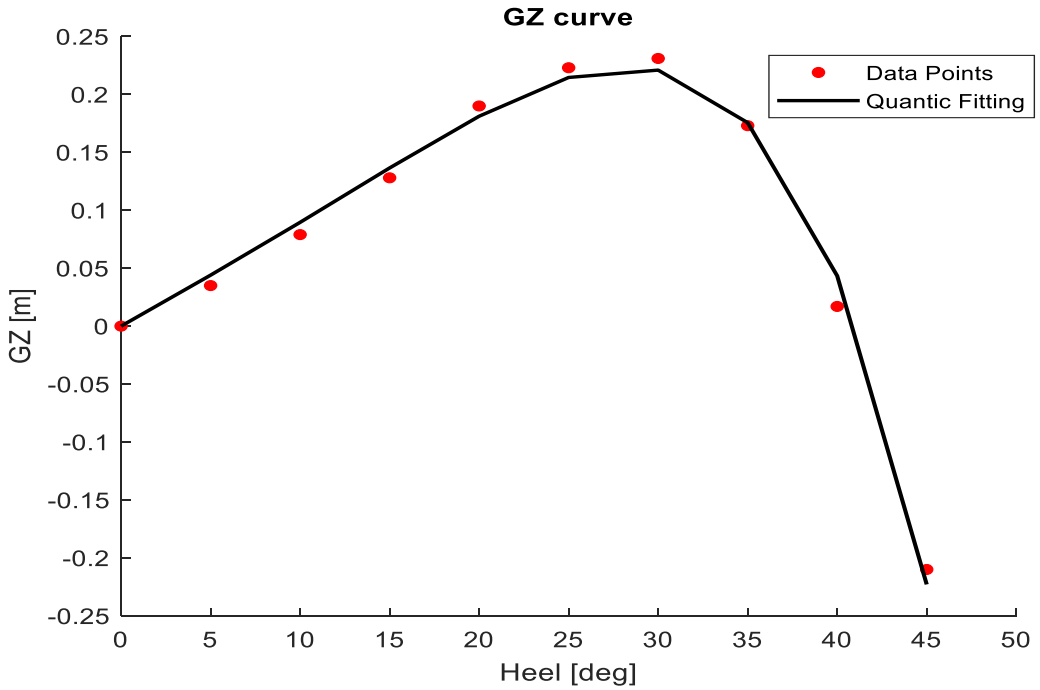

Figure 5.15: GZ curve in calm water fitting

The results for the restoring coefficients are:

$$I_3 = 0.796 \; and \; I_5 = -5.359$$

The equation(4.26) is solved numerically for each wave case and wave direction for a time duration of 500 seconds. Following the process used in Section 5.2.1.3, some results are presented in the figures (5.16) & (5.17).

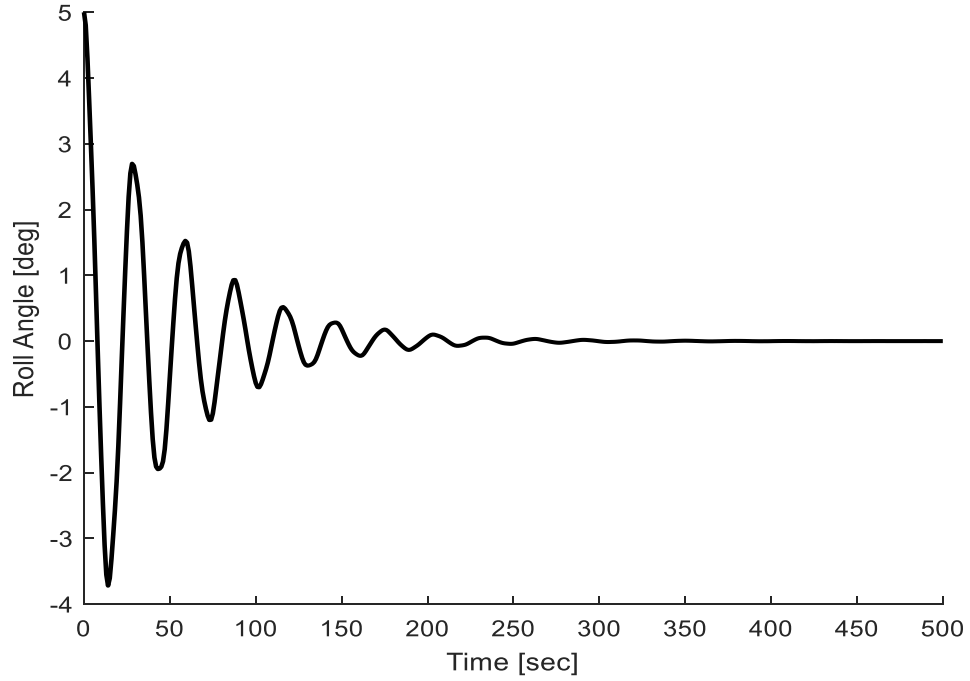

Figure 5.16: Roll response time history for a wave of Hw=9.5 in following seas where parametric roll is not detected

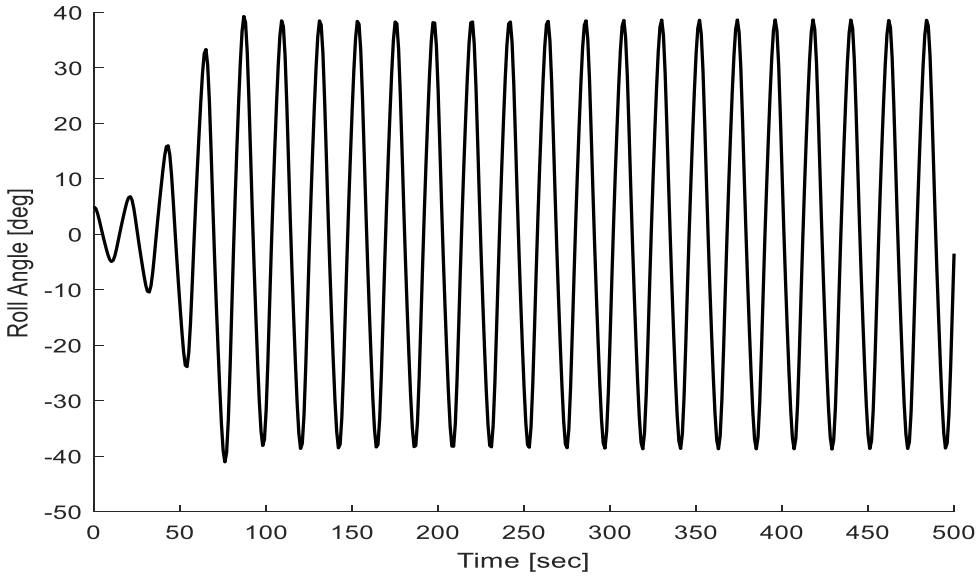

Figure 5.17: Roll response time history for a wave of Hw=13.3 m in head seas where parametric roll is detected

For the wave scattering diagram, the roll angle ϕ_i in each sea state will be established from the previously calculated max roll angles by linear interpolation.Following the same process used in section 5.2.1.3 the Table (5.24) includes the results and Table (5.25) the cases with a roll amplitued over 25 degrees:

Table 5.24: Wave direction and ratio of encounter to natural roll frequency

Ship speed & Wave direction	ω_{enc} / ω_{roll}
21.82 kn 0° Head	0.910
18.90 kn 30° Head	1.242
10.91 kn 60° Head	2.152
Vs=0	3.391
10.91 kn 120° Following	4.636
18.90 kn 150° Following	5.545
21.82 kn 180° Following	5.873

Table 5.25: Cases of different sea states with roll angles over 25 degrees

	Tz[s]=average zero up-crossing wave period															
Hs[m]	3.5	4.5	5.5	6.5	7.5	8.5	9.5	10.5	11.5	12.5	13.5	14.5	15.5	16.5	17.5	18.5
0.5	1.3	133.7	865.6	1186	634.2	186.3	36.9	5.6	0.7	0.1	0	0	0	0	0	0
1.5	0	29.3	986	4976	7738	5569.7	2375.7	703.5	160.7	30.5	5.1	0.8	0.1	0	0	0
2.5	0	2.2	197.5	2158.8	6230	7449.5	4860.4	2066	644.5	160.2	33.7	6.3	1.1	0.2	0	0
3.5	0	0.2	34.9	695.5	3226.5	5675	5099.1	2838	1114.1	337.7	84.3	18.2	3.5	0.6	0.1	0
4.5	0	0	6	196.1	1354.3	3288.5	3857.5	2685.5	1275.2	455.1	130.9	31.9	6.9	1.3	0.2	0
5.5	0	0	1	51	498.4	1602.9	2372.7	2008.3	1126	463.6	150.9	41	9.7	2.1	0.4	0.1
6.5	0	0	0.2	12.6	167	690.3	1257.9	1268.6	825.9	386.8	140.8	42.2	10.9	2.5	0.5	0.1
7.5	0	0	0	3	52.1	270.1	594.4	703.2	524.9	276.7	111.7	36.7	10.2	2.5	0.6	0.1
8.5	0	0	0	0.7	15.4	97.9	255.9	350.6	296.9	174.6	77.6	27.7	8.4	2.2	0.5	0.1
9.5	0	0	0	0.2	4.3	33.2	101.9	159.9	152.2	99.2	48.3	18.7	6.1	1.7	0.4	0.1
10.5	0	0	0	0	1.2	10.7	37.9	67.5	71.7	51.5	27.3	11.4	4	1.2	0.3	0.1
11.5	0	0	0	0	0.3	3.3	13.3	26.6	31.4	24.7	14.2	6.4	2.4	0.7	0.2	0.1
12.5	0	0	0	0	0.1	1	4.4	9.9	12.8	11	6.8	3.3	1.3	0.4	0.1	0
13.5	0	0	0	0	0	0.3	1.4	3.5	5	4.6	3.1	1.6	0.7	0.2	0.1	0
14.5	0	0	0	0	0	0.1	0.4	1.2	1.8	1.8	1.3	0.7	0.3	0.1	0	0
15.5	0	0	0	0	0	0	0.1	0.4	0.6	0.7	0.5	0.3	0.1	0.1	0	0
16.5	0	0	0	0	0	0	0	0.1	0.2	0.2	0.2	0.1	0.1	0	0	0

Since all the parameters have been determined the final level concerns the total value of the C2 which is reckoned as:

$$C2 = \left[\sum_{i=1}^{3} C2^{head}(Fn_i) + C2^{0}(Fn_0 = 0) + \sum_{i=1}^{3} C2^{following}(Fn_i)\right] / 7 = 0.00381$$

Table 5.26: Results for Level 2B of Parametric Rolling

Vessel	Loadcase		C2	R_{PR1}	Status
Feedermax	FLD	Full Load Departure	0.00381	0.025	PASS

In conclusion, the vessel is considered not to be vulnerable to Level 2 criterion of parametric rolling.

5.4. Application of Vulnerability criterion for Excessive Acceleration

5.4.1. Application of Vulnerability Assessment for "5,200 TEUs Post-Panamax"

5.4.1.1.Level 1 Vulnerability Check

Following the process analyzed in [3],the application of 3 different loading conditions will be evaluated.The first one refers to the ballast condition which is considered as the worst case scenario for the excessive acceleration criterion. The second and the third one were chosen since their GM value was near the threshold. The second one is not applicable and the third one is, both with a slight difference to the limit value. The basic particulars of the loading conditions are presented in Table(5.27).

Table 5.27: Loading conditions particulars

	Ballast Arrival	20T/TEU Arrival	Empt.Cont. Arrival
L_{WL} [m]	259.41	266.18	260.45
d [m]	7.47	13.17	8.27
C_M	0.947	0.979	0.964
C_B	0.41	0.586	0.459
KG [m]	11.82	16.31	16.49
GM [m]	9.95	3.15	4.31
$H_{NAV.DECK}$ [m]	46.5	46.5	46.5

The criteria are applicable when for the examined loadcase the following conditions are satisfied simultaneously, following[3]. Where [H] is the vertical distance from the waterline to the examined position, which in our case is the navigational deck.

$$H > 0.7 \cdot B \; and \; GM > 0.08 \cdot B$$

$$H = H_{NAV.DECK} - d = 39.03 > 28.14 \; and \; GM = 9.95 > 3.22 \; applicable$$

Table 5.28: Check for applicability of the EA criterion

	Thresholds	Ballast Arrival	20T/TEU Arrival	Empt.Cont. Arrival
H [m]	28.14	39.03	33.33	38.23
GM [m]	3.22	9.95	3.15	4.31
Applicability		**PASS**	**FAIL**	**PASS**

A ship is not considered vulnerable to excessive acceleration when:

$$\varphi \cdot kL \cdot \left(g + \frac{4\pi^2 h}{T_r^2} \right) < R_{EA1} = 4.64 \; [m/s^2]$$

The examined location is located 84.2 m forward of A.P. so:

$$x = 84.2\,m \rightarrow\ 0.2 \cdot L < x < 0.65 \cdot L\ \rightarrow kL = 1.0$$

$$C = 0.373 + 0.023 \cdot \left(\frac{B}{T}\right) - 0.043 \cdot \left(\frac{L_{WL}}{100}\right) = 0.3852$$

$$T_r = \frac{2C \cdot B}{GM^{0.5}} = 9.82\ [s]$$

Wave steepness according to the Table (4.2) for roll period T_s=9.82 s

$$s = 0.08$$

Effective wave slope coefficient *r*:

$$OG = KG - d = 4.35\ [m]$$

$$\tilde{B} = \frac{2\pi^2 B}{g \cdot T_r^2} = 0.839$$

$$\tilde{T} = \frac{4\pi^2 \cdot C_B \cdot d}{g \cdot T_r^2} = 0.1278$$

$$\beta = \frac{\sin(\tilde{B})}{\tilde{B}} = 0.8867$$

$$\tau = \frac{\exp(-\tilde{T})}{\tilde{T}} = 6.8835$$

$$K_1 = g \cdot \beta \cdot T_r^2 \cdot \frac{\left(\tau + \tau \cdot \tilde{T} - \frac{1}{\tilde{T}}\right)}{4\pi^2} = -1.2475$$

$$K_2 = g \cdot \tau \cdot T_r^2 \cdot \frac{(\beta - cos\tilde{B})}{4\pi^2} = 36.0381$$

$$F = \beta \cdot \left(\tau - \frac{1}{\tilde{T}}\right) = -0.8324$$

$$r = \frac{K_1 + K_2 + OG \cdot F}{\frac{B^2}{12 \cdot C_B \cdot d} - \frac{C_B \cdot d}{2} - OG} = 0.8183$$

Logarithmic decrement of roll decay δ_Φ:

$$\delta_\varphi = 0.5\pi \cdot R_{PR} = 0.3951$$

$$\varphi = 4.43 \cdot r \cdot \frac{s}{\delta^{0.5}} = 0.4614[rad]$$

h is the distance of roll axis assumed to be located at the midpoint between the examined d and KG.

$$h = H_{NAV.DECK} - \left(\frac{KG + d}{2}\right) = 36.855\ [m]$$

$$\varphi \cdot kL \cdot \left(g + \frac{4\pi^2 h}{T_r^2}\right) = 11.49 > R_{EA1} = 4.64\ [m/s^2]$$

Following the same methodology the results for the Level 1 Vulnerability check of the examined loadcases are presented in Table (5.29):

Table 5.29: Results for Level 1 for the loading conditions examined

Values	Ballast Arrival	Design Draft Arrival	Empty Cont.
x [m]	84.2	84.2	84.2
kL	1.0	1.0	1.0
C	0.3852	0.3287	0.3728
Tr [s]	9.82	14.89	14.438
s	0.08	0.049	0.051
OG [m]	4.35	3.14	8.22
$\tilde{B}$	0.839	0.3647	0.388
$\tilde{T}$	0.1278	0.14	0.0733
β	0.8867	0.978	0.9751
τ	6.8835	6.2078	12.6815
K_1	-1.2475	-3.4393	-1.7627
K_2	36.0381	14.9686	32.477
F	0.8324	-0.9126	-0.9402
r	0.8183	0.829	0.9064
δ_φ	0.3951	0.5166	0.5221
φ [rad]	0.4614	0.2504	0.2834
h [m]	36.855	31.76	34.12
$\varphi \cdot kL \cdot \left(g + \frac{4\pi^2 h}{T_r^2}\right)$ [m/s²]	11.49	3.872	4.612

Table 5.30: Results for Level 1 Vulnerability Check

Vessel	Loadcase	Lat.Acc.	R_{EA1}	Status
Post-Panamax	Ballast Arrival	11.49	4.64	**FAIL**
	Design Arrival	3.8716	4.64	**PASS**
	Empty Cont.	4.612	4.64	**PASS**

Finally, an analysis on the critical GM values for Level 1 of excessive accelerations was carried out. Specifically, in Figure (5.18) are presented the drafts and the corresponding GM values which equal the lateral acceleration to the R_{EA1} threshold. A safe area to operate is marked and an unsafe one too where the lateral accelerations will be high enough to

conclude to a Level 2 vulnerability analysis. Eventually, the safe but not applicable area concerns the GM threshold the regulations include in order to apply the criterion.

As observed, for the excessive accelerations criterion, lower GM values are considered safer. As the GM lowers, the period of natural roll gets higher. Hence, for the same roll amplitude the rate of roll velocity change gets lower and concludes to lower lateral accelerations.

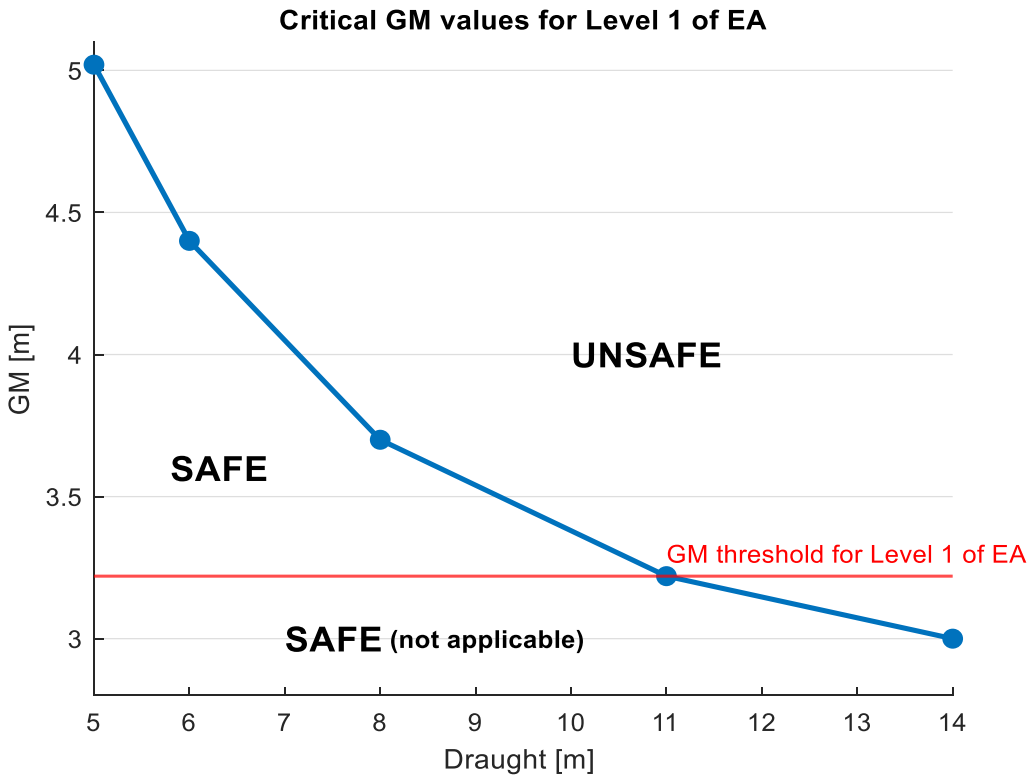

Figure 5.18: Critical GM values for Level 1 of EA

5.4.2.2.Level 2 Vulnerability Check

In this thesis the calculations for the Level 2 were carried out using a constant effective wave slope coefficient as it was computed in Level 1 vulnerability check for excessive accelerations. Also, the equivalent linear roll damping coefficient was calculated as proposed in the explanatory notes [3].

Using the fitting proposed in eq.(4.91) the linear, quadratic and cubic roll damping coefficients are calculated.

$$\frac{B_{44}(\varphi_\alpha)\cdot\omega_\varphi^2}{2W\cdot GM} \Rightarrow \mu + \frac{4}{3\pi}\cdot\beta\cdot\omega_\varphi\cdot\varphi_\alpha + \frac{3}{8}\cdot\delta\cdot\omega_\varphi^2\cdot\varphi_\alpha^2$$

$$\mu = 0.0054 \quad \beta = 0.1627 \quad \delta = 0.3104$$

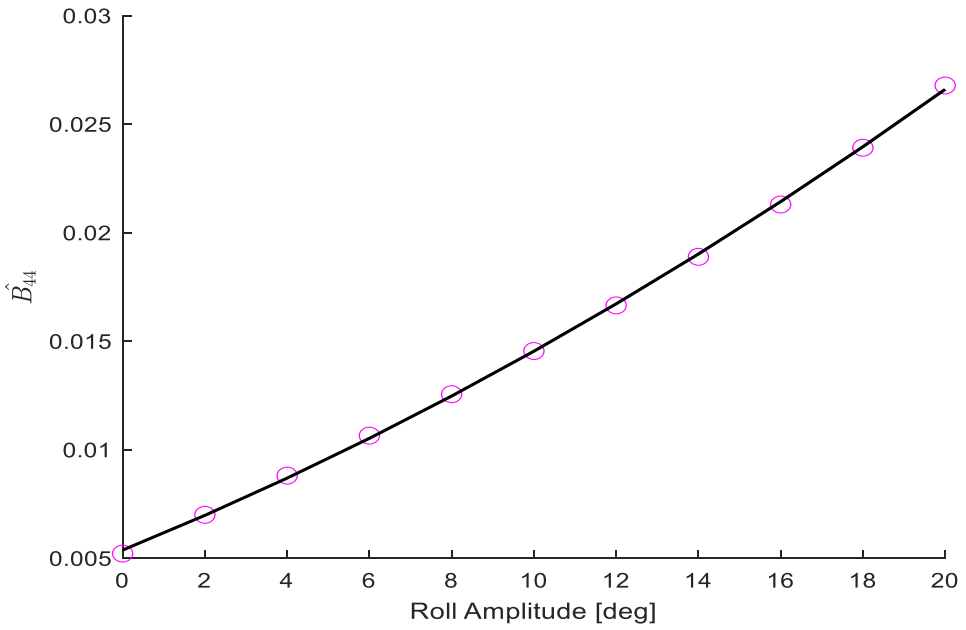

Figure 5.19: Least square fitting for Ballast Arrival

Following the regulations [3] and the appropriate calculations, the results are presented in Table (5.31).

$$\sigma_{LAi}^2 = \frac{3}{4}\int_{\omega_1}^{\omega_2} \Big(a_y(\omega)\Big)^2 Szz(\omega)\, d\omega$$

Table 5.31: Results for standard deviation of lateral acceleration (σ_{LAi})

H[m] / Tz[s]	3.5	4.5	5.5	6.5	7.5	8.5	9.5	10.5	11.5	12.5	13.5	14.5	15.5	16.5	17.5	18.5
0.5	6.38E-05	2.04E-04	1.20E-03	2.56E-03	2.96E-03	2.64E-03	2.12E-03	1.64E-03	1.26E-03	9.65E-04	7.48E-04	5.87E-04	4.66E-04	3.75E-04	3.05E-04	2.51E-04
1.5	5.74E-04	1.84E-03	1.08E-02	2.30E-02	2.66E-02	2.38E-02	1.91E-02	1.48E-02	1.13E-02	8.69E-03	6.73E-03	5.28E-03	4.20E-03	3.38E-03	2.75E-03	2.26E-03
2.5	1.59E-03	5.11E-03	3.01E-02	6.40E-02	7.39E-02	6.60E-02	5.31E-02	4.11E-02	3.14E-02	2.41E-02	1.87E-02	1.47E-02	1.17E-02	9.38E-03	7.63E-03	6.28E-03
3.5	3.12E-03	1.00E-02	5.89E-02	1.25E-01	1.45E-01	1.29E-01	1.04E-01	8.05E-02	6.16E-02	4.73E-02	3.67E-02	2.88E-02	2.28E-02	1.84E-02	1.50E-02	1.23E-02
4.5	5.16E-03	1.65E-02	9.74E-02	2.07E-01	2.39E-01	2.14E-01	1.72E-01	1.33E-01	1.02E-01	7.82E-02	6.06E-02	4.75E-02	3.78E-02	3.04E-02	2.47E-02	2.03E-02
5.5	7.71E-03	2.47E-02	1.45E-01	3.10E-01	3.58E-01	3.19E-01	2.57E-01	1.99E-01	1.52E-01	1.17E-01	9.05E-02	7.10E-02	5.64E-02	4.54E-02	3.69E-02	3.04E-02
6.5	1.08E-02	3.45E-02	2.03E-01	4.33E-01	4.99E-01	4.46E-01	3.59E-01	2.78E-01	2.12E-01	1.63E-01	1.26E-01	9.92E-02	7.88E-02	6.34E-02	5.16E-02	4.24E-02
7.5	1.43E-02	4.59E-02	2.71E-01	5.76E-01	6.65E-01	5.94E-01	4.78E-01	3.70E-01	2.83E-01	2.17E-01	1.68E-01	1.32E-01	1.05E-01	8.44E-02	6.87E-02	5.65E-02
8.5	1.84E-02	5.90E-02	3.48E-01	7.40E-01	8.54E-01	7.63E-01	6.14E-01	4.75E-01	3.63E-01	2.79E-01	2.16E-01	1.70E-01	1.35E-01	1.08E-01	8.82E-02	7.26E-02
9.5	2.30E-02	7.37E-02	4.34E-01	9.24E-01	1.07E+00	9.53E-01	7.67E-01	5.93E-01	4.54E-01	3.49E-01	2.70E-01	2.12E-01	1.68E-01	1.35E-01	1.10E-01	9.06E-02
10.5	2.81E-02	9.01E-02	5.30E-01	1.13E+00	1.30E+00	1.16E+00	9.37E-01	7.24E-01	5.54E-01	4.26E-01	3.30E-01	2.59E-01	2.06E-01	1.65E-01	1.35E-01	1.11E-01
11.5	3.37E-02	1.08E-01	6.36E-01	1.35E+00	1.56E+00	1.40E+00	1.12E+00	8.69E-01	6.65E-01	5.11E-01	3.96E-01	3.10E-01	2.47E-01	1.98E-01	1.61E-01	1.33E-01
12.5	3.98E-02	1.28E-01	7.52E-01	1.60E+00	1.85E+00	1.65E+00	1.33E+00	1.03E+00	7.86E-01	6.03E-01	4.68E-01	3.67E-01	2.91E-01	2.34E-01	1.91E-01	1.57E-01
13.5	4.65E-02	1.49E-01	8.77E-01	1.87E+00	2.15E+00	1.92E+00	1.55E+00	1.20E+00	9.17E-01	7.04E-01	5.45E-01	4.28E-01	3.40E-01	2.73E-01	2.23E-01	1.83E-01
14.5	5.36E-02	1.72E-01	1.01E+00	2.15E+00	2.49E+00	2.22E+00	1.79E+00	1.38E+00	1.06E+00	8.12E-01	6.29E-01	4.94E-01	3.92E-01	3.15E-01	2.57E-01	2.11E-01
15.5	6.13E-02	1.96E-01	1.16E+00	2.46E+00	2.84E+00	2.54E+00	2.04E+00	1.58E+00	1.21E+00	9.28E-01	7.19E-01	5.64E-01	4.48E-01	3.60E-01	2.93E-01	2.41E-01
16.5	6.94E-02	2.22E-01	1.31E+00	2.79E+00	3.22E+00	2.88E+00	2.31E+00	1.79E+00	1.37E+00	1.05E+00	8.15E-01	6.39E-01	5.08E-01	4.08E-01	3.32E-01	2.73E-01

Using the below equations the final results are presented in the table 5.32.

$$C_i = \exp[-R_2^2 \,/\, (2 \cdot \sigma_{LAi}^2)]$$

$$C = \sum_{i=1}^{N} W_i C_i = 5.06e-10 < R_{EA2}$$

Following the above method the calculations for the second loading condition under investigation is presented.

Table 5.32: Results for the value of C_i

H[m] / Tz[s]	3.5	4.5	5.5	6.5	7.5	8.5	9.5	10.5	11.5	12.5	13.5	14.5	15.5	16.5	17.5	18.5
0.5	9.68E-06	1.66E-05	2.88E-05	7.56E-05	3.06E-04	7.77E-04	1.21E-03	1.42E-03	1.42E-03	1.30E-03	1.14E-03	9.73E-04	8.21E-04	6.90E-04	5.79E-04	4.88E-04
1.5	8.71E-05	1.50E-04	2.60E-04	6.80E-04	2.76E-03	6.99E-03	1.09E-02	1.28E-02	1.28E-02	1.17E-02	1.03E-02	8.76E-03	7.39E-03	6.21E-03	5.21E-03	4.39E-03
2.5	2.42E-04	4.15E-04	7.21E-04	1.89E-03	7.66E-03	1.94E-02	3.03E-02	3.55E-02	3.55E-02	3.26E-02	2.85E-02	2.43E-02	2.05E-02	1.72E-02	1.45E-02	1.22E-02
3.5	4.74E-04	8.14E-04	1.41E-03	3.70E-03	1.50E-02	3.81E-02	5.94E-02	6.96E-02	6.96E-02	6.38E-02	5.59E-02	4.77E-02	4.02E-02	3.38E-02	2.84E-02	2.39E-02
4.5	7.84E-04	1.35E-03	2.34E-03	6.12E-03	2.48E-02	6.29E-02	9.82E-02	1.15E-01	1.15E-01	1.06E-01	9.23E-02	7.88E-02	6.65E-02	5.59E-02	4.69E-02	3.95E-02
5.5	1.17E-03	2.01E-03	3.49E-03	9.14E-03	3.71E-02	9.40E-02	1.47E-01	1.72E-01	1.72E-01	1.58E-01	1.38E-01	1.18E-01	9.94E-02	8.35E-02	7.01E-02	5.90E-02
6.5	1.64E-03	2.81E-03	4.88E-03	1.28E-02	5.18E-02	1.31E-01	2.05E-01	2.40E-01	2.40E-01	2.20E-01	1.93E-01	1.64E-01	1.39E-01	1.17E-01	9.79E-02	8.24E-02
7.5	2.18E-03	3.74E-03	6.49E-03	1.70E-02	6.89E-02	1.75E-01	2.73E-01	3.19E-01	3.20E-01	2.93E-01	2.57E-01	2.19E-01	1.85E-01	1.55E-01	1.30E-01	1.10E-01
8.5	2.80E-03	4.80E-03	8.34E-03	2.18E-02	8.85E-02	2.24E-01	3.50E-01	4.10E-01	4.10E-01	3.77E-01	3.29E-01	2.81E-01	2.37E-01	1.99E-01	1.67E-01	1.41E-01
9.5	3.49E-03	6.00E-03	1.04E-02	2.73E-02	1.11E-01	2.80E-01	4.37E-01	5.13E-01	5.13E-01	4.70E-01	4.12E-01	3.51E-01	2.96E-01	2.49E-01	2.09E-01	1.76E-01
10.5	4.27E-03	7.33E-03	1.27E-02	3.33E-02	1.35E-01	3.43E-01	5.34E-01	6.26E-01	6.26E-01	5.75E-01	5.03E-01	4.29E-01	3.62E-01	3.04E-01	2.56E-01	2.15E-01
11.5	5.12E-03	8.79E-03	1.53E-02	4.00E-02	1.62E-01	4.11E-01	6.41E-01	7.51E-01	7.51E-01	6.89E-01	6.03E-01	5.15E-01	4.34E-01	3.65E-01	3.07E-01	2.58E-01
12.5	6.05E-03	1.04E-02	1.80E-02	4.72E-02	1.91E-01	4.85E-01	7.57E-01	8.87E-01	8.88E-01	8.14E-01	7.13E-01	6.08E-01	5.13E-01	4.31E-01	3.62E-01	3.05E-01
13.5	7.06E-03	1.21E-02	2.10E-02	5.51E-02	2.23E-01	5.66E-01	8.83E-01	1.04E+00	1.04E+00	9.50E-01	8.31E-01	7.10E-01	5.99E-01	5.03E-01	4.22E-01	3.55E-01
14.5	8.14E-03	1.40E-02	2.43E-02	6.36E-02	2.58E-01	6.53E-01	1.02E+00	1.19E+00	1.19E+00	1.10E+00	9.59E-01	8.19E-01	6.91E-01	5.80E-01	4.87E-01	4.10E-01
15.5	9.30E-03	1.60E-02	2.77E-02	7.26E-02	2.94E-01	7.46E-01	1.16E+00	1.36E+00	1.36E+00	1.25E+00	1.10E+00	9.35E-01	7.89E-01	6.63E-01	5.57E-01	4.69E-01
16.5	1.05E-02	1.81E-02	3.14E-02	8.23E-02	3.34E-01	8.46E-01	1.32E+00	1.55E+00	1.55E+00	1.42E+00	1.24E+00	1.06E+00	8.94E-01	7.51E-01	6.31E-01	5.31E-01

Table 5.33: Results for Level 2 excessive accelerations

Vessel	Loadcase		C	R_{EA2}	Status
Post-Panamax	BA	Ballast Arrival	5.06E-10	0.00039	PASS
	EC	Empty Cont. Arrival	1.02E-25	0.00039	PASS

Using the DNV world scatter diagram from Table (5.16) the results are displayed in Table (5.34).

Table 5.34: Results for Level 2 for DNV Wave Scatter

Vessel	Loadcase		C	R_{EA2}	Status
Post-Panamax	BA	Ballast Arrival	2.36E-13	0.00039	**PASS**
	EC	Empty Cont. Arrival	1.72E-33	0.00039	**PASS**

5.4.2. Application of Vulnerability Assessment for "2,200 TEUs Feedermax"

5.4.2.1.Level 1 Vulnerability Check

Table 5.35: Loadcase Ballast Arrival particulars

L_{WL} [m]	179.45
d [m]	5.97
C_M	0.947
C_B	0.444
KG [m]	9.21
GM [m]	7.15
$H_{NAV.DECK}$ [m]	36.15

$$H > 0.7 \cdot B \; and \; GM > 0.08 \cdot B$$

$$H = H_{NAV.DECK} - d = 30.18 > 21.14 \;\; and \;\; GM = 7.15 > 2.416 \;\; applicable$$

Following the above methodology of Section 5.4.1.1 the results for the examined loadcase are presented below in Table(5.36) &(5.37):

Table 5.36: Results for Level 1 for the Ballast Arrival

Values	Ballast Arrival
x [m]	37.9
kL	1.0
C	0.4122
Tr [s]	9.311
s	0.084
OG [m]	3.24
$\tilde{B}$	0.701
$\tilde{T}$	0.1231
β	0.92
τ	7.1856
K_1	-1.1239
K_2	24.129
F	-0.8657
r	0.8379
δ_φ	0.4526
φ [rad]	0.4635
h [m]	28.56
$\varphi \cdot kL \cdot \left(g + \frac{4\pi^2 h}{T_r^2}\right)$ [m/s²]	10.575

Table 5.37: Results for Level 1 Vulnerability Check

Vessel	Loadcase		Lat.Acc.	R_{EA1}	Status
Feedermax	BA	Ballast Arrival	10.575	4.64	**FAIL**

5.4.2.2.Level 2 Vulnerability Check

Using the fitting proposed in eq.(4.91) the linear, quadratic and cubic roll damping coefficients are calculated.

$$\frac{B_{44}(\varphi_\alpha)\cdot\omega_\varphi^2}{2W\cdot GM}\Rightarrow \mu+\frac{4}{3\pi}\cdot\beta\cdot\omega_\varphi\cdot\varphi_\alpha+\frac{3}{8}\cdot\delta\cdot\omega_\varphi^2\cdot\varphi_\alpha^2$$

$$\mu=0.0192\quad \beta=0.1029\quad \delta=0.1769$$

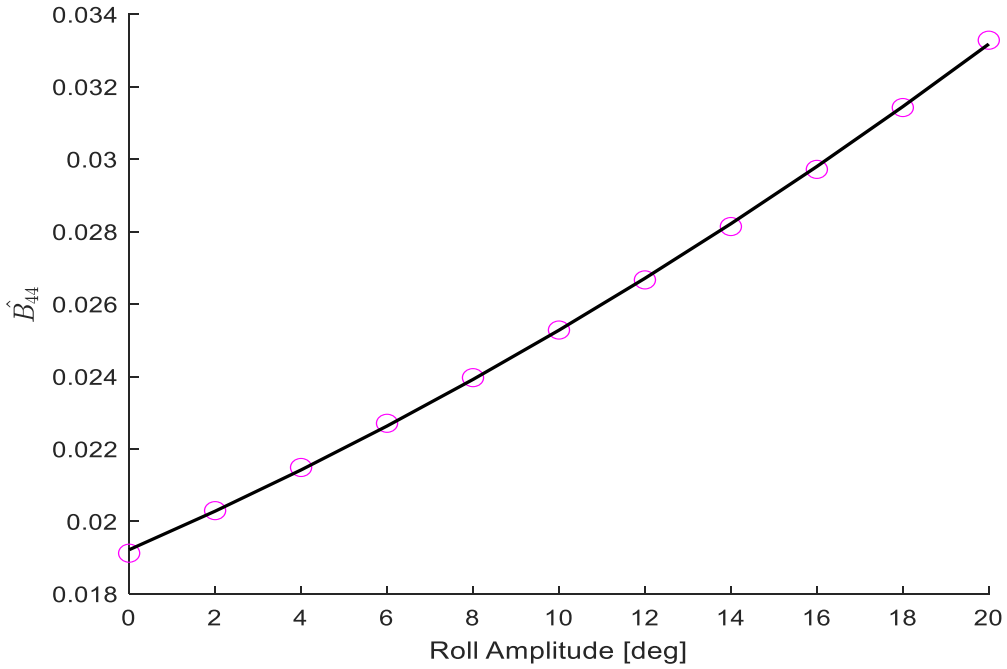

Figure 5.20: Least square fitting for Ballast Arrival

Following the draft regulations and the appropriate calculations, the table of results below is presented.

$$\sigma_{LAi}^2=\frac{3}{4}\int_{\omega_1}^{\omega_2}\Big(a_y(\omega)\Big)^2\,Szz(\omega)\,d\omega$$

Table 5.38: Results for standard deviation of lateral acceleration (σ_{LAi})

H[m] / Tz[s]	3.5	4.5	5.5	6.5	7.5	8.5	9.5	10.5	11.5	12.5	13.5	14.5	15.5	16.5	17.5	18.5
0.5	7.35E-05	3.02E-04	1.31E-03	2.18E-03	2.23E-03	1.88E-03	1.47E-03	1.13E-03	8.59E-04	6.60E-04	5.14E-04	4.06E-04	3.25E-04	2.64E-04	2.17E-04	1.81E-04
1.5	6.61E-04	2.72E-03	1.18E-02	1.96E-02	2.01E-02	1.70E-02	1.33E-02	1.01E-02	7.73E-03	5.94E-03	4.63E-03	3.65E-03	2.93E-03	2.38E-03	1.96E-03	1.62E-03
2.5	1.84E-03	7.54E-03	3.28E-02	5.44E-02	5.58E-02	4.71E-02	3.69E-02	2.82E-02	2.15E-02	1.65E-02	1.29E-02	1.01E-02	8.13E-03	6.61E-03	5.43E-03	4.51E-03
3.5	3.60E-03	1.48E-02	6.43E-02	1.07E-01	1.09E-01	9.23E-02	7.23E-02	5.52E-02	4.21E-02	3.24E-02	2.52E-02	1.99E-02	1.59E-02	1.29E-02	1.06E-02	8.85E-03
4.5	5.95E-03	2.44E-02	1.06E-01	1.76E-01	1.81E-01	1.53E-01	1.19E-01	9.12E-02	6.96E-02	5.35E-02	4.16E-02	3.29E-02	2.63E-02	2.14E-02	1.76E-02	1.46E-02
5.5	8.89E-03	3.65E-02	1.59E-01	2.63E-01	2.70E-01	2.28E-01	1.78E-01	1.36E-01	1.04E-01	7.99E-02	6.22E-02	4.91E-02	3.94E-02	3.20E-02	2.63E-02	2.18E-02
6.5	1.24E-02	5.10E-02	2.22E-01	3.68E-01	3.77E-01	3.18E-01	2.49E-01	1.90E-01	1.45E-01	1.12E-01	8.69E-02	6.86E-02	5.50E-02	4.47E-02	3.67E-02	3.05E-02
7.5	1.65E-02	6.79E-02	2.95E-01	4.90E-01	5.02E-01	4.24E-01	3.32E-01	2.53E-01	1.93E-01	1.49E-01	1.16E-01	9.13E-02	7.32E-02	5.94E-02	4.89E-02	4.06E-02
8.5	2.12E-02	8.72E-02	3.79E-01	6.29E-01	6.45E-01	5.45E-01	4.26E-01	3.26E-01	2.48E-01	1.91E-01	1.49E-01	1.17E-01	9.40E-02	7.64E-02	6.28E-02	5.22E-02
9.5	2.65E-02	1.09E-01	4.74E-01	7.86E-01	8.06E-01	6.80E-01	5.32E-01	4.07E-01	3.10E-01	2.38E-01	1.86E-01	1.47E-01	1.17E-01	9.54E-02	7.84E-02	6.52E-02
10.5	3.24E-02	1.33E-01	5.79E-01	9.60E-01	9.84E-01	8.31E-01	6.50E-01	4.97E-01	3.79E-01	2.91E-01	2.27E-01	1.79E-01	1.43E-01	1.17E-01	9.58E-02	7.96E-02
11.5	3.89E-02	1.60E-01	6.94E-01	1.15E+00	1.18E+00	9.97E-01	7.80E-01	5.96E-01	4.54E-01	3.49E-01	2.72E-01	2.15E-01	1.72E-01	1.40E-01	1.15E-01	9.55E-02
12.5	4.59E-02	1.89E-01	8.20E-01	1.36E+00	1.40E+00	1.18E+00	9.22E-01	7.04E-01	5.37E-01	4.13E-01	3.21E-01	2.54E-01	2.03E-01	1.65E-01	1.36E-01	1.13E-01
13.5	5.35E-02	2.20E-01	9.56E-01	1.59E+00	1.63E+00	1.37E+00	1.08E+00	8.21E-01	6.26E-01	4.81E-01	3.75E-01	2.96E-01	2.37E-01	1.93E-01	1.58E-01	1.32E-01
14.5	6.18E-02	2.54E-01	1.10E+00	1.83E+00	1.88E+00	1.58E+00	1.24E+00	9.47E-01	7.22E-01	5.55E-01	4.32E-01	3.41E-01	2.74E-01	2.22E-01	1.83E-01	1.52E-01
15.5	7.06E-02	2.90E-01	1.26E+00	2.09E+00	2.15E+00	1.81E+00	1.42E+00	1.08E+00	8.25E-01	6.34E-01	4.94E-01	3.90E-01	3.13E-01	2.54E-01	2.09E-01	1.73E-01
16.5	8.00E-02	3.29E-01	1.43E+00	2.37E+00	2.43E+00	2.05E+00	1.61E+00	1.23E+00	9.35E-01	7.19E-01	5.60E-01	4.42E-01	3.54E-01	2.88E-01	2.37E-01	1.97E-01

Using the below equations the final results are presented in the table 5.39.

$$C_i = \exp[-R_2^2 \,/\, (2 \cdot \sigma_{LAi}^2)]$$

Table 5.39: Results for Level 2 excessive accelerations

Vessel	Loadcase		C	R_{EA2}	Status
Feedermax	BA	Ballast Arrival	6.965E-14	0.00039	PASS

5.4.3. Relationship between Level 1 check of EA and IMO Cargo Securing Manual [41]

The cargo securing manual of a containership contains the strength limit of lashing equipment in connection with the accelerations on different decks and for different directions. Following the advanced calculation method presented in Annex 13 of [41], the accelerations are calculated for different vertical and longitudinal locations as presented in Fig.(5.21).

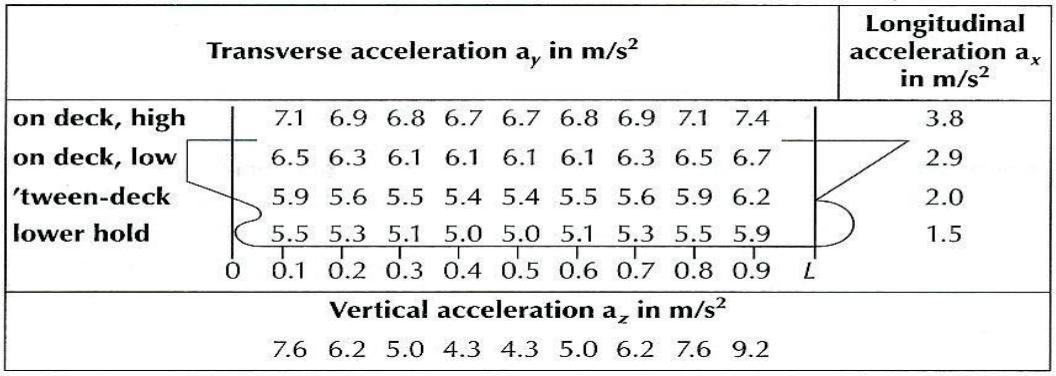

Figure 5.21: Basic acceleration data [41]

The table presented in Fig.(5.21) is considered valid following specific operational conditions explained in [41]. For ships with a different length of 100 m and a service speed other than 15 knots a correction formula is adopted. Also, for ships with a ratio B/GM less than 13 thre is also a correction.

Following the above method of [41] for the calculation of accelerations the relationship between the two regulations are compared. The results concern calculations for the metacentric height, the service speed and the length of the vessel.

Firstly, concerning the length of the vessel the corresponding lateral accelerations are calculated. The results of Figures (5.22) & (5.23) are calculated for IMO CSS and they are compared to the ones calculated for level 1 of EA for a step of 0.1*L_{BP} .

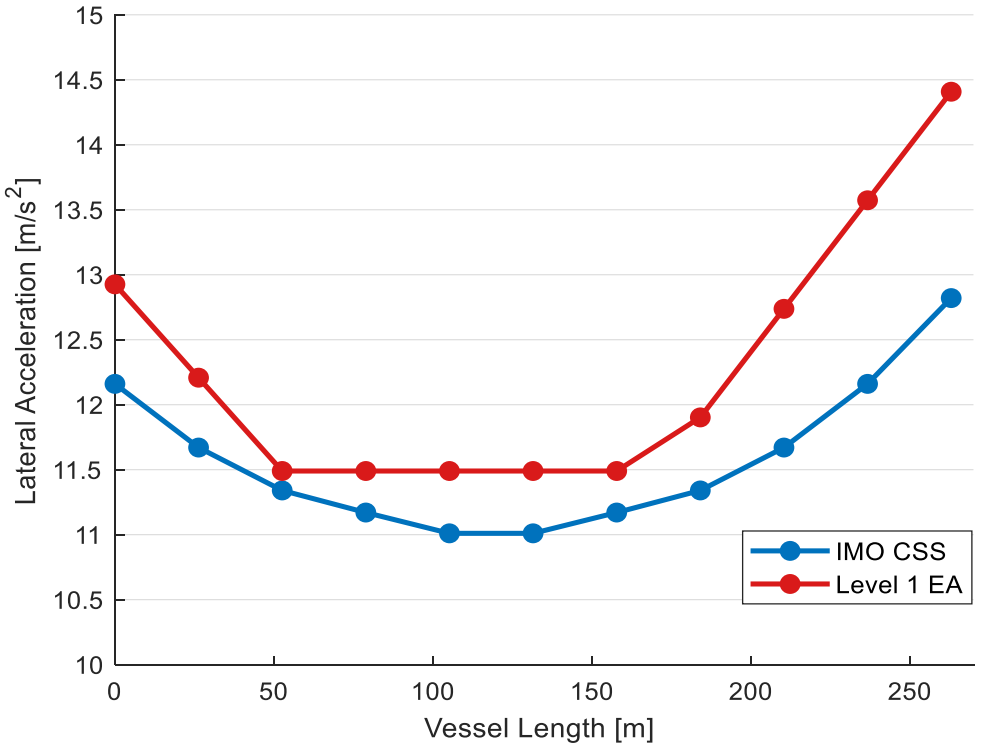

Figure 5.22: Lateral accelerations for longitudinal positions of Lvl 1 EA and IMO CSS for Ballast Arrival

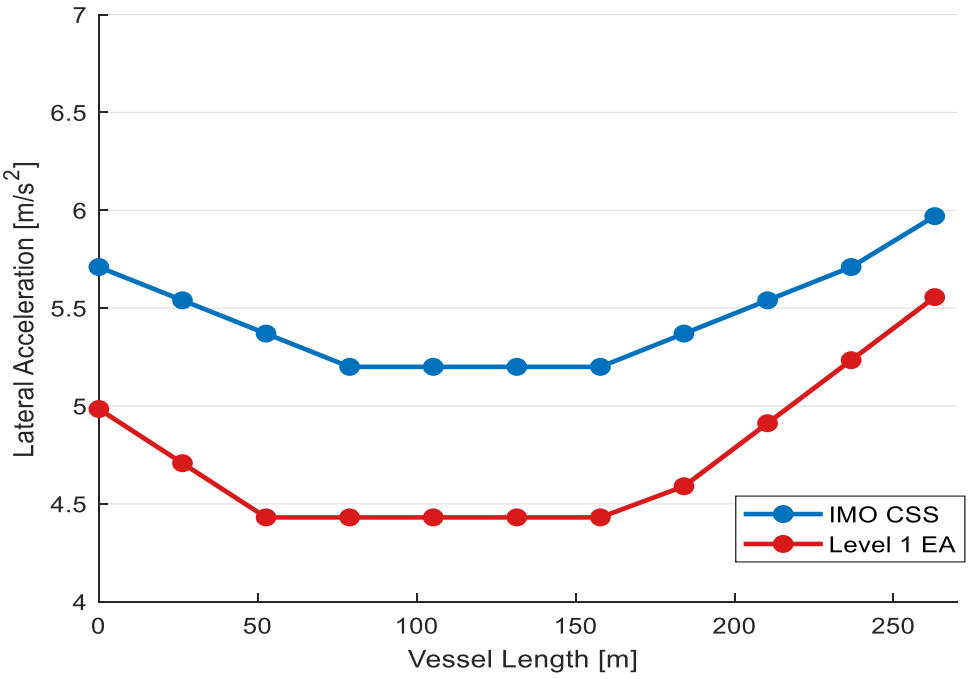

Figure 5.23: Lateral accelerations for longitudinal positions of Lvl 1 EA and IMO CSS for Emp. Cont. Arrival

*M*oreover, another examination is considered as the value of speed changes. Level 1 of excessive acceleration is not affected by the speed so its value is steady, in contrast to CSS Annex 13. As the speed progresses the value of acceleration is increasing linearly. The results are presented in Figures (5.24).

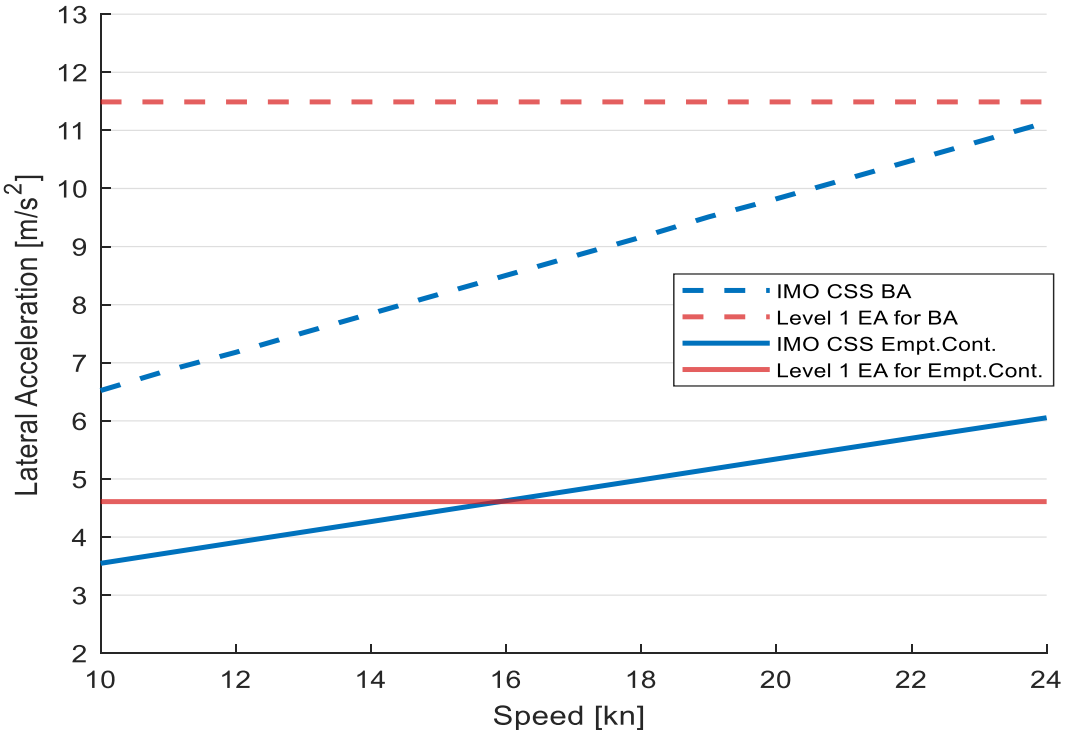

Figure 5.24: Lateral accelerations to different speeds for Level 1 EA and IMO CSS

Finally, the relationship for the loadcase examined in Level 1 of excessive accelerations is presented for various values of GM. It is obvious that the line concering the CSS Annex 13 increases with a linear rate as the GM value is increasing. In addition, the line concerning the loadcase examined in Level 1 of excessive acceleration is strongly affected by the GM increase starting from an insignificant value and reaching a high value of acceleration as the GM increases. The results are presented in Figures (5.25).

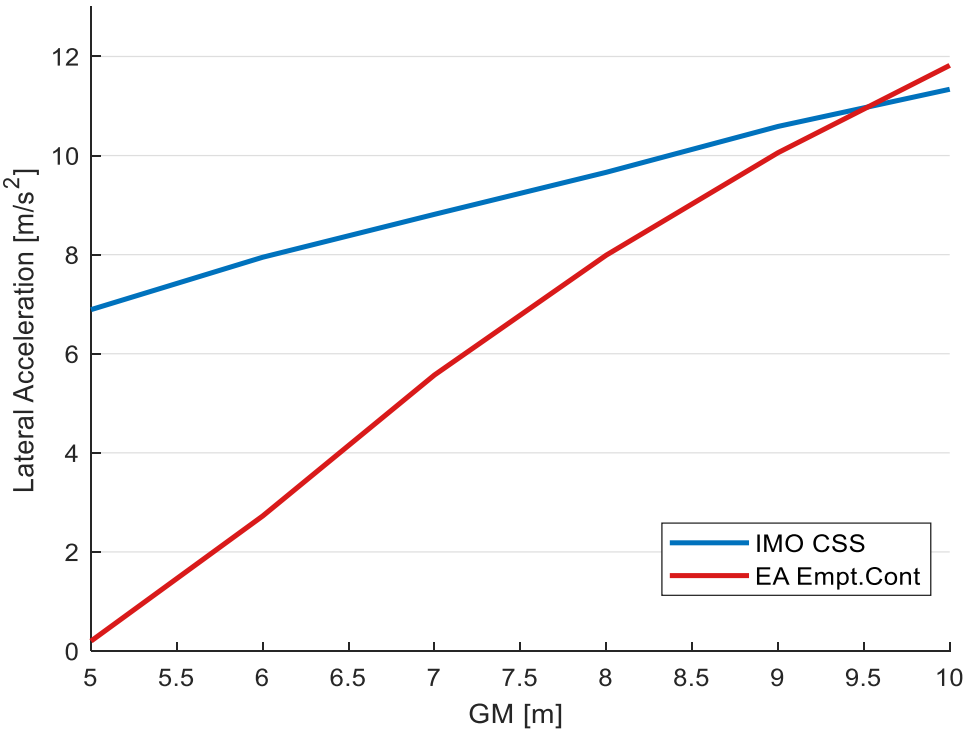

Figure 5.25: Comparison of Lvl 1 EA to CSS Annex 13 for examined LC

The conclusion drawn from the analysis above is that the Level 1 of EA is highly dependent to the GM. For that reason, for two different loadcases with a significant difference of the GM value the comparison provides two really different solutions. Specifically, for the high GM loadcase the excessive acceleration criterion provides higher lateral accelerations than the ones calculated for IMO CSS, opposing to the lower GM loading conditions that provides lower.

Chapter 6 Impact of bilge keel

Bilge keels are structures of small width placed perpendicular to ship's hull on the curve shaped as a permanent fin and running along much of the ship's length. They account as passive stability systems and they are commonly built as a pair one in each side symmetrically to the keel. Bilge keels contribute to the increase of the hydrodynamic resistance to rolling, by reducing the amplitude of roll. The performance of the bilge keels is mainly affected by their surface area and they perform better for large heel angles. Finally, bilge keels remain as the cheapest solution to reduce effectively rolling and that is the reason they are used on a large scale in every vessel type. In this chapter, the influence of bilge keel area and dimensions will be investigated in order to examine their effect on the criteria. It has been decided to conduct the calculations for a bilge keel area with a span of 0 to 80 m^2 with steps of 10 m^2 and the length of it in reference to the length of the ship with a span from 0% to 40% of ship's length. The results produced will be analyzed below.

The analysis will be applied on the examined Post-Panamax vessel and the loading case used to assess the criteria of parametric rolling vulnerability. Specifically, the impact of bilge keels on the vulnerability assessment will be analyzed by changing their basic design parameters. Following Level 1 Vulnerability Criterion for Parametric Rolling and the equation (4.14) an analysis for the impact on the factor R_{PR} was concluded. The case used concerns the C_M >0.96, where a change in Ak can produce higher values of R_{PR} coefficient.

As the bilge keel area is increasing so does the R_{PR} factor following a linearized curve. Although, the increase is not so drastic in order to avoid the vulnerability of Level 1 as the maximum value presented in Table (6.1) is too low compared to the value of $\Delta GM/GM$. In conclusion, even though the increase of the R_{PR} value is visible, is not significant enough to avoid a Level 2 vulnerability check. In this situation more loading conditions where the boundaries for Level 1 are closer are examined. Loading cases with higher GM values were taken into account. Specifically, as the GM value gets higher the value of of $\Delta GM/GM$ becomes lower and according to equation (4.13), more loading conditions will be checked. A design draught departure condition and a ballast arrival were used. Results are presented in Table (6.1).

Table 6.1: Results for Level 1 Vulnerability Check

Vessel	Loadcase	ΔGM/GM	Maximum Rpr	Status
Post-Panamax	Full Load Departure	2.129	0.484	**PASS**
	Design draught Departure	0.9429	0.484	**PASS**
	Ballast Arrival	0.6453	0.484	**PASS**

Although these cases seem to be more prone than FLD they still do not reach the threshold limit and thus the conclusion is that a too significant raise of bilge keel area could actually made ship not vulnerable to first check but for certain loading conditions.

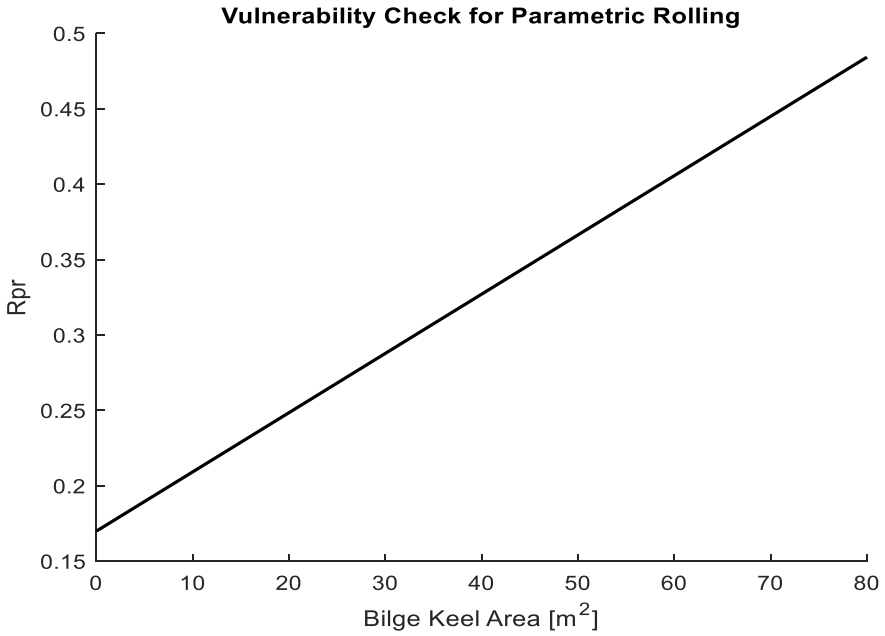

Figure 6.1: Bilge Keel Area effect to Rpr Index

For Level 2A vulnerability criterion for parametric rolling the coefficient R_{PR} is presented for the adequate requirements. Same as Level 1, the threshold of R_{PR0}=0.06 is too low to be affected by the C1 factor and so the increase of bilge keel area can reduce the value of C1 but not affect it enough to bypass the check. The difference of C1 factor is presented in the Figure (7.2).

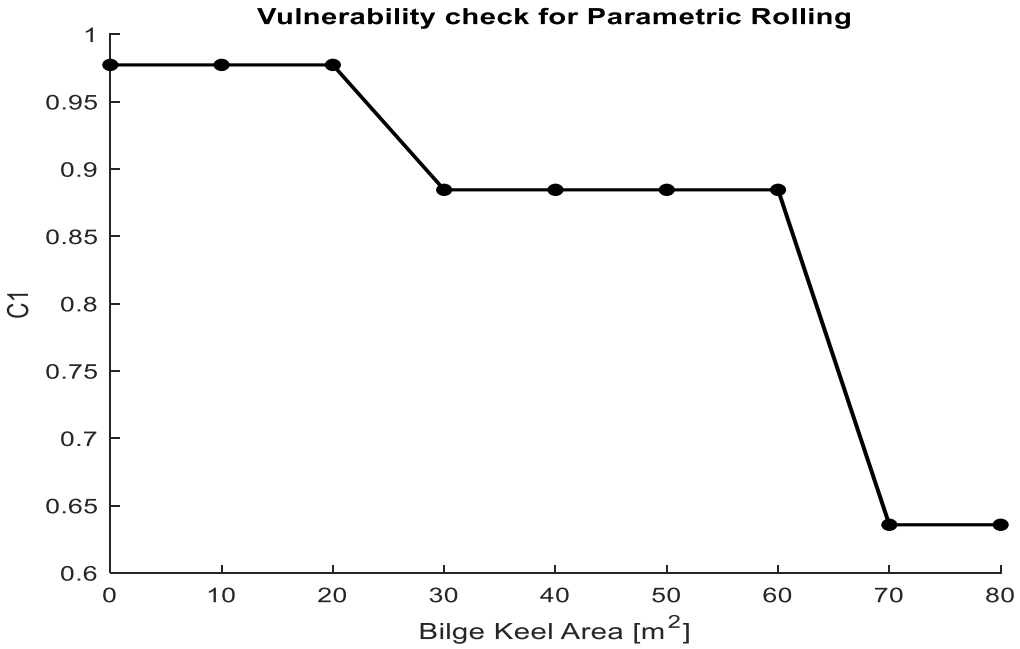

Figure 6.2: Bilge Keel Area effect to C1 Vulnerability Index

Furthermore, the bilge keel concerns the calculation of roll damping coefficient B_{44} as the bilge keel component B_{BK}. In this step, calculations were conducted for different ratios of the length of bilge keel to the length of the ship. The purpose is to define if the increase of the ratio can impact the total roll damping and so the resistance to rolling. The span used here is from 0% to 40%. As shown in figure (7.3) the B_{BK} coefficient is increasing as the ratio becomes bigger. Definitely, it was computed that a 10% increase in the ratio results in a 2% increase of the total B_{44} roll damping coefficient. This raise is not significant but should not be neglected as the B_{BK} coefficient plays a secondary role compared to the other coefficients.

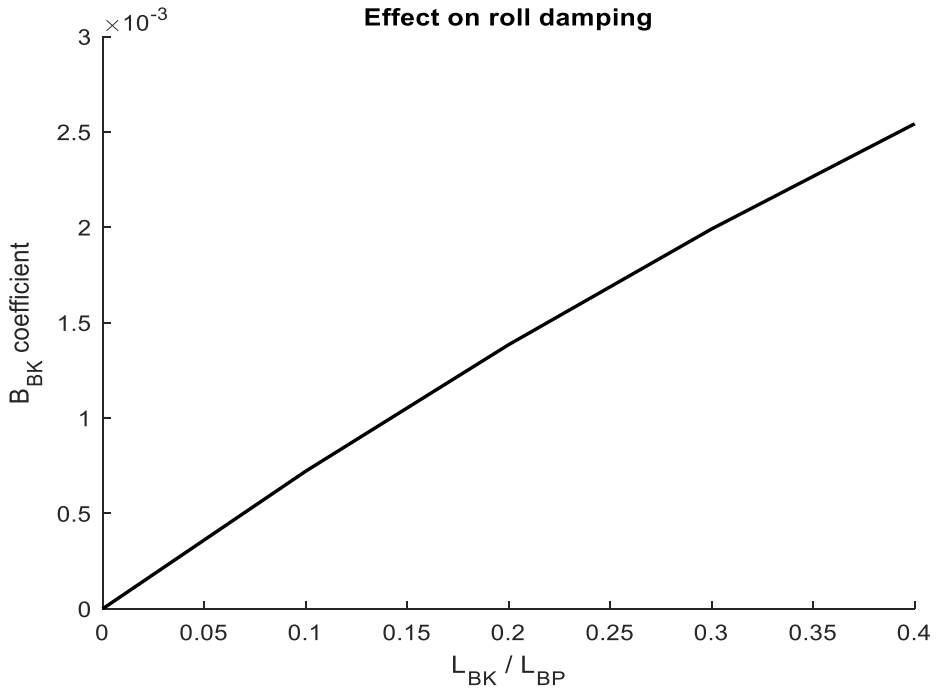

Figure 6.3: Length ratio effect on roll damping coefficient of bilge keel

Concerning Level 1 Vulnerability for Excessive Acceleration, it is proven that metacentric height plays a significant role for the lateral acceleration that will be developed on the deck under examination. Since the criterion is applied only for GM values higher than 3.22 [m], two loading conditions were taken into account as in chapter 5. The Ballast Arrival with a too high GM value and another one with a close to threshold GM value. In Figure (6.4), it is proven that in a high GM case the difference in the bilge keel area will not affect at all the vulnerability of the criterion. In Figure (6.5), though a small change in the bilge keel area can actually become effective enough to avoid a Level 2 check.

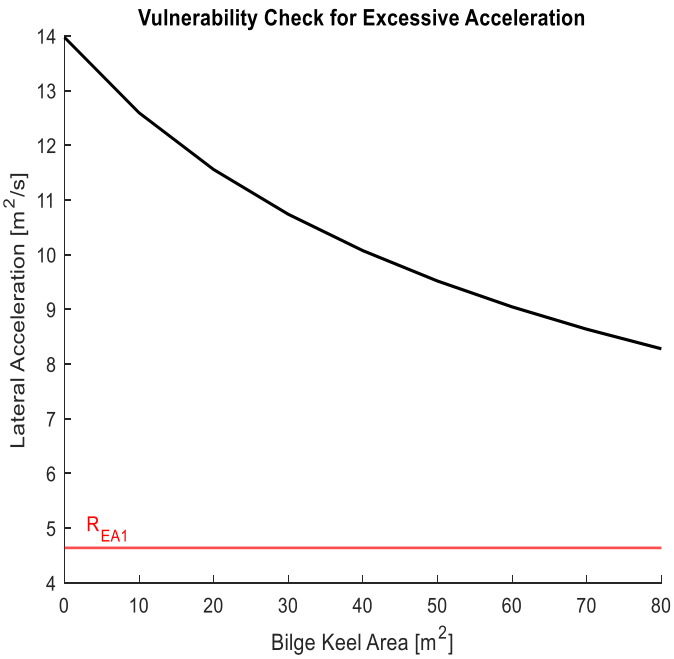

Figure 6.4: Effect to lateral acceleration for high GM Loadcase

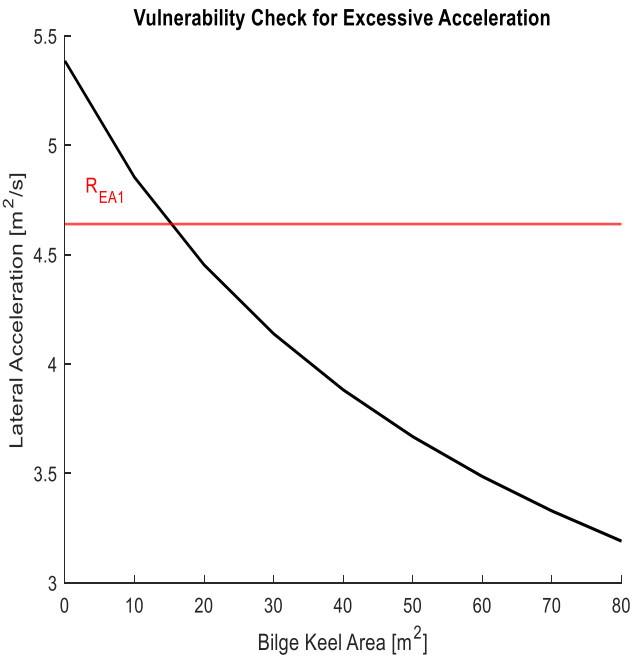

Figure 6.5: Effect to lateral acceleration for low GM Loadcase

Consequently, the variations in bilge keel area and length do not result to the change of the verdict of the vulnerability criteria. Although, their effect should not be ignored as they can actually reduce the ship rolling and thus vessels can become more immune to these phenomena.

Chapter 7 Discussion & Conclusions

This thesis presents the intact stability regulations and applies them to containerships of modern hull designs. Specifically, the IMO Weather Criterion and the IMO Second Generation Intact Stability criteria for parametric rolling and excessive accelerations are evaluated through their application. In addition, significant accidents are described and an analysis on bilge keel design is performed in order to examine its effect on the satisfaction of the criteria. Specifically, the next conclusions have been derived.

Firstly, the parametric rolling vulnerability assessment demands complex calculations. Level 1 and Level 2A are straightforward although it is easy for a ship to fail them. On the contrary, the vessels pass Level 2B easily. For Level 2B, it shall be noted that many wave cases lead to parametric roll detection but because of their small probability of occurrence according to the wave scatter diagram, their effect is not strongly considered. Also, cases with high wave heights that conclude to a roll angle larger than 25 degrees are not considered into the calculation of the vulnerability index $C2$ as the representative wave heights Hri are too small. So, a significant change to the design process of containerships concerning the current form of parametric roll criterion is not so probable. Although, it can provide operational guidance and limitations for each vessel and critical information on how the master can confront adverse weather conditions.

Concerning the criterion of excessive acceleration, it is clear that a vulnerability check on the bridge contributes towards the avoidance of accidents for the crew. Although, for containerships, large transverse accelerations are connected with the cargo security and the probability of lashings failure which can cause stability failures and cargo shifting. Since the bridge deck is high enough to cover the height of TEUs bays, Level 1 can connect with cargo securing, but since the bridge location is mostly amidship, the more significant accelerations at the vessel's bow are not taken into account. The operational window of GM value is also another question that rises through this criterion and should be examined in a larger extent. Also, same concerns as the parametric rolling criterion are visible. Even though, the vessels fail the first level easily, they pass the second level quite easy. The reason seems to be the small values of the short-term probability index. Finally, an attempt to examine the effect of the bilge keel design on the satisfaction of the criteria was carried out. As a result, the variations in the particulars proved to have small impact towards the vulnerability criteria. Nevertheless, bilge keels effects should not be neglected as they can be useful towards increasing roll damping.

References

[1] IMO SDC 6.5, 2018: "*Finalization of Second Generation Intact Stability Criteria*", Sub-committee on ship design and construction, 6_{th} session, 1 November 2018

[2] IMO SDC 4/5/1/Add.1, 2016: "*Draft explanatory notes on the vulnerability of ships to the parametric roll stability failure mode*", Sub-committee on ship design and construction, 4_{th} session, 11 November 2016

[3] IMO SDC 4/5/1/Add.4, 2016: "*Draft explanatory notes on the vulnerability of ships to the excessive acceleration stability failure mode*", Sub-committee on ship design and construction, 4_{th} session, 11 November 2016

[4] Spyrou, K.J. "*Δυναμική Ευστάθεια Πλοίου*", Ακαδημαικά Συγγράμματα Κάλλιπος, 2015

[5] Themelis, N. "*Probabilistic Assessment of Ship Dynamic Stability in Waves*", PhD Thesis, National Technical University of Athens, 2008

[6] Grinnaert, F. "*Analysis and implementation of second generation criteria in a stability computer code*", PhD Thesis, Universitè de Bretagne-Brest, 2017

[7] Sjule, A. "*Evaluation of vulnerability to parametric rolling*", MSc Thesis, KTH Royal Institute of Technology in Stockholm, 2016

[8] Panagiotelis, S. "*Evaluation of IMO's Second Generation Intact Stability criteria-Investigation for the possible impact on RoRo/RoPax ship design and operation*", Diploma Thesis, National Technical University of Athens, 2017

[9] Moulos, V. "*Probabilistic Assessment of ship stability in the framework of IMO's Second Generation Intact Stability criteria*", Diploma Thesis, National Technical University of Athens, 2019

[10] Dousia, G."*Numerical Analysis of Parametric Roll Resonance of a Containership Sailing in Nonlinear Longitudinal Seas* ", Diploma Thesis,National Technical University of Athens,2015

[11] Petacco, N. "*Second Generation Intact Stability criteria: Analysis,Implementation and Applications to significant ship typologies*", PhD Thesis, University of Genova, 2019

[12] Boccadamo G. & Rosano G. "*Excessive Acceleration Criterion Application to Naval Ships*", University of Naples, 2019

[13] Federal Bureau of Marine Casualty Investigation, " *Fatal accident on board the CMV CHICAGO EXPRESS during Typhoon 'HAGUPIT' on 24 September 2008 off the coast of Hong Kong*",Investigation Report 510/08,Federal Higher Authority subordinated to Ministry of Transport, Hamburg, Germany, November 2009

[14] France W.N. et al. , "*An investigation of head-sea parametric rolling and its influence on container lashing systems*", SNAME Annual Meeting 2001

[15] Danish Maritime Accident Investigation Board, "*Svendborg Maersk Heavy weather damage on 14 February 2014*", Spetember 2014

[16] Federal Bureau of Marine Casualty Investigation, " *Loss overboard of 10 containers from JRS CANIS at estuary of Elbe River on 12 January 2007*",Investigation Report 45/07,Federal Higher Authority subordinated to Ministry of Transport, Hamburg, Germany, November 2007

[17] Federal Bureau of Marine Casualty Investigation, " *Fatal accident on board the CMV CCNI GUAYAS during Typhoon 'KOPPU' on 15 September 2009 in the sea area off Hong Kong*",Investigation Report 391/09,Federal Higher Authority subordinated to Ministry of Transport, Hamburg, Germany, June 2011

[18] Federal Bureau of Marine Casualty Investigation, " *Person overboard from MS BELUGA STIMULATION on 27 October 2006 in the German Bight*", Investigation Report 510/08,Federal Higher Authority subordinated to Ministry of Transport, Hamburg, Germany, June 2008

[19] American Bureau of Shipping, *"Assessment of parametric roll resonance in the design of container carriers*", September 2004

[20] Rahola, J. "*The Judging of the Stability of Ships and The Determination of The Minimum Amount of Stability*", PhD thesis, Technical University of Finland, Helsinki 1939

[21] IMO, *"Recommendation on a severe wind and rolling criterion (Weather Criterion) for the intact stability of passenger and cargo ships of 24 metres in length and over. Resolution A.562(14)"*, International Maritime Organization,London, UK, 1982

[22] Francescutto, A. "*Is it really impossible to design safe ships? Transaction of Royal Institute of Naval Architect"*, 135:163–173, 1993

[23] IMCO, "*Recommendation on intact stability for passenger and cargo ships under 100 metres in length. Resolution A.167(AS.IV)*", Inter-Governmental Maritime Consultative Organization, London, UK, 1968

[24] Spyrou, K.J. 2005: "*Design Criteria for Parametric Rolling*", Oceanic Engineering International, Vol. 9, No. 1, 2005, pp. 11-27

[25] Spyrou K.J., Tigkas I.,Scanferla G., Pallikaropoulos N.,Themelis N. "Prediction potential of the parametric rolling behavior of a post-panamax containership", *Ocean Engineering,* 2008

[26]Spyrou, K.J. "*A basis for a developing a rational alternative to the weather criterion:problems and capabilities*." Proceedings, 6th International Ship Stability Workshop, Webb Institute, New York, (2002)

[27] IMO, *Adoption of the international code on Intact Stability. Resolution MSC.267(85)*, International Maritime Organization, London, UK, December 2008

[28] IMO, "*MSC.1/Circ 1200 Interim Guidelines for Alternative Assessment of the Weather Criterion*" International Maritime Organization, London, UK, May 2006

[29]Shigunov, V., Rathje, H., El Moctar O., Altmayer, B., "*On the Consideration of Lateral Accelerations in Ship Design Rules*", 12th International Ship Stability Workshop, USA 2011

[30] IMO, "*MSC.1/Circ.1627 Interim Guidelines On the Second Generation Intact Stability Criteria*"

[31] Umenda, N., Hashimoto H., Vassalos D., Urano S. & Okou K., 2003, "*Nonlinear analysis of parametric rolling in longitudinal and quartering seas with realistic modeling of roll-restoring moment*",8th International Conference on the Stability of Ships and Ocean Vehicles

[32] Yamagata, M. 1959, "*Standard of stability adopted in Japan."* Transactions of Institution of Naval Architects

[33]Register of Shipping of the USSR, *"Standards of stability of sea-going vessels and coasters.",*Technical report, Mosrskoi Transport, Moscow,RU,1961

[34] L.L. Goldberg & T.H. Sarchin, *"Stability and buoyancy criteria for u.s. naval surface ship."* Transactions of American Society of Naval Architects and Marine Engineers 1962

[35]Francescutto, A. *2002, "Experimental Tests on Ships with Large Values of B/T, OG/T and Roll Period"* Proceedings of the 6th Intact Ships Stability Workshop

[36] Kato, H. 1965, *"Effects of bilge keels on the rolling of ships."* J.Society of Naval Architecture of Japan 117(in Japanese)

[37] Chakrabarti, S. 2000, "*Empirical calculation of roll damping for ships and barges"*, Ocean Engineering 2001

[38] Falzarano et.al 2015, "*An overview of the prediction methods for roll damping of ships"* Ocean Systems Engineering 2015

[39] Schmitke, R. 1978, "*Ship sway, roll, yaw motions in oblique seas"* SNAME Trans.,86

[40]Soding, H. 1979, " *Discussion to paper by Blume"*

[41] IMO 2011, "*Code of safe practice for Cargo Storage and Security"*

[42] Tae-Young Park, Chang-Doo Jang, Yong-suk Suh and Bong-Jae Kim, *"A parametric study based on spectral fatigue analysis for 170k LNG"* International Journal of Naval Architecture and Ocean Engineering 2011

[43]Malcom McLean - Wikipedia

[44] SS Ideal X - Maritime Logistics Professional (maritimeprofessional.com)

[45] Namsung Shipping

[46] Our Fleet of Vessels | MSC

[47]Container ship - Wikipedia

[48]https://www.shutterstock.com/